Cretaceous Research 143 (2023) 105415

Contents lists available at ScienceDirect

Cretaceous Research

journal homepage: www.elsevier.com/locate/CretRes

Carbon isotopes, palynology and stratigraphy of the Santonian–Campanian boundary: The GSSP auxiliary sections, Seaford Head (England) and Bocieniec (Poland), and correlation between the Boreal and Tethyan realms

Ian Jarvis [a, *], Martin A. Pearce [b], Johannes Monkenbusch [c], Agata Jurkowska [d], Clemens V. Ullmann [e], Zofia Dubicka [f], Nicolas Thibault [c]

[a] Department of Geography, Geology and the Environment, Kingston University London, Penrhyn Road, Kingston-upon-Thames KT1 2EE, UK
[b] Department of Earth Sciences, Natural History Museum, Cromwell Road, London SW7 5BD, UK
[c] Department of Geosciences and Natural Resource Management, University of Copenhagen, Øster Voldgade 10, DK-1350 Copenhagen C, Denmark
[d] Faculty of Geology, Geophysics and Environmental Protection AGH, University of Science and Technology, Mickiewicza 30, PL 30-059 Kraków, Poland
[e] Camborne School of Mines and the Environment and Sustainability Institute, University of Exeter, Penryn Campus, Penryn, Cornwall TR10 9FE, UK
[f] Faculty of Geology, University of Warsaw, Al. Zwirki I Wigury 93, 02-089 Warszawa, Poland

ARTICLE INFO

Article history:
Received 9 August 2022
Received in revised form
25 October 2022
Accepted in revised form 1 November 2022
Available online 8 November 2022

Keywords:
Santonian
Campanian boundary
Campanian GSSP
Palynology
Dinoflagellate cysts
Carbon isotope stratigraphy

ABSTRACT

The stratigraphy and palynology of the upper Santonian–lower Campanian (*Uintacrinus socialis–Gonioteuthis quadrata* zones) Newhaven Chalk are described for the Campanian auxiliary GSSP section at Seaford Head, England. A new high-resolution bulk-sediment carbonate carbon stable-isotope ($\delta^{13}C_{carb}$) curve provides the basis to refine the carbon-isotope event (CIE) stratigraphy of the section. Results are compared to a complementary palynological study of a second Campanian auxiliary GSSP section (*U. socialis–O. pilula* zones) at Bocieniec, Poland. Palynological assemblages are dominated by organic-walled dinoflagellate cysts (dinocysts; 208 taxa) at both sites. A stratigraphic framework is established via review of published lithostratigraphic, macrofossil, foraminifera and calcareous nannofossil records from the study sites. Carbon isotope curves with 13 major named CIEs provide a basis for correlation of Seaford Head and Bocieniec to sections at: Trunch, England; Poigny, France; Lägerdorf, Germany; and the Campanian GSSP at Gubbio, Italy. Correlations are constrained by biostratigraphic records, including dinocyst events. The Late Santonian $\delta^{13}C$ Event (LSE, previously termed the Santonian–Campanian Boundary Event, SCBE) provides a key correlation level between Boreal and Tethyan sections and enables the placement of base Campanian markers: extinction levels of the crinoid *Marsupites* and the planktonic foraminifera *Dicarinella asymetrica*; the first appearance of the calcareous nannofossil *Aspidolithus parcus parcus*; and the C34n/C33r magnetozone boundary (the primary Campanian marker), in both Boreal and Tethyan sections. A holostratigraphy for the Santonian–Campanian boundary interval that integrates CIEs, macrofossils, benthic and planktonic foraminifera, calcareous nannofossils, dinocysts and magnetostratigraphy is presented. *Rhynchodiniopsis juneae* sp. nov. is described.

1. Introduction

Following votes of the Campanian Working Group, the Cretaceous Subcommission, and the International Commission on Stratigraphy, the lower boundary of the Campanian Stage was ratified by the International Union of Geological Sciences (IUGS) on October 5th, 2022, with Bottaccione (Gubbio, Italy) as the Global Boundary Stratotype Section and Point (GSSP), and the base of Chron C33r as the primary stratigraphic marker.

The C33r palaeomagnetic reversal corresponds to the top of the Cretaceous Long Normal Superchron C34n (e.g. Ogg, 2020) which, together with the approximately coincident last appearance datum level (LAD) of the planktonic foraminifera *Dicarinella asymetrica* (Sigal) (Gale et al., in press; Premoli Silva, 1977; Marks, 1984; Premoli Silva and Sliter, 1995), provide robust base Campanian markers that are well documented in deeper water Tethyan successions. These are

* Corresponding author.
E-mail address: i.jarvis@kingston.ac.uk (I. Jarvis).

https://doi.org/10.1016/j.cretres.2022.105415

exemplified by the Cretaceous–Paleogene magnetostratigraphic reference section and boundary stratotype at Gubbio (Lowrie and Alvarez, 1977; Premoli Silva and Sliter, 1995; Coccioni and Premoli Silva, 2015; Miniati et al., 2020), the GSSP auxiliary section at Postalm in Austria (Gale et al., in press; Wolfgring et al., 2018a), and multiple ocean drilling cores (e.g. Petrizzo, 2000; Petrizzo et al., 2011, 2020; Ando et al., 2013).

The LAD of the crinoid *Marsupites testudinarius* (Schlotheim) has previously been widely used as the stage boundary marker, particularly in epicontinental chalk facies (e.g. Birkelund et al., 1984; Schulz et al., 1984; Hancock and Gale, 1996; Hampton et al., 2007; Gale et al., 2008, 2020). The taxon is distributed throughout northern and eastern Europe and extends from the US Gulf Coast through the Western Interior Basin to British Columbia in North America (e.g. Cobban, 1995; Gale et al., 2007; Haggart and Graham, 2018). It is known from Madagascar (Walaszczyk et al., 2014) and occurs widely in Western Australia (Gale et al., 1995). However, *Marsupites* is absent from deeper water, low-latitude, and ocean basin sections.

The base of Chron C33r was selected as the primary marker for the base of the Campanian Stage based on the argument that magnetic reversals are global and potentially identifiable in all palaeoenvironments (Gale et al., in press). Sadly, the magnetic reversal is rarely unambiguously identifiable outside oceanic seafloor sections and successions yielding *Marsupites* have failed to provide reliable palaeomagnetic records. However, in addition to the use of the *D. asymetrica* planktonic foraminifera LAD, high-resolution correlation of the boundary interval between sections is possible using carbon isotope stratigraphy (e.g. Jarvis et al., 2002, 2006; Voigt et al., 2010; Joo and Sageman, 2014; Thibault et al., 2016; Chenot et al., 2018; Deville de Periere et al., 2019; Takashima et al., 2019; Eldrett et al., 2021; Ifrim and Stinnesbeck, 2021; Pearce et al., 2022) and occurrences of evolutionary subspecies in the *Aspidolithus parcus* (Stradner) Noël coccolith lineage (e.g. Kita et al., 2017; Miniati et al., 2020; also referred to *Brionsonia parca* (Stradner) Bukry). These biostratigraphic and chemostratigraphic criteria provide important secondary markers bracketing the boundary horizon (Gale et al., in press).

The base of the Campanian Stage was assigned a nominal age of 83.65 Ma by Gale et al. (2020) for the 2020 Geologic Time Scale. However, an astronomically tuned age for the base of Chron C33r is 82.875 Ma (Wu et al. in Ogg, 2020), which is further constrained by a high-precision U–Pb zircon date of 83.27 ± 0.11 Ma for a bentonite below it (Wang et al., 2016). Most recently, an age of 82.7 ± 0.6 Ma for the base of Chron C33r was derived by Shen et al. (2022) using magnetostratigraphy, radiometric dating, and averaged sediment accumulation rate in a borehole sequence from NE China. Notably, a superspline age of 82.8 Ma was adopted for the base Campanian by Gradstein and Agterberg (2022).

Integration of macrofossil, microfossil and nannofossil markers with the reference magnetostratigraphy and $\delta^{13}C$ chemostratigraphy available from the GSSP is facilitated by reference to GSSP auxiliary sections at: Seaford Head Sussex, England; Bocieniec near Kraków, Poland; Postalm, Austria; Smoky Hill Kansas, USA; and Tepeyac, Mexico (Gale et al., in press). Palynology data are lacking from most of these sections, although Jarvis and Pearce (in Gale et al., in press figs. 13, 16) presented summary range charts for selected organic-walled dinoflagellate cysts (dinocysts) from Seaford Head and Bocieniec.

In this paper, we present new high-resolution carbon and oxygen stable-isotope data for the upper Santonian and lower Campanian of Seaford Head, together with the first detailed palynological records for the Santonian–Campanian boundary intervals of the Seaford Head and Bocieniec sections. Macrofossil, foraminifera and calcareous nannofossil biostratigraphic markers and carbon isotope events that bracket the stage boundary interval are critically reviewed, and key dinocyst datum levels and palynological assemblage changes are identified and placed within the associated biostratigraphic and chemostratigraphic framework. It is demonstrated that dinocyst biostratigraphy offers robust tie points that can exceed the correlation precision provided by published foraminifera and calcareous nannofossil records.

The holostratigraphy developed, combining biostratigraphy, chemostratigraphy and magnetostratigraphy, provides increased resolution and greater confidence for the definition of the Santonian–Campanian boundary and the global correlation of the boundary succession.

2. Auxiliary GSSPs for the Santonian–Campanian boundary

2.1. Seaford Head, England

The Chalk sea-cliff section at Seaford Head, southern England (Fig. 1) has been proposed as an international reference section for both the Coniacian–Santonian and Santonian–Campanian boundaries (Birkelund et al., 1984; Hancock and Gale, 1996; Lamolda and Hancock, 1996; Hampton et al., 2007). Seaford town is located on the south coast of England between Brighton and Eastbourne, East Sussex (Fig. 1). A 2.5 km long section of Chalk cliffs between Hope Gap (50.7561°N 0.1388°E) and Seaford Head (50.7644°N 0.1087°E) exposes a continuous succession of soft, white nannofossil chalks of latest Turonian to Campanian age, typical of this interval in the Anglo-Paris Basin (Mortimore, 1986; Mortimore and Pomerol, 1987). The complete section is accessible at beach level at low spring tides, but it is strongly tide dependant and subject to rapid erosion and frequent large rock falls; progressive retreat of the Chalk cliffs due to coastal erosion (Hurst et al., 2016; Robinson, 2020) is continually exposing fresh rock and fossils for sampling and analysis. The section forms part of the Beachy Head West Marine Conservation Zone (MCZ), the Seaford to Beachy Head Site of Special Scientific Interest (SSSI), and the Seaford Head Local Nature Reserve (LNR) (Moffat et al., 2020).

An approximately 10° northerly dip on the Seaford Head Anticline and the NW–SE orientation of the cliffs in the western half of the traverse provide a continuous shallow-dipping NW-younging section at beach level. This extends from below the Castrum at 50.7583°N 0.1230°E (Mortimore et al., 2001 fig. 3.96; Mortimore, 2021 fig. 6.2), where the uppermost Turonian Navigation Hardgrounds and Navigation Marls in the Lewes Nodular Chalk are exposed at the cliff base, to the cliff termination in the lower Campanian Culver Chalk at the top of Seaford Head.

2.1.1. Lithostratigraphy and macrofossil biostratigraphy

The whole Chalk succession at Seaford Head is well dated by calcitic macrofossils, principally inoceramid bivalves, crinoids and echinoids (Barrois, 1876; Rowe, 1900; Brydone, 1914; Mortimore, 1986, 2021; Wood and Mortimore, 1988; Mortimore et al., 2001; Gale, 2018, 2019). The lithostratigraphy of the section, based largely on the work of Mortimore (1986), is well established (e.g. Wood and Mortimore, 1988; Jenkyns et al., 1994; Mortimore et al., 2001; Jarvis et al., 2006; Hampton et al., 2007; Thibault et al., 2016; Mortimore, 2021) and includes a large number of regional named marker beds, mostly corresponding to marls, distinctive flint layers, and beds of fossils (Fig. 2), many of which can be correlated throughout southern England and northern France.

The Santonian–Campanian stage boundary lies within the Newhaven Chalk Formation comprising soft to medium indurated, smooth white chalks with numerous marl seams and flint bands (Mortimore, 1986; Bristow et al., 1997). The basal marker is Buckle

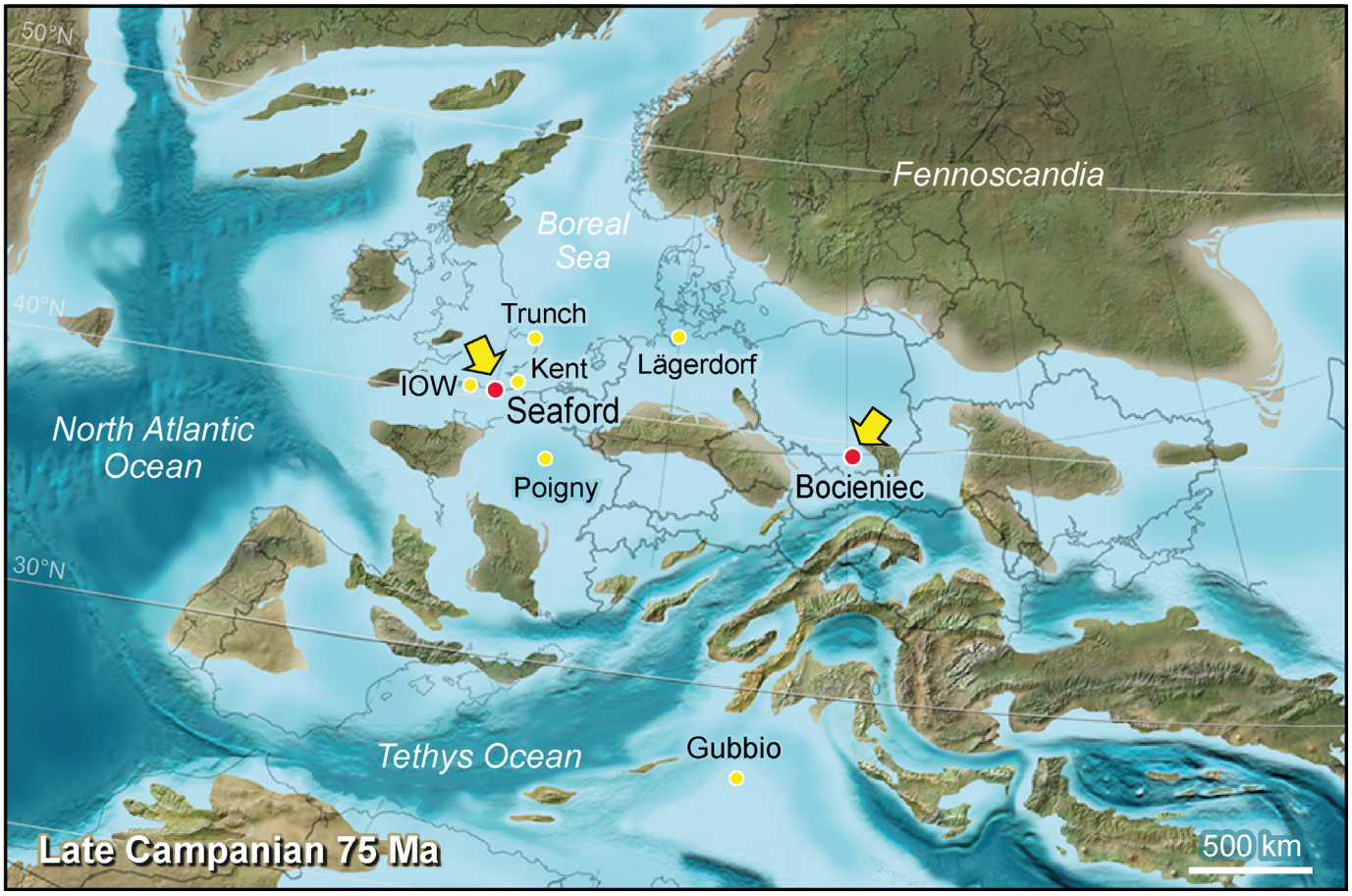

Fig. 1. Campanian palaeogeography of Europe with geographic location of the Seaford Head and Bocieniec GSSP auxiliary sections and main comparative study sites. The GSSP is located at Gubbio, northern Italy. Palaeogeographic map modified from Blakey (2012) with Poland palaeogeography revised after Niechwedowicz et al. (2021). Lines of palaeolatitude (light grey) are shown for reference. IOW, Isle of Wight, Whitecliff.

Marl 1 at Seaford Head, the boundary stratotype and holostratotype section for the Formation (Figs. 2, 3; Mortimore, 1986; Rawson et al., 2001; Hopson, 2005). This represents a change from the Seaford Chalk Formation below, which is largely marl-free and is characterised by soft, relatively featureless, flinty chalks containing several conspicuous semi-tabular flint marker beds. The Newhaven Chalk is subdivided into 5 Bed units, in ascending order, the Splash Point, Old Nore, Peacehaven, Meeching and Bastion Steps Beds, that include more than 30 named marker beds (Figs. 2, 3; Mortimore, 1986).

Echinoderms provide the principal macrofossil zonal and marker taxa for the Santonian–Campanian boundary interval in chalk facies. The lowest occurrence of the crinoid *Uintacrinus socialis* Grinnel, the index species of the *U. socialis* Zone, generally taken to mark the base of the upper Santonian in Europe (Gale et al., 2020), is recorded 20 cm above Buckle Marl 1 at Seaford Head. As summarised in Figs. 2 and 3, the Newhaven Chalk comprises the *Uintacrinus socialis, Marsupites laevigatus, Marsupites testudinarius, Uintacrinus anglicus, Offaster pilula* and the lowest part of the *Gonioteuthis quadrata* macrofossil zones, and microcrinoid zones mid-SaR4–low CaR4 of Gale (2018, 2019).

In this paper we distinguish between first and last appearance datum levels (FAD, LAD), which are interpreted to represent evolutionary first appearance and extinction events, and records of lowest and highest occurrences (LO, HO) of taxa in regional sections. Diachroneity of the latter may occur due to, for example, differences in sampling resolution, ecological and facies controls, provincialism and biotic migration, and preservation effects.

The LO of the crinoid *Marsupites laevigatus* (Forbes) is recorded 1 m above the Hawks Brow Flint and that of *M. testudinarius* (Schlotheim) immediately above the Brighton Marl. The HO and inferred LAD of *M. testudinarius* is recorded in Friar's Bay Marl 1 at Seaford Head (Figs. 2, 3). *Uintacrinus anglicus* Rasmussen occurs through a 1.3 m interval including Friar's Bay Marl 2, with the LO of the small holasteroid echinoid *Offaster pilula* Lamarck recorded 50 cm below the Black Rock Marl.

Offaster pilula occurs principally at three levels at Seaford Head that provide regional biostratigraphic markers (Figs. 2, 3): **Op1** of Gale (2018), an approximately 1 m thick interval with abundant small *O. pilula* (<15 mm in length), 0.5–1.3 m above the Black Rock Marl; **Op2**, a 4 m thick interval yielding small *O. pilula* from beneath the Old Nore Marl to the Peacehaven Marl. This equates to the 'lower *O. pilula* belt' of Brydone (1912, 1914); **Op3**, a 7 m thick section from the level of the Meeching Paired Marls to Telscombe Marl 3. This is the 'upper *O. pilula* belt' of Brydone (1912, 1914). There is an overall increase in size of individuals through Op3; the lower part of the bed contains *O. pilula planata* Brydone and the upper part, between Telscombe Marls 1–3, *O. pilula convexa* Brydone (Brydone, 1939). The upper part, yielding large *O. pilula* (reaching >30 mm in length), has been termed the Planoconvexa Bed (Fig. 3; Brydone, 1939; Ernst, 1972). Telscombe Marl 3 is taken to mark the base of the *G. quadrata* Zone, although belemnites are rare and small *O. pilula* continue to occur uncommonly above (Brydone, 1912; Mortimore, 1986; Smith and Wright, 2003).

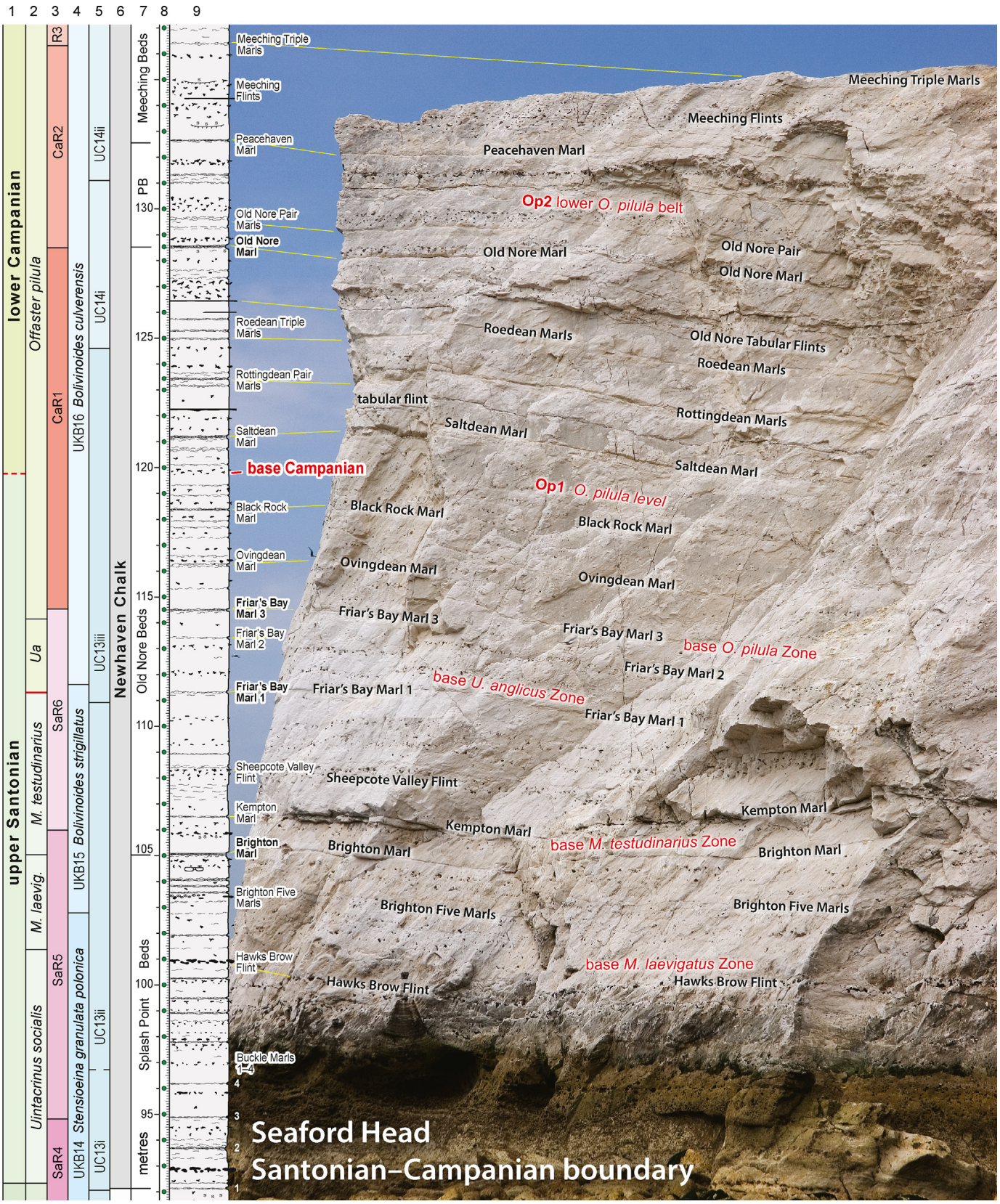

Fig. 2. Field photograph of the Newhaven Chalk Santonian–Campanian boundary succession in the Seaford Head cliff, East Sussex. The section is annotated to show the positions of key lithostratigraphic marker beds and biostratigraphic datum levels. A corresponding lithological log and stratigraphic framework is provided for comparison. Stratigraphy columns: **1**, substage; **2**, macrofossil zone; **3**, microcrinoid zone (Gale, 2018, 2019); **4**, UKB benthic foraminifera zone (after Hart et al., 1989); and **5**, calcareous nannofossil zone (after Fritsen et al., 1999); **6**, formation; **7**, beds; **8**, scale with palynological sample positions (green filled circles); **9**, Lithology. *M. laevig.*, *Marsupites laevigatus*; *Ua*, *Uintacrinus anglicus*; PB, Peacehaven Beds. The base of the upper Santonian is placed at the lowest occurrence of *Uintacrinus socialis* (above Buckle Marl 1). The Santonian–Campanian boundary has

Successive forms of the large holasteroid echinoid *Echinocorys scutata* Leske form a lineage in the Anglo-Paris Basin that evolved from a low variant of *E. scutata* in the *M. coranguinum* Zone and provide useful biostratigraphic markers in the upper Santonian–lower Campanian (Griffith and Brydone, 1911; Brydone, 1912, 1914; Gaster, 1924, 1937; Willcox, 1953). These variants comprise (as summarised in Gale, 2018 fig. 8; Mortimore, 2021 fig. 7.17; Wood and Mortimore, 1988 fig. 18): (1) *E. s. elevata* Brydone, the typical form of the *Marsupites* zones; (2) *E. s. tectiformis* Griffith and Brydone, occurring between Friar's Bay Marl 1 and the Saltdean Marl; (3) *E. s. depressula* Brydone ranging from 70 cm above the Saltdean Marl to the Old Nore Marl; and (4) *E. s. truncata* Brydone, characteristic of chalks between the Old Nore Marl and the Peacehaven Marl. The Peacehaven Marl marks a major change in *Echinocorys* morphology, with the disappearance of the *E. s. elevata–E. s. truncata* lineage. A succession of informally designated morphotypes of *Echinocorys scutata cincta* Brydone followed by *Echinocorys* 'large forms' of Gaster (1924) from above the Meeching Marl Pair, characterise the upper beds of the Newhaven Chalk.

Other useful macrofossil biostratigraphic markers within the Newhaven Chalk include two levels containing the distinctive, highly specialized small holasteroid echinoid genus *Hagenowia* (Gale, 2018): **H1**, *Hagenowia anterior* Ernst and Schulz ssp. B occurs uncommonly in the uppermost *U. anglicus* Zone and the immediately overlying chalk; **H2,** *Hagenowia blackmorei* Wright and Wright occurs in an approximately 1.5 m thick interval immediately above the Meeching Paired Marl, in the lower part of Op2.

A refined biostratigraphy based on roveacrinid microcrinoids extracted from washed chalk residues, has recently been developed by Gale (2018, 2019), with 3 zones (SaR4–SaR6) spanning the upper Santonian to basal Campanian and 3 more (CaR1–CaR3) comprising the lower Campanian *O. pilula* to basal *G. quadrata* zones (Fig. 3). Seaford Head and other East Sussex Chalk localities provide the type sections for all these zones.

Composite moulds of the giant (the World's largest, reaching diameters of >1 m) ammonite *Parapuzosia* spp. are recorded sporadically throughout the stage boundary interval between the Hawks Brow Flint and Peacehaven Marl (Mortimore, 1986, 2021; Ifrim et al., 2021). Records within the upper Santonian are attributed to the typical Santonian species (Kennedy, 2019) *Parapuzosia (Parapuzosia) leptophylla* (Sharpe). Above Friar's Bay Marl 1, giant ammonites newly ascribed to the species *Parapuzosia (Parapuzosia) seppenradensis* (Landois) occur, and are particularly common in the lower Campanian upper Old Nore and Peacehaven Beds (Fig. 3) between the Saltdean Marl and Peacehaven Marl (Ifrim et al., 2021 fig. 3). Scattered records of belemnites, inoceramid bivalves, brachiopods and other macrofossil taxa similarly offer little biostratigraphic resolution.

2.1.2. Micropalaeontology

The microfaunal and nannofloral biostratigraphy of the Seaford Head section have been documented by Hampton et al. (2007) who recorded LO and HO datum levels for key taxa, although detailed range charts were not provided. As summarised in Fig. 3, the Newhaven Chalk comprises UK benthic foraminifera zones high UKB14–low UKB16 of Hart et al. (1989), British Geological Survey benthic foraminifera zones BGS18i to low BGS20i of Wilkinson (2011), and calcareous nannofossil zones UC13i–high UC14ii of Fritsen et al. (1999).

2.1.2.1. Benthic foraminifera. The micropalaeontological zonation of the upper Santonian–lower Campanian Chalk is based principally on evolutionary lineages and species of the benthic foraminifera genera *Bolivinoides* and *Stensioeina*. The base of our study section lies within the upper part of the *Stensioeina granulata polonica* UK benthic foraminifera Zone UKB14 (Hart et al., 1989; Fig. 3) and the top of BGS17iii (Wilkinson, 2011).

The LO of persistent *S. granulata polonica* Witwicka, the basal marker for Zone BGS17, occurs in the Seaford Chalk at Seaford Head coincident with the LO *Cibicides beaumontianus* (d'Orbigny) and the HO of *Stensioena granulata granulata* (Olbertz), just below the Michel Dean Flint and the FAD of the inoceramid bivalve *Cladoceramus undulatoplicatus* (Roemer), the basal Santonian marker (Hampton et al., 2007; Lamolda et al., 2014; Thibault et al., 2016). Very rare *S. granulata polonica* range 6.5 m lower, into the upper Coniacian between the Cuckmere Sponge Bed and the Tarring Neville Flint. Both LO datum levels at Seaford Head are somewhat lower than the BGS17 Zone regional base placement at the Chartham Flint (3 m above the LO of *S. granulata polonica* at Seaford Head) interpreted by Wilkinson (2011, 2013). The HO of the index taxon occurs together with the LO of *Gavelinella stelligera* (Marie) at Whitaker's 3-inch Flint (= Rough Brow Flint), a major middle Coniacian marker bed, and associated elsewhere with the LO of *Cibicides beaumontianus* (d'Orbigny) (Wilkinson, 2011; = base BGS17ii). As noted above, *C. beaumontianus* ranges down at Seaford Head to below the Michel Dean Flint, although a significant increase in abundance was noted in the sponge bed above the Short Brow Flint by Hampton et al. (2007), 22 m higher in the section.

The LOs of *G. cristata cristata* (Goel) and *Stensioeina exsculpta gracilis* Brotzen [together with LO of the calcareous nannofossil marker species *Arkhangelskiella cymbiformis* Vekshina (basal marker for the UC13i Zone of Fritsen et al., 1999)] occur in Buckle Marl 1 at the base of the Newhaven Chalk at Seaford Head (Hampton et al., 2007), and immediately below the LO of *U. socialis*, base marker of the upper Santonian (Fig. 3). The LO of *Gavelinella cristata brotzeni* (Goel) has been recorded approximately 3 m below the top of the Seaford Chalk. The microfauna throughout most of the Newhaven Chalk, between the Buckle Marls and the Telscombe Marls, is characterised by the presence of both *G. cristata cristata* and *G. cristata brotzeni*, the latter occurring very commonly. The LO of *Stensioenia granulata incondita* Koch is seen in Buckle Marl 2.

The base of the BGS18 Zone is defined by the FAD of *G. cristata cristata*, and its incorporated Subzone 18i by the FADs of *G. cristata cristata* and *Gavelinella stelligera* to the FAD of *Stensioeina granulata perfecta* Koch (Wilkinson, 2011, 2013). The first of these datum levels occurs at Buckle Marl 1 at Seaford Head but the second lies 16 m lower, at Whitaker's 3-Inch Flint. The LO of *G. cristata cristata* is used to place the base of BGS18 in Fig. 3, but it is noted that this is higher than the stratigraphic position inferred by Wilkinson (2011, 2013). The bases of the BGS18ii *S. granulata perfecta* Subzone and the BGS18iii *B. strigillatus* Subzone have been interpreted to approximate to the base of the *U. socialis* Zone (Buckle Marl 1) and to immediately below the Hawks Brow Flint, respectively, and the base of BGS18iv to the base of the *U. anglicus* Zone (Wilkinson, 2011, 2013). These subzone boundaries (dashed lines on Fig. 3) cannot be

traditionally been placed at the highest occurrence (HO) of *Marsupites testudinarius* (= base *U. anglicus* Zone). The position of the stage boundary (bold red annotation) is here based on the projected stratigraphic position for the Chron C34n/C33r boundary, derived from biostratigraphic and carbon isotope correlation to the magnetostratigraphically well-characterised Gubbio GSSP section (see text). Palaeomagnetic data obtained directly from Seaford Head (Barchi, 1995; Montgomery et al., 1998) has proven unreliable. See Fig. 3 for additional information sources and stable isotope curves. (For interpretation of the references to colour in this figure legend, the reader is referred to the Web version of this article).

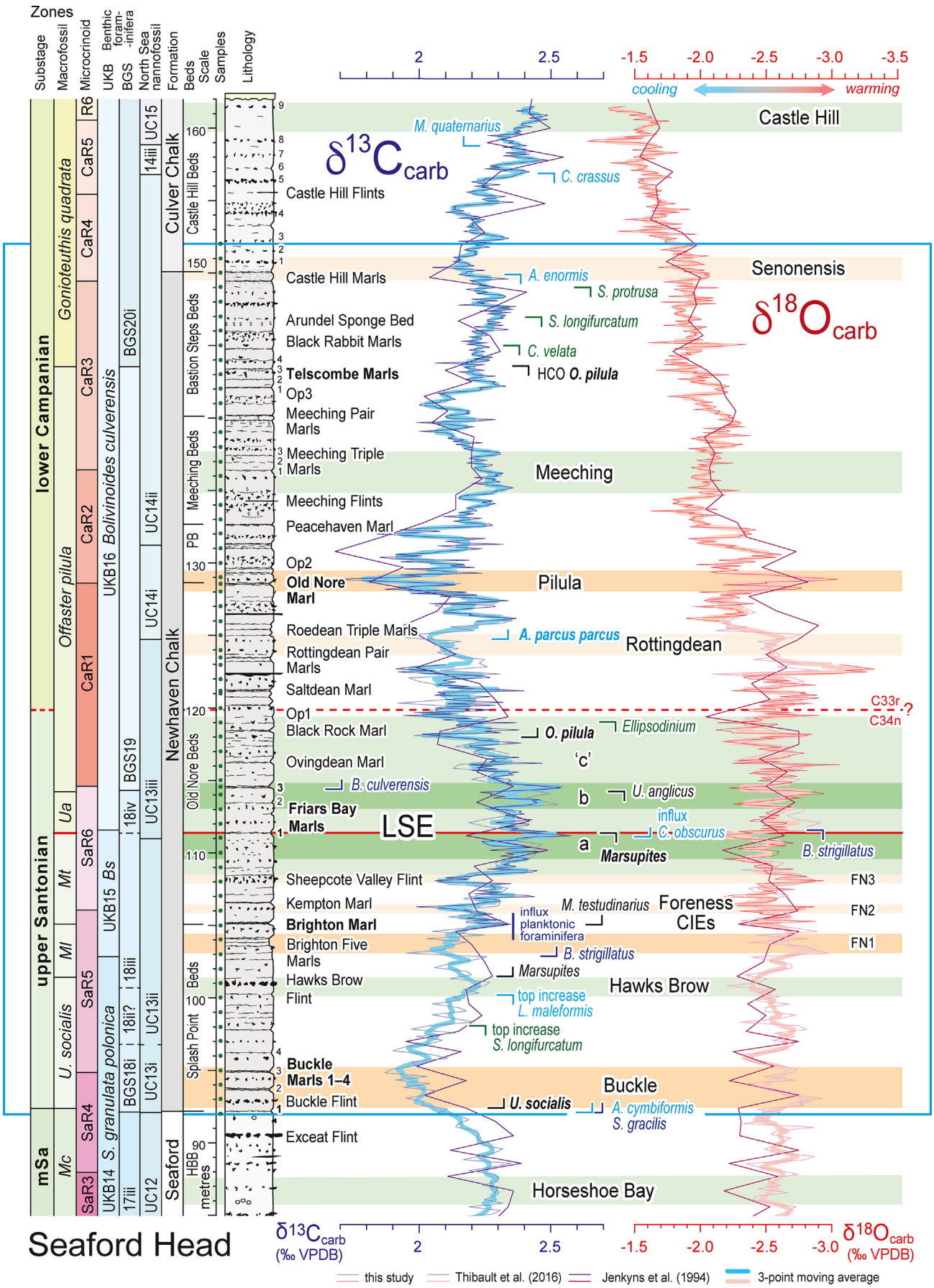
Zones
Substage
Macrofossil
Microcrinoid
UKB Benthic foram-inifera
BGS
North Sea nannofossil
Formation
Beds
Scale
Samples
Lithology
lower Campanian
upper Santonian
mSa
Mc
Gonioteuthis quadrata
Offaster pilula
U. socialis
Ml
Mt
Ua
S. granulata polonica
Bolivinoides culverensis
Bs
SaR3
SaR4
SaR5
SaR6
CaR1
CaR2
CaR3
CaR4
CaR5
R6
UKB14
UKB15
UKB16
17iii
18ii?
18iii
18iv
BGS18i
BGS19
BGS20i
UC12
UC13i
UC13ii
UC13iii
UC14i
UC14ii
14iii
UC15
Seaford
Newhaven Chalk
Culver Chalk
Splash Point Beds
Old Nore Beds
PB
Meeching Beds
Bastion Steps Beds
Castle Hill Beds
HBB
metres
Seaford Head
δ13Ccarb
δ18Ocarb
2
2.5
-1.5
-2.0
-2.5
-3.0
-3.5
cooling
warming
Castle Hill
Senonensis
Meeching
Pilula
Rottingdean
Foreness CIEs
Hawks Brow
Buckle
Horseshoe Bay
LSE
M. quaternarius
C. crassus
Castle Hill Flints
Castle Hill Marls
A. enormis
S. protrusa
Arundel Sponge Bed
S. longifurcatum
Black Rabbit Marls
C. velata
Telscombe Marls
HCO O. pilula
Op3
Meeching Pair Marls
Meeching Triple Marls
Meeching Flints
Peacehaven Marl
Op2
Old Nore Marl
Roedean Triple Marls
A. parcus parcus
Rottingdean Pair Marls
Saltdean Marl
C33r
C34n
?
Op1
Black Rock Marl
O. pilula
Ellipsodinium
Ovingdean Marl
'c'
B. culverensis
b
U. anglicus
Friars Bay Marls
influx C. obscurus
a
Marsupites
B. strigillatus
Sheepcote Valley Flint
FN3
Kempton Marl
M. testudinarius
FN2
Brighton Marl
influx planktonic foraminifera
Brighton Five
FN1
Marls
B. strigillatus
Hawks Brow Flint
Marsupites
top increase L. maleformis
top increase S. longifurcatum
Buckle Marls 1–4
Buckle Flint
U. socialis
A. cymbiformis
S. gracilis
Exceat Flint
δ13Ccarb (‰ VPDB)
δ18Ocarb (‰ VPDB)
this study
Thibault et al. (2016)
Jenkyns et al. (1994)
3-point moving average

placed precisely at Seaford Head using available foraminiferal records (Hampton et al., 2007).

The top of the UKB14 *Stensioeina granulata polonica* Zone is defined by the FAD of *Bolivinoides strigillatus* (Chapman) in the mid-upper Santonian (Hart et al., 1989). *Bolivinoides strigillatus*, the index taxon of UKB15, a total range zone (Hart et al., 1989), ranges from the base of the Brighton Five Marls, coincident with the highest common occurrence (HCO) of *S. exsculpta exsculpta* (Reuss), to immediately above Friar's Bay Marl 1 and the HO of *M. testudinarius* (Figs. 2, 3). However, *Stensioenia exsculpta exsculpta* continues to be recorded in low numbers through the lower part of the lower Campanian. The *B. strigillatus* Zone is characterized by a reduction in the numbers of *Eponides concinna* Brotzen compared with the underlying section, and moderately high numbers of *S. granulata perfecta* Koch. The LO of *Bolivinoides strigillatus* has been considered previously as a potential proxy for the Santonian–Campanian boundary (Birkelund et al., 1984), but this is discounted because it has been recorded from the base of the *U. socialis* Zone in northern Germany (Koch, 1977).

UKB16, the *Bolivinoides culverensis* Zone, extends from the HO of *B. strigillatus* above Friar's Bay Marl 1 to the HO of *B. culverensis* Barr; the latter species is consistently common up to approximately 14 m below the top of the section, 2 m below Castle Hill Marl 1 (Fig. 3). The evolutionary change from *B. strigillatus* to *B. culverensis* (Barr, 1966, 1967) that occurs between Friar's Bay Marls 1 and 3 provides an important marker event (Hampton et al., 2007) spanning the *U. anglicus* Zone. The base of BGS18iv is assumed to approximate to the base of the *U. anglicus* Zone; the FAD of *B. culverensis* defines the base of BGS19 (Wilkinson, 2011, 2013), coincident with the top of the *U. anglicus* Zone (Fig. 3).

Gavelinella usakensis (Vasilenko) one of the two index species for UKB17, the concurrent range zone of *Gavelinella monterelensis* (Marie) and *G. usakensis*, has a LO below Black Rabbit Marl 2 in the *G. quadrata* Zone at Seaford Head (Fig. 3), but *G. monterelensis*, a typical upper Campanian *Belemnitella mucronata* Zone species (Hart et al., 1989), does not occur in the section. The LO of *G. usakensis* marks the base of Zone BGS20i (Fig. 3; Wilkinson, 2011, 2013). There is a significant change in the benthic microfauna between the Black Rock Marl and the Saltdean Marl, interval of the Op1 *O. pilula* event and the inferred position of the stage boundary (Fig. 3), marked primarily by changes in the genus *Stensioeina* (Hampton et al., 2007). At this level the last occurrences of both *S. granulata perfecta* and *S. exsculpta exsculpta* are recorded, the latter coincident with the first occurrence of very early forms of *Stensioeina pommerana*, *S. "praepommerana"* of Hampton et al. (2007); there is also a major increase in the abundance of *S. granulata incondita*.

The LO of true *Stensioeina pommerana* Brotzen occurs between the Rottingdean Pair Marls (Fig. 3). The section between the Roedean Triple Marls and the Peacehaven Marl is characterised by rare to common *S. exsculpta gracilis* Brotzen. The lowest record of *S. exsculpta gracilis* at Roedean Triple Marl 3 was considered by Hampton et al. (2007) to be a transitional form between *S. exsculpta exsculpta* and *S. exsculpta gracilis*. *Gavelinella pseudoexcolata* Kalinin is recorded for the first time from the level of the Telscombe Marls. The HOs of *S. exsculpta gracilis* and common *B. culverensis* occur 1.5 m below the Castle Hill Marls at the top of the Newhaven Chalk. The HO of *S. granulata incondita* lies 2 m higher, between Castle Hill Flints 2 and 4, in the basal Culver Chalk.

2.1.2.2. Planktonic foraminifera. Planktonic foraminifera occur throughout the Seaford Head section, but in insufficient numbers and with too low a diversity to be employed for detailed biostratigraphy (Hampton et al., 2007). The majority of Tethyan species that are widely used for zonation and global correlation (cf. Coccioni and Premoli Silva, 2015) are absent. However, the base of the *Bolivinoides strigillatus* Zone UKB15 (at the level of the Brighton Five and Brighton marls, Fig. 3) is marked by a major influx of planktonic foraminifera, particularly double-keeled taxa such as *Globotruncana linneiana* (d'Orbigny) and *G. bulloides* Vogler, both typical northern European Santonian taxa (cf. Peryt et al., 2022). This "flooding" event is coincident with the highest occurrence of *Globigerinelloides rowei* (Barr) (Hampton et al., 2007), a taxon proposed by Bailey et al. (1983, 1984) as a potential marker for the top of the Santonian Stage (see also Hart et al., 1989), but situated here at the top of the mid-upper Santonian *M. laevigatus* Zone.

2.1.2.3. Calcareous nannofossils. Calcareous nannofossils are used widely for the zonation and correlation of NW European chalks (e.g. Burnett et al., 1998; Burnett and Whitham, 1999; Fritsen et al., 1999; Surlyk et al., 2013; Eldrett et al., 2021). The Boreal nannofossil zonation of Burnett et al. (1998) has been widely adopted, but the stratigraphic positions of some zonal boundaries have been subject to significant revision (see below). The zonal markers cited by Burnett et al. (1998) have proven to be robust and reliable, but the subzonal markers less so; the subzonation developed by Hampton and Gallagher (in Fritsen et al., 1999) for the Chalk of the North Sea Basin offers an alternative scheme that is used herein.

At Seaford Head, the HO of *Lithastrinus septenarius* Forchheimmer in the middle Santonian, 2.6 m below Whitaker's 3-inch Flint, defines the top of Zone UC11 of Burnett et al. (1998) and places the sediments above in Zone UC12. The LO of *Arkhangelskiella cymbiformis* Vekshina defining the base of Zone UC13 (Burnett et al., 1998) and Subzone UC13i of Fritsen et al. (1999) occurs at Buckle Marl 1 (Fig. 3), the base of the Newhaven Chalk and top of the *M. coranguinum* Zone at Seaford Head (Hampton et al., 2007). The LO of *Cylindralithus crassus* Stover, the basal marker for Subzone UC13ii (Fritsen et al., 1999) lies in the mid-*U. socialis* Zone above Buckle Marl 4, and an influx of *Calculites obscurus* (Deflandre) Prins and Sissingh, the basal marker of Subzone 13iii, occurs immediately below Friar's Bay Marl 1 (Fig. 3).

It is notable that the placement of calcareous nannofossil zones UC12 and UC13 at Seaford Head differs substantially from the general interpretation of Burnett et al. (1998) for northern Europe, who placed the base of UC12 (HO of *L. septenarius*) at the top of the *M. coranguinum* Zone and the base of UC13 (LO of *A. cymbiformis*)

Fig. 3. Stratigraphy and $\delta^{13}C_{carb}$ and $\delta^{18}O_{carb}$ stable isotope profiles of the Santonian–Campanian boundary interval, Seaford Head. Blue box indicates the interval of the palynological study. Lithostratigraphy and marker bed names after Mortimore (1986, 2021); Op1–3 events of Gale (2018). mSa, middle Santonian; *Mc*, *Micraster coranguinum*; *Ml*, *Marsupites laevigatus*; *Mt*, *Marsupites testudinarius*; *Ua*, *Uintacrinus anglicus*; *Bs*, *Bolivinoides strigillatus*; HBB, Haven Brow Beds; PB, Peacehaven Beds. Microcrinoid zones after Gale (2018, 2019). UKB benthic foraminifera zones of Hart et al. (1989); BGS zones after Wilkinson (2011, 2013). North Sea nannofossil zonation after Fritsen et al. (1999). Systematic offsets between the carbon isotope profiles of different authors are corrected by subtracting 0.15‰ and 0.1‰ $\delta^{13}C_{carb}$ from the data sets of Jenkyns et al. (1994) and Thibault et al. (2016), respectively. The smoothed 3-point moving average $\delta^{13}C_{carb}$ curve is based on a concatenation of our data and the offset-corrected values of Thibault et al. (2016). The companion $\delta^{18}O_{carb}$ curves required no offset correction of the Thibault et al. (2016) data. Note that the $\delta^{18}O_{carb}$ scale has been reversed (values decrease to the right) to emphasise cooling vs. warming trends. Key biostratigraphic marker levels derived from the lowest (LO) and highest (HO) occurrences of macrofossils (black), foraminifera (dark blue), calcareous nannofossils (pale blue) and dinocysts (green) are indicated, together with the correlated position of the C34n/C33r boundary (red dashed line), the base Campanian primary marker (Gale et al., in press). Carbon isotope events (CIEs) after Jarvis et al. (2006), Thibault et al. (2016) and this study; green horizontal bars indicate the extent of positive CIEs, pink bars are negative CIEs. The prominent $\delta^{13}C_{carb}$ maximum with double peaks (a, b) at the level of the Friars Bay Marls is referred to the Late Santonian CIE (LSE, formerly termed the Santonian–Campanian Boundary Event, SCBE) to reflect its position below the stage boundary. Placement of peak 'c' follows Gale et al. (in press). (For interpretation of the references to colour in this figure legend, the reader is referred to the Web version of this article).

within the lowest *O. pilula* Zone. *Arkhangelskiella cymbiformis* ranges down into the *M. coranguinum* Zone in NE England (Burnett and Whitham, 1999); it provides a potential proxy for the Santonian and not the lower Campanian *O. pilula* Zone as indicated by Burnett et al. (1998).

The base of Zone UC14 and Subzone UC14i, defined by the LO of *Aspidolithus parcus parcus* (Stradner) Noël, occurs immediately below Roedean Triple Marl 1 and 4 m below the Old Nore Marl in the mid-*O. pilula* Zone (Fig. 3). The LO *Reinhardtites levis* Prins and Sissingh (base Subzone 14ii) has been recorded 2.5 m above the Old Nore Marl at the summit of the Op2 'lower *O. pilula* belt' (Hampton et al., 2007). There are, however, some concerns about the general reliability of this nannofossil bioevent. There is a continuous evolutionary trend between the parent species *Reinhardtites anthophorus* and *R. levis*, with a progressive reduction of the central area openings. Moreover, syntaxial recrystallization of the inner cycle of *R. anthophorus* can easily occur to such an extent as to make it look like *R. levis*.

The HO of *Aspidolithus enormis* (Shumenko), another regional marker (Burnett et al., 1998 fig. 6.5), lies between the two Castle Hill Marls, towards the base of the *G. quadrata* Zone. The HO of *Cylindralithus crassus* Stover, taken by Hampton et al. (2007) to mark the base of Subzone 14iii (cf. Fritsen et al., 1999), lies in the lower *G. quadrata* Zone, above Castle Hill Flint 5. Thibault et al. (2016) argued that the LO of *Monomarginatus quaternarius* Wind and Wise below Castle Hill Flint 8 (Fig. 3) should be used as the base marker for Zone UC15 in the Boreal Realm.

2.1.3. Palynology

Prince (1997) studied 140 samples taken at approximately 1 m intervals upwards from Belle Tout Marl 3 (middle Coniacian) to the section top at Seaford Head, processing 80 g of each using the method of Batten and Morrison (1983). The resulting preparations proved to be nearly barren of palynomorphs and were not counted. Subsequent analysis of an equivalent Chalk section at Whitecliff, Isle of Wight, using a new processing method, offered good recovery of palynomorphs (Prince, 1997; Prince et al., 1999). The good recovery from Seaford Head achieved in the present study demonstrates that the method of Batten and Morrison (1983) is unsuitable for these sediments.

2.1.4. Carbon isotope stratigraphy

Carbon isotope stratigraphy has proven to be a valuable tool for the dating and correlation of Cretaceous sections since the seminal work of Scholle and Arthur (1980) that included key Santonian–Campanian bulk carbonate carbon-isotope ($\delta^{13}C_{carb}$) profiles from the Chalk of the Isle of Wight and the Norfolk Trunch borehole. Data from English, German and Danish chalks, including Santonian data from Seaford Head (Thibault et al., 2016), were used by Cramer and Jarvis (2020) to construct their global Upper Cretaceous carbon isotope reference curve.

Jenkyns et al. (1994) published the first bulk oxygen and carbon stable-isotope data together with a measured section for the middle Santonian to lower Campanian of Seaford Head. Jarvis et al. (2006) provided a new summary log for the middle Coniacian–lower Campanian with an interpretation of the carbon isotope stratigraphy, incorporating the Santonian–Campanian data of Jenkyns et al. (1994) and showing the correlation of a succession of named Carbon Isotope Events (CIEs). This log was presented at 1:100 scale by Thibault et al. (2016 appendix 1) who published new detailed carbon and oxygen stable isotope curves for the middle Coniacian–lower Campanian based on 25 cm interval sampling of a 91 m thick section.

The $\delta^{13}C_{carb}$ profile for the Santonian–Campanian stage boundary interval shows a falling trend through the uppermost middle Santonian towards a broad minimum spanning a 2 m thick interval between the Buckle Flint and Buckle Marl 3, at the base of the *U. socialis* Zone (Fig. 3). This 0.2‰ negative excursion, termed the Buckle CIE by Jarvis et al. (2006), constitutes the minimum of a long-term trough falling to 1.9‰ $\delta^{13}C_{carb}$ at the base of the upper Santonian from a maximum of 2.3‰ at the summit of the middle Santonian (note: $\delta^{13}C_{carb}$ values reported here have been recalibrated relative to our new data set – see Section 3.1). The long-term $\delta^{13}C_{carb}$ trend above the Buckle CIE shows rising values through the Santonian that reach a broad maximum with two peaks and values of 2.5–2.6‰ that span the top *M. testudinarius* to basal *O. pilula* zones – the Santonian–Campanian Boundary Event (SCBE) of Jarvis et al. (2006), now renamed the Late Santonian Event (LSE, Fig. 3) to reflect the higher position of the newly ratified stage boundary.

Superimposed on the generally rising $\delta^{13}C_{carb}$ trend though the Santonian is a small peak in 1 m of sediment centred on the Hawks Brow Flint – the Hawks Brow CIE at the top of the *U. socialis* Zone, and a short trough spanning the 1 m of the Brighton Five Marls in the mid-*M. laevigatus* Zone – the Foreness CIE sensu Thibault et al. (2016 fig. 2). The Buckle CIE and LSE provide robust datum levels for correlation between the North Sea, English, French, German and Polish Chalk (e.g. Thibault et al., 2016; Deville de Periere et al., 2019; Eldrett et al., 2021; Pearce et al., 2022), with the double peak of the LSE well-expressed at Seaford Head.

Carbon isotope values fall through the top Santonian and lower Campanian towards a minimum of 1.8‰ $\delta^{13}C_{carb}$ at the level of the Old Nore to Peacehaven marls at Seaford Head, in the middle of the *O. pilula* Zone (Fig. 3) – the "pillula Zone event" of Thibault et al. (2016). Only the low-resolution $\delta^{13}C_{carb}$ data of Jenkyns et al. (1994) have previously been available for the remainder of the section at Seaford Head (Fig. 3). These display a long-term rising trend towards a maximum at the section top of 2.4‰ $\delta^{13}C_{carb}$, with a minor negative excursion at the Telscombe Marls tentatively assigned to the "senonensis Zone event", and the top of the succession above Castle Hill Marl 7 identified with the "papillosa Zone event" by Thibault et al. (2016). This correlation is revised here in the light of our new stable isotope and palynological results (Section 7.5).

2.1.5. Magnetostratigraphy

A magnetostratigraphic study of the Seaford Head section by Montgomery et al. (1998) placed the base of Chron C33r in the mid-*U. socialis* Zone. This has been shown to be unreliable (Hampton et al., 2007; Thibault et al., 2016) due to the very weak palaeomagnetic signal. A higher position for the reversal, in the mid-*O. pilula* Zone below the Old Nore Marl, has been advocated by Mortimore (e.g. Mortimore, 2021 figs. 7.4, 7.17; Mortimore et al., 2001) based on the unpublished thesis study of Barchi (1995). However, this placement is not underpinned by any magnetic polarity data from Seaford Head, which yielded very weak natural remanent magnetization, but by a poorly constrained correlation to Précy-Boran in the Paris Basin and Lägerdorf, Germany, with untested magnetostratigraphic interpretations for these sections (Barchi, 1995 fig. 73). The stratigraphic position of the C34n/C33r polarity reversal at Seaford requires reassessment.

2.1.6. A Campanian GSSP auxiliary section

The Seaford Head section had been proposed as a candidate GSSP for the Campanian Stage (Birkelund et al., 1984; Gale et al., 1995; Hancock and Gale, 1996) but this was subsequently rejected due to a paucity of stratigraphically significant ammonites and planktonic foraminifera and the poor magnetostratigraphic record that, together, limit its potential for global correlation (Hampton et al., 2007). Nonetheless, the section remains an important permanent and accessible protected reference section for Chalk stratigraphy and has been designated as a Campanian GSSP auxiliary

section (Gale et al., in press) to constitute a stratigraphic standard for the Santonian to lower Campanian Chalk of NW Europe.

2.2. Bocieniec, Poland

Bocieniec near Kraków in southern Poland was proposed by Dubicka et al. (2017) as a Campanian GSSP candidate section. The abandoned Bocieniec quarry in the village of Laski Dworskie, 25 km north of Kraków (Fig. 1; 50.2726°N 19.9336°E), exposes 5.4 m of Santonian–Campanian sediments overlying 5–10 cm of Cenomanian–Turonian? conglomerate resting unconformably on Jurassic limestones (Rutkowski, 1965; Dubicka et al., 2017). The Santonian–Campanian succession is thin, but provides important data on biostratigraphy (crinoids, planktonic and benthic foraminifera, calcareous nannofossils), magnetostratigraphy, and a detailed carbon isotope curve.

2.2.1. Lithostratigraphy and macrofossil biostratigraphy

The Santonian–Campanian succession at Bocieniec (Fig. 4; Dubicka et al., 2017) comprises a thin basal glauconitic marl, overlain by 4.8 m of monotonous grey marls, capped by 0.6 m of opoka (a carbonate-siliceous rock containing opal-CT that forms a siliceous rock framework with an insignificant amount of detrital quartz and clays; Jurkowska, 2022) with cherts (siliceous nodules composed of >50% opal-CT; Jurkowska and Świerczewska-Gładysz, 2020). New fossil collecting by Gale (in Gale et al., in press) indicates that the LO of *U. socialis* occurs towards the bottom of the section, and the cirripede *Eoverruca hewitti* Withers (see Gale, 2015) is abundant up to about 0.5 m above the base (A.S. Gale pers. comm., 2021). This species typically occurs some way above the base of the *U. socialis* Zone in England (Kent, Suffolk, Sussex) and France (Dieppe, Sens) (A.S. Gale pers. comm., 2021). However, *E. hewitti* has been recorded from the upper lower Campanian in southern Poland in glauconitic sediments just above a hardground (Jagt et al., 2008). This younger occurrence has a comparable lithological association to that seen at Bocieniec and indicates that the species is likely in-part facies controlled and not restricted to one narrow stratigraphic interval.

Uintacrinus socialis ranges up to 2.2 m in the section with the LO and HO of *Marsupites laevigatus* observed at around 2.4 m and 3.2 m, respectively (Fig. 4; Gale et al., in press). The LO of *M. testudinarius* lies a short distance above the HO of *M. laevigatus* and ranges up to 4.2 m (higher in the section than the 3.48 m recorded by Dubicka et al., 2017). *Uintacrinus anglicus* has not been observed, suggesting a possible unrecorded hiatus within the marls representing the basal Campanian. However, despite the presence of *Uintacrinus socialis* and *Marsupites* spp., it is notable that microcrinoids have not been recovered from the succession (A.S. Gale pers. comm., 2021), so the absence of *U. anglicus* at the top of the marls and from the lithological transition to opoka (Jurkowska, 2022) may be a product of the facies change towards an environment unfavourable for these crinoids. Other key macrofossil records are a specimen of *Gonioteuthis granulataquadrata* (Stolley) from around 4.9 m and records of *Offaster pilula* between 4.98 and 5.28 m (Dubicka et al., 2017), both taxa being recovered from the opoka facies at the section top (Fig. 4).

2.2.2. Micropalaeontology

2.2.2.1. Benthic foraminifera. The Bocieniec section has yielded abundant and well-preserved stratigraphically important benthic foraminifera of the genera *Bolivinoides*, *Gavelinella* and *Stensioeina* (Dubicka et al., 2017). *Stensioeina gracilis*, *Gavelinella pertusa*, and *G.* ex gr. *stelligera* occur throughout almost the whole section from the base of the Bocieniec marls. This places the lowest marls within the middle–upper Santonian *Stensioeina gracilis* Zone of Dubicka (in Walaszczyk et al., 2016).

A succession of stratigraphically significant LOs have been recorded though the section (Dubicka et al., 2017) and provide the basis for applying the benthic foraminifera zonation of Dubicka (in Walaszczyk et al., 2016) to the succession. In stratigraphic order these are: the LO of *Gavelinella costulata* (Marie) at 0.88 m; the LO of *Stensioeina perfecta* Koch transitional to *Stensioeina pommerana* Brotzen (1.28 m), and the LO of *Bolivinoides strigillatus* at 1.68 m which marks the base of the *B. strigillatus* Zone (Fig. 4). The LO of true *S. pommerana* at 2.58 m marks the base of its eponymous zone. The LO of *B. culverensis* is recorded at 3.58 m (base *B. culverensis* Zone), and the LO of *G.* ex gr. *clementiana* (d'Orbigny) lies at 4.38 m (base *G. clementiana* Zone).

These bioevents are generally considered to be stratigraphically important markers of the Santonian–Campanian boundary interval in most areas of the European epicontinental Upper Cretaceous (e.g. Gale et al., in press; Vasilenko, 1961; Koch, 1977; Monciardini et al., 1980; Hart et al., 1989; Schönfeld, 1990; Wilkinson, 2011; Walaszczyk et al., 2016; Guzhikov et al., 2021).

2.2.2.2. Planktonic foraminifera. Planktonic foraminifera are common and relatively diverse through the entire Bocieniec section (Dubicka et al., 2017). They are represented by the main morphological groups, including biserial heterohelicids, planispiral *Globigerinelloides*, low-trochospiral hedbergellids, high-trochospiral globular chambered morphotypes, as well as double-keeled globotruncanids, marginotruncanids, dicarinellids and contusotruncanids. Unkeeled taxa have a continuous record through the Santonian–Campanian part of the section but the occurrence of keeled taxa is more variable.

Marginotruncanids together with *Globotruncana*, comprise the most abundant groups of keeled foraminifera at the base of the marls (Dubicka et al., 2017). The former become much rarer upwards and are more discontinuously recorded in samples. Coincident with the decline in marginotruncanids, globotruncanids start to increase in abundance and become the most common foraminifera among deep-dwelling forms. Dicarinellids are very rare at Bocieniec. The HO of the key biostratigraphic marker species *Dicarinella asymetrica* has been recorded at 4.38 m (Fig. 4). However, the level of this bioevent is poorly constrained, relying on only 3 discontinuous occurrences of the taxon. The base of the Campanian at Bocieniec is taken at 4.45 m where Dubicka et al. (2017) placed the base of Chron C33r, within the lower part of the *Gavelinella clementiana* benthic foraminifera Zone of Dubicka (in Walaszczyk et al., 2016).

2.2.2.3. Calcareous nannofossils. The calcareous nannoflora of the Bocieniec section shows a moderate preservation. The following sequence of events across the boundary, from bottom to the top of the section (Fig. 4), was documented by Dubicka et al. (2017): the presence of *Lithastrinus septenarius* Forchheimer at 0.58 m; a top increase of *Calculites obscurus* (Deflandre) Prins and Sissingh at 1.28 m, marking a change from an interval of frequent abundance to rare abundance upwards; the top increase of *Lucianorhabdus maleformis* Reinhardt at 1.68 m, marking a change from an interval of frequent abundance to absent or rare abundance upwards; the HO of *Hexalithus gardetiae* Bukry and the LO of small *Orastrum campanensis* (Cepek) at 2.08 m; the base of a second increase in *C. obscurus* marked by a change from rare to frequent abundances at 2.78 m; the LO of *Lapideacassis cornuta* (Forchheimer and Stradner) at 3.38 m; rare occurrences of *Watznaueria britannica* (Stradner) noted solely at 3.98 m, along with the LO of large *Orastrum campanensis*; the LO of *Reinhardtites levis* Prins and Sissingh in Sissingh and the HO of small *R. anthophorus* (Deflandre) at 4.38 m; the HO of *Zeugrhabdotus biperforatus* (Gartner) at the top of the marls at 4.78 m; the LO of *Aspidolithus parcus parcus* at 5.18 m.

The presence of *A. cymbiformis* at the base of the section indicates sediments that are not older than Zone UC13 of Fritsen et al. (1999). This is consistent with the late Santonian age indicated by

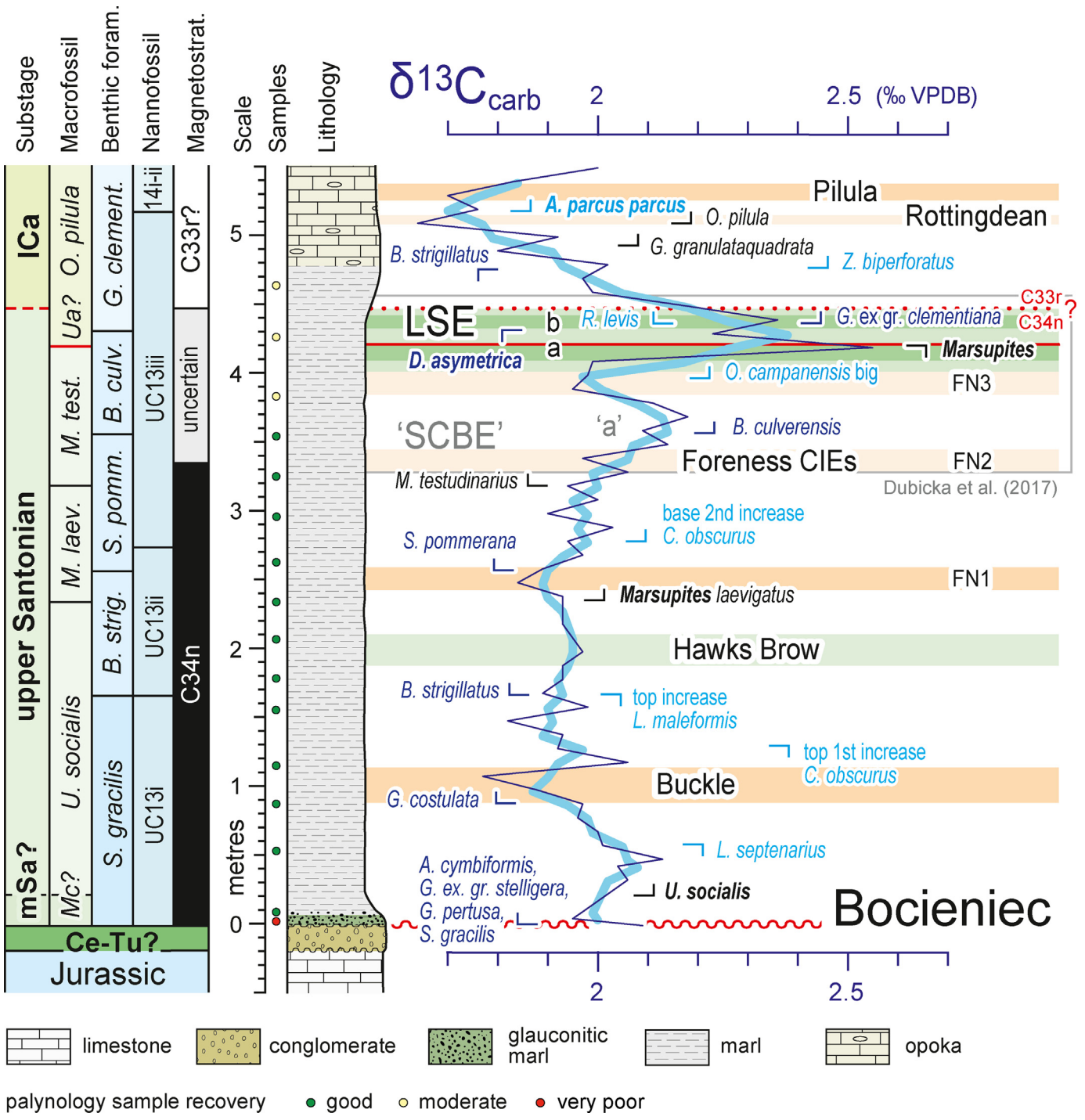

Fig. 4. Stratigraphy and $\delta^{13}C_{carb}$ stable isotope profile of the Santonian–Campanian boundary interval, Bocieniec. Stratigraphy after Dubicka et al. (2017) with amended macrofossil ranges from Gale et al. (in press) and reinterpreted substages and macrofossil zones (this paper). Carbon isotope stratigraphy is derived from this paper (see text). Key fossil datum levels (black, macrofossils; dark blue, foraminifera; pale blue, calcareous nannofossils) are shown. The extent of the LSE as interpreted by Dubicka et al. (2017; = SCBE of those authors) is indicated by the grey box, with their peak a (grey) corresponding to the positive $\delta^{13}C_{carb}$ excursion in the lower part of the magnetostratigraphically uncertain interval. New crinoid records from the section (Gale et al., in press) indicate that the LSE is restricted to the large double peak towards the top of the section (see text for discussion). MSa, middle Santonian; lCa, lower Campanian; *Mc*, *Micraster coranguinum*; *M. laev.*, *Micraster laevigatus*; *M. test.*, *Marsupites testudinarius*; *Ua*, *Uintacrinus anglicus*, *B. strig*, *Bolivinoides strigillatus*; *S. pomm.*, *Stensioeina pommerana*; *B. culv.*, *Bolivinoides culverensis*; *G. clement.*, *Gavelinella clementiana*. (For interpretation of the references to colour in this figure legend, the reader is referred to the Web version of this article).

the macrofossils, and not earliest Campanian as interpreted by Burnett et al. (1998; see Section 2.2.2.3, above). The primary marker *Cylindralithus crassus* used to define the base of UC13ii and top of UC14ii in the North Sea (Fritsen et al., 1999) and recognised at Seaford Head (Hampton et al., 2007) is absent at Bocieniec. However, the top increase of *Lucianorhabdus maleformis* at 1.68 m was used by Dubicka et al. (2017) to define the base of UC13ii (Fig. 4) by comparison to the Seaford Head section where this event occurs within the lower part of UC13ii (Hampton et al., 2007), below the Hawks Brow Flint (Fig. 3). The base of a second significant increase in *Calculites obscurus* at 2.78 m was interpreted by Dubicka et al. (2017) as the equivalent of the base of common *C. obscurus* below

Friar's Bay Marl 1 at Seaford Head which marks the base of Subzone UC13iii (Hampton et al., 2007). The FO of *Aspidolithus parcus parcus* in opoka at 5.18 m marks the base of Zone UC14 (Fig. 4). Subzones UC14i and UC14ii cannot be distinguished at Bocieniec as the LO of *Reinhardtites levis*, marker event for the base of UC14ii, has been recorded below the LO of *A. parcus parcus*. However, as noted above (Section 2.1.2.3), the identification of *R. levis* can be problematic and may have been compromised by the moderate preservation of nannofossils in the section.

2.2.3. Palynology

To our knowledge, no palynological study of the Bocieniec section has been undertaken prior to the current work.

2.2.4. Carbon isotope stratigraphy

The carbon isotope curve for Bocieniec (Fig. 4) shows a long-term falling trend upwards from the base towards a minimum and small negative $\delta^{13}C_{carb}$ excursion with a minimum value of 1.84‰ in the lower *Marsupites laevigatus* Zone. This was interpreted to represent the Foreness Event by Dubicka et al. (2017).

A well-developed 0.5‰ $\delta^{13}C_{carb}$ peak spanning the interval 4.18–4.48 m, with a maximum value of 2.55‰ coincident with the HO *M. testudinarius*, occurs at the top of the marls. Based on a lower recorded HO of *M. testudinarius* at 3.48 m, this was interpreted by Dubicka et al. (2017) to be the higher of the twin peaks (peak b) that typically characterise the LSE (their SCBE), as observed at Seaford Head (Figs. 3, 4; Jarvis et al., 2006; Thibault et al., 2016); the smaller peak between 3.48 and 3.78 m on the rising trend below was considered to represent peak a (grey annotation in Fig. 4). However, a revised position for the HO of *M. testudinarius* derived from subsequent collecting by Gale (in Gale et al., in press), which places the HO at the base of the upper main peak (Fig. 4), suggests that this represents the lower of the LSE pair (i.e. peak a). Since *U. anglicus* is absent, a minor hiatus has been postulated at ca. 4.4 m on which the upper part of the LSE (peak b) and the *U. anglicus* Zone are missing (Gale et al., in press).

A marked minimum of 1.64–1.70‰ $\delta^{13}C_{carb}$ in opoka facies between 5.08 and 5.28 m has been interpreted (Dubicka et al., 2017) to represent the "pillula Zone Event" of Thibault et al. (2016).

2.2.5. Magnetostratigraphy

The magnetostratigraphy at Bocieniec demonstrates that C34n extends up into the range of *M. testudinarius*, and that the highest metre of the section is reversed, with an intervening 1.1 m thick zone of uncertain polarity (Fig. 4; Gale et al., in press; Dubicka et al., 2017). Significantly, the HO of *Dicarinella asymetrica* lies 30 cm above the HO of *Marsupites testudinarius*, towards the top of the interval of uncertain polarity (Fig. 4). The LO of the calcareous nannofossil *A. parcus parcus* occurs at 5.18 m in opoka facies, in the lower part of Chron C33r.

2.2.6. A Campanian GSSP auxiliary section

The most important feature of the Bocieniec section is that it yields key Chalk macrofossil and benthic foraminifera index species constrained by a carbon isotope curve, together with a magnetostratigraphy and records of the key Santonian–Campanian boundary planktonic foraminifera and calcareous nannofossil markers *D. asymetrica* and *A. parcus parcus*. This provides a basis for correlation between Boreal Chalk successions and Tethyan carbonates, exemplified by the Gubbio GSSP (Gale et al., in press).

3. Material and methods

The uppermost Turonian–lower Campanian section exposed between Hope Gap and Seaford Head was logged by IJ in June 1993 and June–August 2018. Our log shows good general agreement with those of Gale (in Jenkyns et al., 1994), Mortimore (1986, 2021 fig 6.11) and Mortimore et al. (2001 figs 3.97–3.102). The 91 m section between Belle Tout Marl 3 (middle Coniacian) and the Old Nore Marl (lower Campanian), logged in 1993, was presented at 1 cm: 1 m by Thibault et al. (2016 Supplementary Material Fig. S1). Sampling for stable isotopes and palynology in September 2018 was referenced to our subsequently compiled 162 m log spanning the entire exposed section, from the uppermost Turonian *Plesiocorys (Sternotaxis) planus* Zone (1.5 m below Navigation Marl 1) to lower Campanian *Gonioteuthis quadrata* Zone (Castle Hill Flint 9). The base of the Thibault et al. (2016) section is located at 37.84 m height on the new complete logged section.

3.1. Carbon isotopes

A total of 537 bulk sediment samples (50 g) were taken at 10 cm intervals within the Santonian–Campanian boundary interval between 105.0–123.0 m and 126.0–161.5 m height from the Seaford Head section (Fig. 3) for stable isotope analysis, to supplement and extend the 25 cm sampling of the uppermost Coniacian to lowest Campanian between 37.8 and 128.6 m by Thibault et al. (2016).

Samples were analysed by JM and CVU at the University of Exeter using a Sercon 20-22 gas source isotope ratio mass spectrometer (GS-IRMS) in continuous flow setup. The analytical method is analogous to Ullmann et al. (2020 supplementary information) and is here explained only in brief.

Approximately 500 μg of bulk carbonate were weighed into borosilicate vials at 1 μg precision to minimise weight-dependent analytical biases. Samples and in-house standards CAR (Carrara Marble, $\delta^{13}C_{carb} = +2.10‰$ VPDB; $\delta^{18}O_{carb} = -2.03‰$ VPDB) and NCA (Namibian carbonatite, $\delta^{13}C_{carb} = -5.63‰$ VPDB; $\delta^{18}O_{carb} = -21.90‰$ VPDB) were flushed with He for 80 s and reacted with nominally anhydrous phosphoric acid (103%) at 70 °C. Instrumental drift as well as analytical bias were corrected using the two in-house standards yielding a reproducibility (two standard deviations; 2 sd) of 0.07‰ for $\delta^{13}C_{carb}$ and 0.15‰ for $\delta^{18}O_{carb}$ ($n = 917$) over the year in which the analyses were conducted. Results for the Seaford Head samples are reported in Appendix B Supplementary data Table 1.

Comparison of our plotted $\delta^{13}C_{carb}$ curve showed a systematic offset in values compared to the previously published curves of Jenkyns et al. (1994) and Thibault et al. (2016). These offsets were corrected by subtracting 0.15‰ and 0.1‰ from the two data sets, respectively (Appendix B Supplementary data Table 1). The new and recalibrated curves show excellent agreement (Fig. 3), and it is notable that even the low-resolution 1-m sampling data of Jenkyns et al. (1994) fully captures key medium-to long-term $\delta^{13}C_{carb}$ trends through the overlapping section. This confirms the viability of using such data to generate a robust high-order $\delta^{13}C$ chemostratigraphic framework for Chalk successions, as done by Jarvis et al. (2006). However, the Jenkyns et al. (1994) $\delta^{13}C_{carb}$ data display higher amplitude scatter than the newer data sets (Fig. 3) and will not be considered further.

Comparison of oxygen isotope values from the three sources showed higher amplitude variation than for carbon but with no systematic offset between the data set of Thibault et al. (2016) and this study (Fig. 3; Appendix B Supplementary data Table 1), but a −0.1‰ correction for bias was applied to the data of Jenkyns et al. (1994). For consistency with the $\delta^{13}C_{carb}$ analysis, the $\delta^{18}O_{carb}$ data of Jenkyns et al. (1994) were not used for compilation purposes. The recalibrated $\delta^{13}C_{carb}$ and the $\delta^{18}O_{carb}$ results of Thibault et al. (2016) from Seaford Head were combined with our new data to generate smoothed 3-point moving average curves to more clearly illustrate key stratigraphic trends (Fig. 3).

The $\delta^{13}C_{carb}$ profile for the Bocieniec succession obtained by Dubicka et al. (2017 supplementary table 2), who analysed 56


Seaford Head
Zones
Substage
Macrofossil
UKB foraminifera
North Sea nannofossil
Formation
Beds
Scale
Samples
Lithology
Marker beds
lower Campanian
upper Santonian
mSa
G. quadrata
Offaster pilula
Ua
Mt
Ml
U. socialis
Mc
UKB16 Bolivinoides culverensis
UKB15 Bs
UKB14 S. g. polonica
UC14ii
UC14i
UC13iii
UC13ii
UC13i
UC12
Culver
Newhaven Chalk
S
Castle Hill
Bastion Steps Beds
Meeching Beds
PB
Old Nore Beds
Splash Point Beds
HBB
metres
Castle Hill Flints
Castle Hill Marls
Arundel Sponge Bed
Black Rabbit Marls
Telscombe Marls
Op3
Meeching Pair Marls
Meeching Triple Marls
Meeching Flints
Peacehaven Marl
Op2
Old Nore Marl
Roedean Triple Marls
Rottingdean Pair Marls
Saltdean Marl
Op1
Black Rock Marl
Ovingdean Marl
Friars Bay Marls
Sheepcote Valley Flint
Kempton Marl
Brighton Marl
Brighton Five Marls
Hawks Brow Flint
Buckle Marls 1–4
Buckle Flint
Exceat Flint
CIEs
Senonensis
Meeching
Pilula
Rottingdean
Late Santonian Event
Foreness CIEs
FN3
FN2
FN1
Hawks Brow
Buckle
C33r ?
C34n ?
'c'
b
a
Eatonicysta? mutabilireta
Palaeoperidinium pyrophorum
Hystrichosphaeropsis ovum
Chatangiella manumii
Montanarocysta aemiliana
Florentinia mayi
Trichodinium castanea
Spiniferites multispinus
Disphaeria macropyla
Rhynchodiniopsis juneae sp. nov.
Turnhosphaera hypoflata
Membranigonyaulax wilsonii
Raphidodinium fucatum
Senoniasphaera macroreticulata
Exochosphaeridium majus robust type
Spinidinium echinoideum
Eisenackia? knokkensis
Rhynchodiniopsis saliorium
Xenascus perforatus
Pervosphaeridium intervelum
Whiteiffia spinosa
Dimidium striatum
Neosphaerodictyon filosum
Odontochitina porifera
Palaeohystrichophora infusorioides
Trimuridinium whitenessense
Membranilarnacia pterococcoides
Cordosphaeridium catherineae
Raetiaedinium truncigerum
Odontochitina diducta
Dinogymnium acuminatum
fungal hyphae
Pervosphaeridium pseudhystrichodinium
Pervosphaeridium monasteriense
Culversphaera velata
Tenua colliveri
Spiniferites ramosus ramosus
Senoniasphaera florireticulata
Odontochitina operculata
Odontochitina costata
Exochosphaeridium majus
Canningia glomerata
Cassiculosphaeridia reticulata
zooclasts (undifferentiated)
Senoniasphaera protrusa
Senoniasphaera congregensa
Circulodinium distinctum
Surculosphaeridium longifurcatum
Canningia senonica
Xenascus ceratioides
Coronifera striolata sensu Schiøler 1992
Ellipsodinium rugulosum
Sentusidinium spp.
Ellipsodinium membraniferum
Senoniasphaera turonica
Heterosphaeridium sp. G. (gracile)
C. velata
P. infusorioides (influx)
P/G ratio increase
X. perforatus
E.? knokkensis
R. junei
C. senonica (C/A)
C. senonica (acme)
S. macroreticulata
S. protrusa (inc)
T. whitenessense
W. spinosa (pers)
E. membraniferum (inc)
R. saliorum
W. spinosa
D. striatum
C. glomerata (C)
O. porifera
S. longifurcatum (inc)
T. whitenessense
C. catherineae
S. congrensa
S. protrusa
S. longifurcatum (temp)
Ellipsodinium spp.
E. membraniferum
acme
S. longifurcatum minimum
Dinocyst semi-quantitative abundance (200 count)
+ outside count
present (1)
frequent (2–9)
common (10–24)
v. common (25–39)
abundant (40–69)
v. abundant (70–99)
dominant (100+)
? includes some uncertain specimens in count

samples taken at 10 cm intervals (Fig. 4), is used for correlation purposes here. Oxygen isotope results were not reported due to issues surrounding analytical data quality (AJ pers. obs.).

3.2. Palynology

For palynological analysis at Seaford Head, 64 samples were taken at approximately 1 m intervals through the upper Santonian–lower Campanian between 92 and 152 m, spanning the complete Newhaven Chalk (Fig. 3). Sample positions were recorded with respect to the detailed drafted logs of IJ (see above).

The Bocieniec section was sampled every 30 cm for palynology (21 samples) by AJ in October 2017 and October 2021 with reference to the published log of Dubicka et al. (2017; Fig. 4). Heavy rain and flooding in July 2021 led to landslides and slumps that obscured the lower section. Samples collected from the section top in 2021 (4.08, 4.48, 4.98, 5.28, 5.48 m) were taken by reference to the marl–opoka facies boundary (Fig. 4).

Weighed (typically 100 g) samples were treated with HCl and HF to remove the carbonate and silicate matrix, and the organic residue was concentrated with a 15 μm sieve mesh (see Lignum et al., 2008; Jarvis et al., 2021). Seaford Head samples were spiked with *Lycopodium clavatum* spore tablets (Department of Geology, Lund University) to enable the determination of palynomorph absolute abundances (cf. Pearce et al., 2003). Bocieniec samples were unspiked. Oxidation was not required for either sample set. Residues were stained with Safranin-0 (red–pink) to enhance visibility (cf. Wood et al., 1996).

Palynology slides were analysed with a Leica DM1000 LED microscope with ×63 and ×100 oil-immersion objectives. A full count was reached when 200 identified dinocysts (excluding spores and pollen, acritarchs and unidentified specimens) were recorded. Subsequently, whole slides were visually scanned for the presence of additional taxa. These were recorded as present (crosses on range charts, e.g. Fig. 5) but were not included in the numerical count data.

All the studied slides are deposited in the Department of Earth Sciences, Natural History Museum, Cromwell Road, London SW7 5BD, UK. Accession numbers: Seaford Head, NHMUK PM FD 1343–1406; Bocieniec NHMUK PM FD 1417–1437. Further details are provided in Appendix B. Supplementary data Tables 2 and 3.

4. Carbon isotope stratigraphy

4.1. Seaford Head

The carbon isotope stratigraphy of the Santonian–Campanian boundary succession at Seaford Head is illustrated in Fig. 3. The curve provides a basis to identify the middle Santonian Horseshoe Bay CIE, the upper Santonian Buckle, Hawks Brow and Foreness CIEs, the LSE (formerly, SCBE), and the lower Campanian Pilula CIE. It confirms the placement of these CIEs by Jarvis et al. (2006) and Thibault et al. (2016), with minor adjustments and refinement (Section 7.2) indicated by the new higher resolution $\delta^{13}C_{carb}$ data.

Thibault et al. (2016) used the low-resolution $\delta^{13}C_{carb}$ data of Jenkyns et al. (1994) as a basis to interpret the isotope stratigraphy of the Campanian section at Seaford Head, with the designation of negative excursions above the old Nore Marl and below the Telscombe Marls as the “pillula Zone event” and “senonensis Zone event”, respectively (referred to here subsequently as the Pilula and Senonensis CIEs). The peak at the section top, above the HO of *M. quaternarius*, was assigned to the “papillosa Zone event” (Papillosa CIE). These 3 CIEs were correlated to corresponding $\delta^{13}C_{carb}$ curves (Thibault et al., 2016 fig. 3) from the Trunch borehole, Norfolk (Jarvis et al., 2006) and Lägerdorf quarry, north Germany (Voigt et al., 2010), with names allocated to the events based on their correlation to the Lägerdorf reference macrofossil biozones.

The new high-resolution $\delta^{13}C_{carb}$ profile (Fig. 3) displays additional structure that reveals three discrete negative excursions in the high upper Santonian (Foreness CIEs FN1–FN3) and other positive and negative excursions that have correlative value (Rottingdean, Meeching and Castle Hill CIEs), while our dinocyst biostratigraphy provides new constraints on the correlation of the Senonensis and Papillosa CIEs (Section 7.2).

4.2. Bocieniec

A revised interpretation of the carbon-isotope stratigraphy of the Bocieniec section is shown in Fig. 4. The negative excursion falling to 1.77‰ $\delta^{13}C_{carb}$ at 1.08 m in the lower *U. socialis* Zone is equated to the Buckle CIE, and the maximum of 1.97‰ at 1.98 m in the upper *U. socialis* Zone to the Hawks Brow CIE. The negative excursion at the base of the *M. laevigatus* Zone between 2.4 and 2.6 m with a minimum of 1.84‰, identified as the Foreness CIE by Dubicka et al. (2017), is considered to represent the Foreness FN1 excursion, the lowest of 3 negative CIEs occurring within the *Marsupites* zones (Section 7.2).

The extended ranges of the crinoid zonal taxa reported by Gale (in Gale et al., in press) has required a reappraisal of the LSE (see Section 2.2.4). Our interpretation (Fig. 4) places the top of LSE peak a at the $\delta^{13}C_{carb}$ maximum of 2.55‰ at 4.18 m, coincident with the HO of *M. testudinarius*. The overlying peak with a value of 2.36‰ at 4.38 m may represent peak b of the LSE, or the peak may be represented in the falling limb of the main peak, below. Gale et al. (in press) placed the whole positive excursion within peak a based on the apparent absence of *U. anglicus*, requiring the presence of a hiatus at around 4.3 m that cuts out the *U. anglicus* Zone. It is equally possible that *U. anglicus* occurs infrequently in the few cm of sediment representing the zone, and has not been recorded, or the taxon is absent from the section due to environmental changes accompanying the facies change towards opoka, above. On balance, the high $\delta^{13}C_{carb}$ value of the second peak favours its identification as peak b of the LSE.

Gale et al. (in press) placed the base of the Campanian at Bocieniec at ca. 4.45 m where Dubicka et al. (2017) positioned the base of Chron C33r, within the lower part of *Gavelinella clementiana* Zone (Fig. 4). This compares to a location at around 4.2 m based on the HO *Marsupites* at the $\delta^{13}C_{carb}$ maximum towards the top of the *Bolivinoides culverensis* Zone. Placement of the Pilula CIE (lower *O. pilula* Zone) in Fig. 4 broadly follows Dubicka et al. (2017). However, the sequential LOs of *O. pilula* at 5.08 m and *A. parcus parcus* at 5.28 m support the tentative identification of the two adjacent small negative excursions as the Rottingdean and Pilula CIEs (Fig. 4; Section 7.2) rather than the Pilula CIE alone.

Fig. 5. Semi-quantitative range chart for stratigraphically significant dinocyst taxa recorded from the Santonian–Campanian boundary interval, Seaford Head. See Fig. 3 for stratigraphy abbreviations and data sources. Significant lowest occurrence (LO), highest occurrence (HO) and acme levels are shown for key taxa. A, abundant; C, common; inc, increase; C/A, common/abundant; pers, persistent. Yellow bars and bold text of species names highlight the ranges of the stratigraphically most significant taxa. Species counts are presented in Appendix B Supplementary data Table 2. (For interpretation of the references to colour in this figure legend, the reader is referred to the Web version of this article).

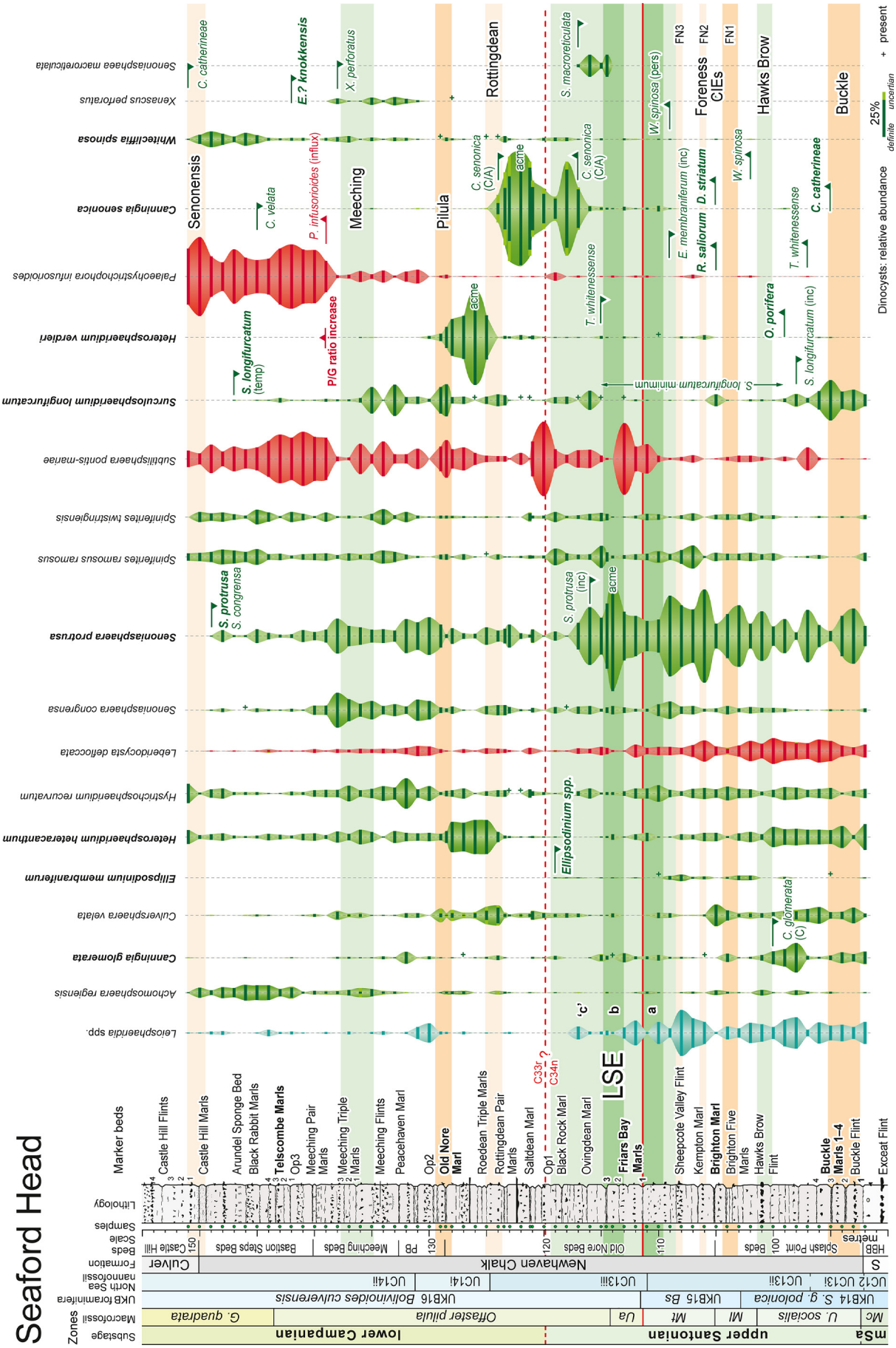
Seaford Head
Zones
Substage
Macrofossil
UKB foraminifera
North Sea nannofossil
Formation
Beds
Scale
Samples
Lithology
Marker beds
Castle Hill Flints
Castle Hill Marls
Arundel Sponge Bed
Black Rabbit Marls
Telscombe Marls
Op3
Meeching Pair Marls
Meeching Triple Marls
Meeching Flints
Peacehaven Marl
Op2
Old Nore Marl
Roedean Triple Marls
Rottingdean Pair Marls
Saltdean Marl
Op1
Black Rock Marl
Ovingdean Marl
Friars Bay Marls
Sheepcote Valley Flint
Kempton Marl
Brighton Marl
Brighton Five Marls
Hawks Brow Flint
Buckle Marls 1–4
Buckle Flint
Exceat Flint
lower Campanian
upper Santonian
msA
Mc
Ml
Mt
Ua
U. socialis
G. quadrata
Offaster pilula
UKB16 Bolivinoides culverensis
UKB15 Bs
UKB14 S. g. polonica
UC14ii
UC13iii
UC12 UC13i
Culver
Newhaven Chalk
Beds
Castle Hill
Baston Steps Beds
Meeching Beds
PB
Old Nore Beds
Splash Point Beds
HBB
metres
LSE
C33r
C34n
a
b
c
FN3
FN2
FN1
Foreness CIEs
Hawks Brow
Buckle
Leiosphaeridia spp.
Achomosphaera regiensis
Cannidia glomerata
Culversphaera velata
Ellipsodinium membraniferum
Heterosphaeridium heteracanthum
Hystrichosphaeridium recurvatum
Leberidocysta deflocculata
Senoniasphaera congrensa
Senoniasphaera protrusa
Spiniferites ramosus
Spiniferites twistringiensis
Subtilisphaera pontis-mariae
Surculosphaeridium longifurcatum
Heterosphaeridium verdieri
Palaeohystrichophora infusorioides
Canninga senonica
Whitecliffia spinosa
Xenascus perforatus
Senoniasphaera macroreticulata
C. catherineae
E.? knokkensis
X. perforatus
C. velata
P. infusorioides (influx)
S. longifurcatum (temp)
P/G ratio increase
Meeching
Pilula
Rottingdean
Senonensis
C. senonica (C/A)
acme
S. protrusa
S. congrensa
S. protrusa (inc)
Ellipsodinium spp.
S. macroreticulata
T. whitenessense
S. longifurcatum minimum
W. spinosa (pers)
E. membraniferum (inc)
D. striatum
R. saliorum
W. spinosa
O. porifera
T. whitenessense
S. longifurcatum (inc)
C. catherineae
C. glomerata (C)
Dinocysts: relative abundance
25%
definite
uncertain
present

5. Palynology results

5.1. Seaford Head

All samples from Seaford Head were productive and yielded well-preserved palynological assemblages, overwhelmingly dominated by organic-walled dinoflagellate cysts (147 taxa) with a species richness per sample of 30–64 taxa. Other marine palynomorphs, including algal cysts, acritarchs and prasinophytes (22 taxa), and fungal hyphae are present throughout. Note that taxa recorded to generic level (as spp.) are included in the counts. Occasional terrestrial palynomorphs, principally bisaccate pollen grains, are recorded in some samples. The ranges of dinocyst taxa considered to be of wider stratigraphic significance are plotted in Fig. 5, the relative abundances of the main elements of the flora are shown in Fig. 6, and key taxa are figured in Figs. 7 and 8. Palynomorph assemblage composition data are summarised in Fig. 9. Appendix A provides a list of palynological taxa identified from the two study; sample counts and statistics are contained in Appendix B Supplementary data Tables 2 and 3.

The dinocyst assemblages are dominated by the areoligeracean genera *Senoniasphaera* and *Heterosphaeridium*, although not consistently by the same species (Fig. 6). From 93 to 116 m, throughout the *U. socialis* to basal *O. pilula* zones, *Senoniasphaera protrusa* (Fig. 8G) dominates (together with high numbers of the prasinophyte *Leiosphaeridia* spp.). The species is superseded as the dominant taxon by *Canningia senonica* (Fig. 7B) across the proposed Santonian–Campanian boundary interval from 117 to 124 m, and this taxon is, in turn, superseded by common to abundant *Heterosphaeridium heteracanthum* (Fig. 7H) and *H. verdieri* (Fig. 7I) in the lower Campanian from 125 to 129 m. These assemblages are typical of the marginal marine *Circulodinium–Heterosphaeridium* (C–H) assemblage (see Pearce et al., 2003). Collectively, representatives of the more distal *Spiniferites–Palaeohystrichophora* (S–P) assemblage (Pearce et al., 2003, 2009; Prince et al., 2008; Jarvis et al., 2021) are subordinate, but are consistently present throughout, indicating a more proximal setting than suggested for Bocieniec (Section 6.2). Absolute abundances (palynomorphs per gram, ppg) are relatively low and range from 90 to 1400 ppg (Fig. 9); these values are consistent with those of the type C–H assemblage recovered from the Chalk of Berkshire, England by Pearce et al. (2003).

Abbreviations used in the following sections and figures are as follows: A = abundant, C = common, CIE = Carbon Isotope Event, FAD = First Appearance Datum, HCO = Highest Common Occurrence, HO = Highest Occurrence, IOW = Isle of Wight, LAD = Last Appearance Datum, LCO = Lowest Common Occurrence, LO = Lowest Occurrence, pers = persistent.

5.1.1. Palynological bioevents

The Seaford Head section yields a limited number of dinocyst biostratigraphic index taxa, presumably due to the relatively marginal position of the area with respect to the palaeoshoreline. However, notable events are indicated in Figs. 5, 6, and are described here in stratigraphic order.

5.1.1.1. Canningia glomerata. *Canningia glomerata* (Fig. 7A) (formerly referred to *Senoniasphaera rotundata*; Fensome et al., 2019b), occurs throughout the upper Santonian–lower Campanian interval at Seaford Head. The frequency and abundance of *C. glomerata* decreases progressively upwards through the study section (Figs. 5, 6). A significant fall in the relative abundance of *C. glomerata* occurs at 100 m at Seaford Head in the upper Santonian (*U. socialis* Zone), immediately below the Hawks Brow CIE.

5.1.1.2. Canningia senonica. Sporadic records of *Canningia senonica* (Fig. 7B) occur throughout the study interval at Seaford Head. However, the species temporarily becomes a dominant component of the dinocyst assemblages within the top LSE and immediately above, between 117 and 124 m, with two large abundance pulses and an acme above the Saltdean Marl (Figs. 5, 6). It represents a consistent and abundant component of the palynology assemblage solely within this interval. Identification of *C. senonica* in non-optimum preserved material can be problematic, so our records include significant numbers of "uncertain" assignments (Figs. 5, 6, Appendix B Supplementary data Table 2). Nonetheless, the same trends are apparent when including only definite records of the species.

5.1.1.3. Cordosphaeridium catherineae. The LO of *Cordosphaeridium catherineae* (Fig. 7C) at Seaford Head is observed at 95 m, in the upper Santonian (lower *U. socialis* Zone) immediately above Buckle Marl 3, at the top of the Buckle CIE (Fig. 5). The species is generally rare and sporadic through the section, but frequent occurrences do occur in the Campanian. The species is recorded to the section top at 151 m in the lower *G. quadrata* Zone, at the top of the Senonensis CIE.

5.1.1.4. Culversphaera velata. *Culversphaera velata* (Fig. 7D) occurs commonly through the study interval at Seaford Head but some identifications remain uncertain (Figs. 5, 6), particularly because the sutural crests are fine and easily damaged. The HO of a definite record of *C. velata* occurs at 145 m in the lower Campanian (basal *G. quadrata* Zone), midway between the Meeching and Senonensis CIEs, although two uncertain records occur above this.

5.1.1.5. Dimidium striatum. *Dimidium striatum* (Fig. 7E) is poorly represented at Seaford, occurs rarely and sporadically with a base at 102 m in the mid-upper Santonian (*M. laevigatus* Zone) between the Hawks Brow and Foreness FN1 CIEs (Fig. 5). The highest occurrence is recorded at 129 m in the lower Campanian (mid-*O. pilula* Zone) within the Pilula CIE.

5.1.1.6. Eisenackia? knokkensis. *Eisenackia*? *knokkensis* (Fig. 7F) is recorded sporadically in low numbers at Seaford Head (Fig. 5). The species occurs at only three levels: 112 m in the in the *U. anglicus* Zone, 121 m–121.2 m around the Saltdean Marl in the lower Campanian (lower *O. pilula* Zone), and at 141–142 m towards the top of the *O. pilula* Zone, between the Meeching and Senonensis CIEs; the last height represents its HO at the locality (Fig. 5).

5.1.1.7. Ellipsodinium *spp.* The HO of *E. membraniferum* (Fig. 7G) at Seaford Head occurs at 119 m in the upper Santonian (basal *O. pilula* Zone), close to the top of the LSE and immediately below the inferred position of the C34n/C33r boundary (Figs. 5, 6). *Ellipsodinium membraniferum* occurs consistently in samples below this and is commonest in the top Santonian *Marsupites laevigatus* and *M. testudinarius* zones. Records of *E. rugulosum* are more sporadic and the species occurs most commonly in the *M. laevigatus* Zone.

Fig. 6. Stratigraphic variation in the relative abundance of major palynological constituents through the Santonian–Campanian boundary interval, Seaford Head. See Fig. 3 for stratigraphy abbreviations and data sources. LOs, HOs and acmes of stratigraphically significant taxa are shown. Bold text of species names indicates the stratigraphically most significant taxa. Bars represent relative abundances determined in individual samples based on 200 dinocyst counts. Blue, acritarch; green, gonyaulacoid dinocysts; red, peridinioid dinocysts. Note the differentiation between definite (dark colour) and uncertain (pale colour) counts of specimens identified at specific level (Appendix B Supplementary data Table 2) contributing to the abundance bars. (For interpretation of the references to colour in this figure legend, the reader is referred to the Web version of this article).

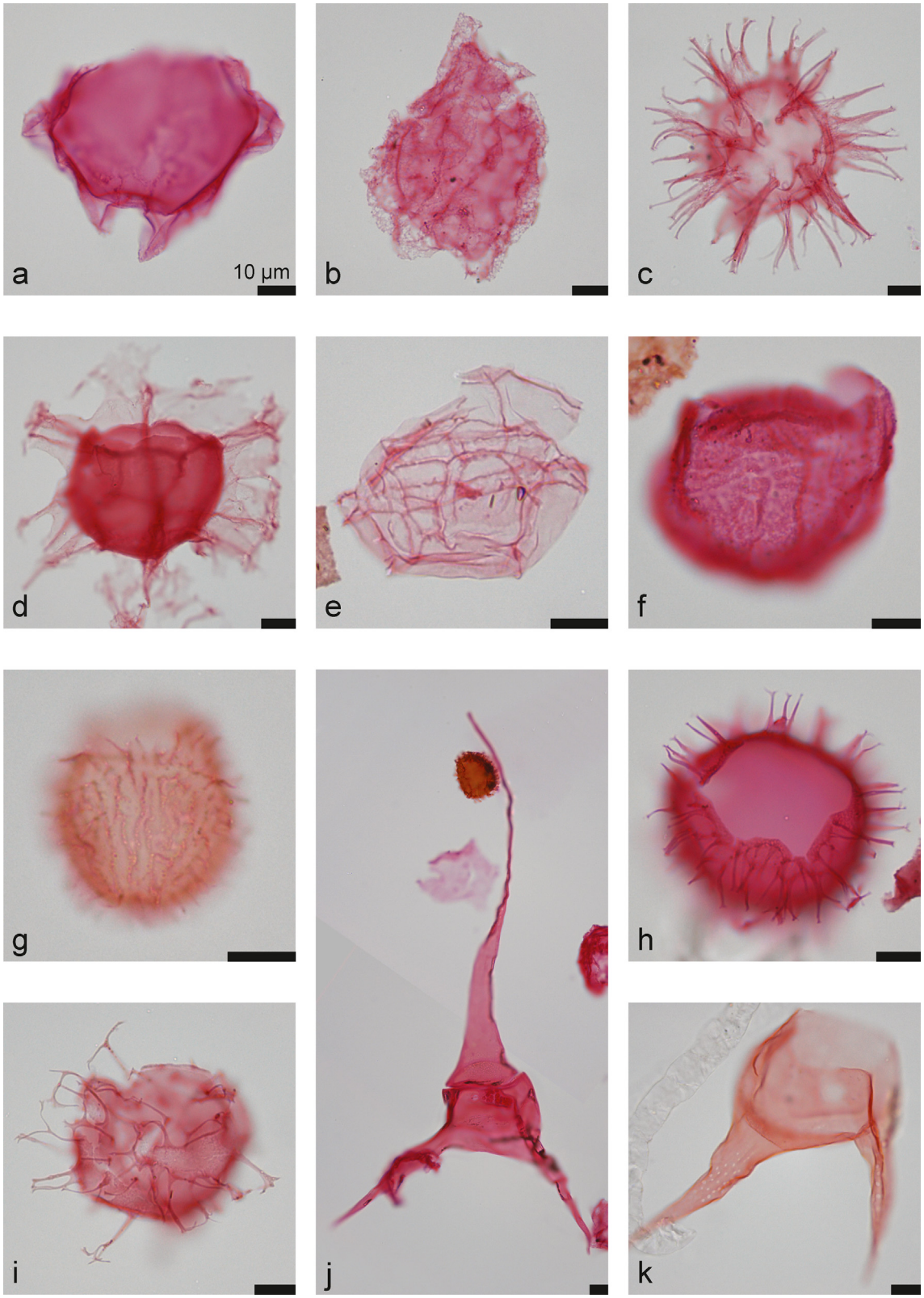

Fig. 7. Selected stratigraphically important dinocyst species from the Santonian–Campanian boundary interval, Seaford Head. **A**. *Canningia glomerata*, 95 m, EF: L43/1. **B**. *Canningia senonica*, 122 m, EF: K38/3. **C**. *Cordosphaeridium catherineae*, 124 m, EF: M16. **D**. *Culversphaera velata*, 128.5 m, EF: H35/1. **E**. *Dimidium striatum*, 129 m, EF: L25/2. **F**. *Eisenackia? knokkensis*, 121.2 m, EF: L33. **G**. *Ellipsodinium membraniferum*, 108 m, EF: L30/3. **H**. *Heterosphaeridium heteracanthum*, 104 m, EF: Q33/1. **I**. *Heterosphaeridium verdieri*, 126 m, EF: H41/4. **J**. *Odontochitina diducta*, 123.4 m, EF: T30. **K**. *Odontochitina porifera*, 137 m, EF: N36/3. Scale bars are 10 µm.

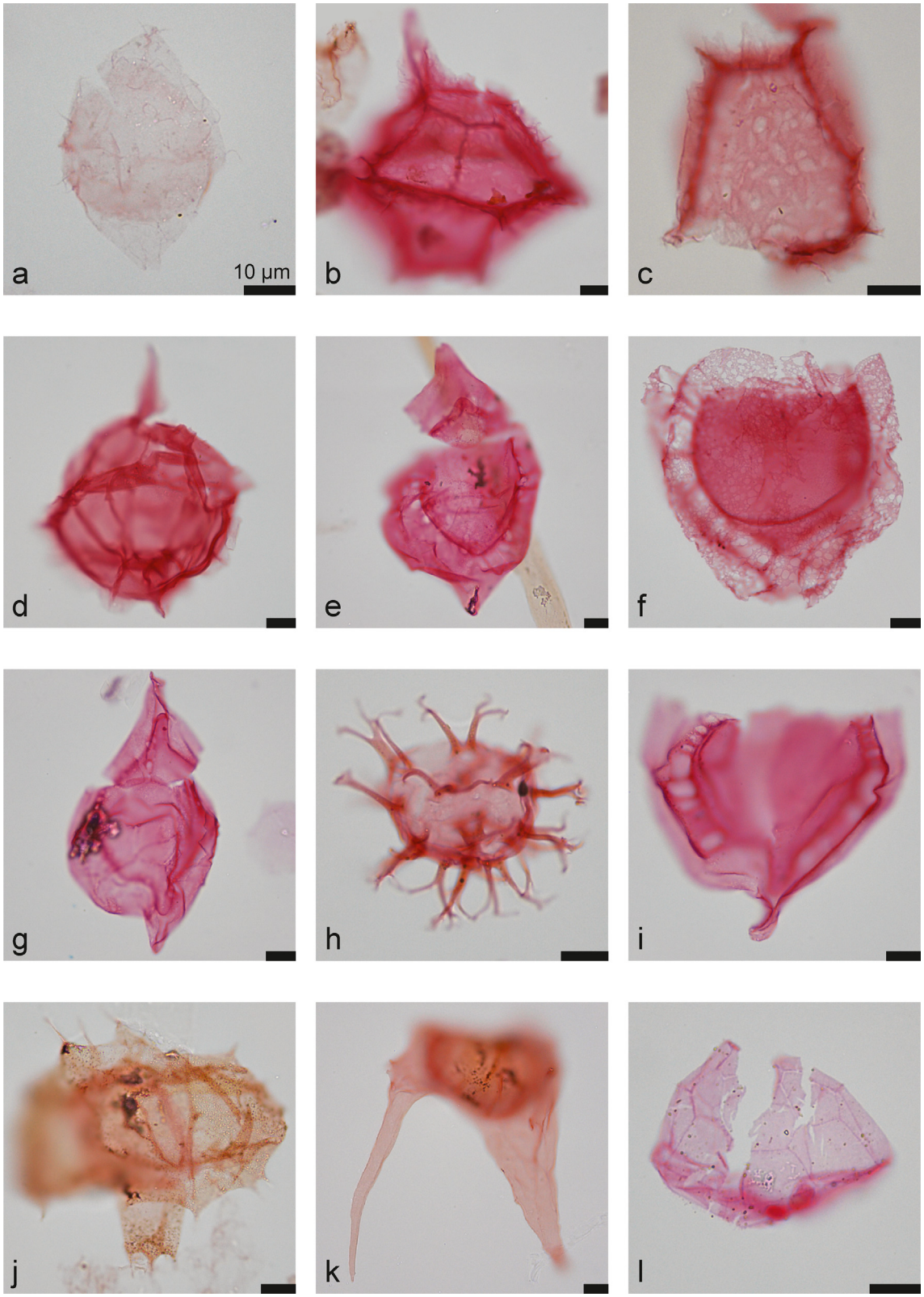

Fig. 8. Selected stratigraphically important dinocyst species from the Santonian–Campanian boundary interval, Seaford Head and Bocieniec. A–K from Seaford Head, L from Bocieniec. **A**. *Palaeohystrichophora infusorioides*, 140 m, EF: O30. **B**. *Rhynchodiniopsis juneae* sp. nov. (holotype), 149 m, EF: K23/4. **C**. *Rhynchodiniopsis juneae* sp. nov. (paratype) operculum demonstrating the distinctive ornament, 144 m, EF: O37. **D**. *Rhynchodiniopsis saliorum*, 128.5 m, EF: Q29. **E**. *Senoniasphaera congrensa*, 123 m, EF: S51/1. **F**. *Senoniasphaera macroreticulata*, 117 m, EF: L44/3. **G**. *Senoniasphaera protrusa*, 108 m, EF: K25/1. **H**. *Surculosphaeridium longifurcatum*, 128.5 m, EF: L38/4. **I**. *Trimuradinium whitenessense*, 115 m, EF: K49/3. **J**. *Whitecliffia spinosa*, 145 m, EF: O17. **K**. *Xenascus perforatus*, 135 m, EF: F25/1. **L**. *Alterbidinium ioannidesii*, 2.63 m, EF: L18/4. Scale bars are 10 µm.

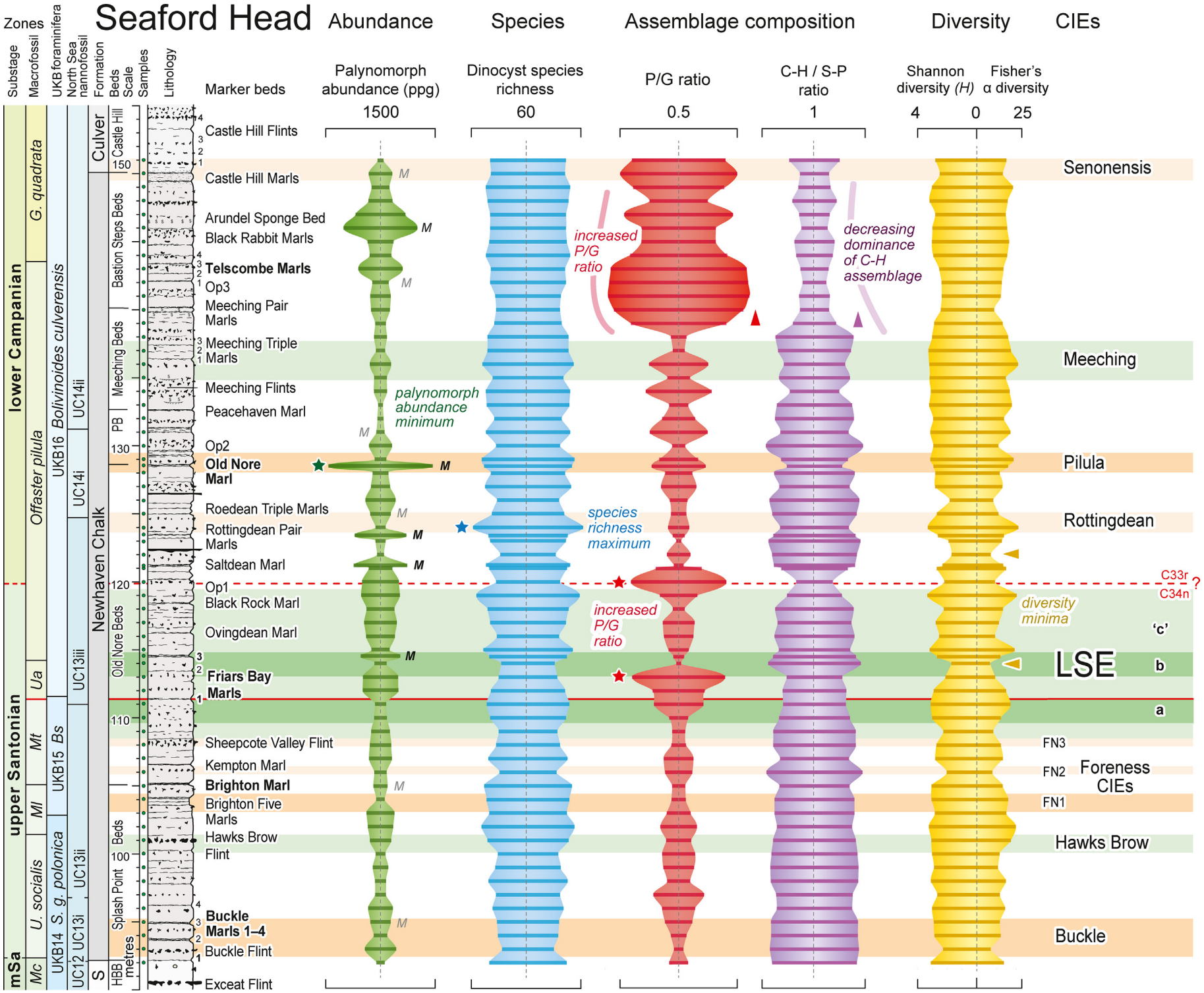
Seaford Head
Zones
Substage
Macrofossil
UKB foraminifera
North Sea nannofossil
Formation
Beds
Scale
Samples
Lithology
Marker beds
Abundance
Species
Assemblage composition
Diversity
CIEs
Palynomorph abundance (ppg)
1500
Dinocyst species richness
60
P/G ratio
0.5
C-H / S-P ratio
1
Shannon diversity (H)
4
0
Fisher's α diversity
25
upper Santonian
lower Campanian
mSa
Mc
U. socialis
S. g. polonica
Offaster pilula
G. quadrata
Ma
Mt
Bs
Ml
UKB14
UKB15
UKB16
Bolivinoides culverensis
UC12
UC13i
UC13ii
UC13iii
UC14i
UC14ii
S
Culver
Newhaven Chalk
HBB
Splash Point Beds
Old Nore Beds
Friars Bay Marls
PB
Meeching Beds
Bastion Steps Beds
Castle Hill
metres
Castle Hill Flints
Castle Hill Marls
Arundel Sponge Bed
Black Rabbit Marls
Telscombe Marls
Op3
Meeching Pair Marls
Meeching Triple Marls
Meeching Flints
Peacehaven Marl
Op2
Old Nore Marl
Roedean Triple Marls
Rottingdean Pair Marls
Saltdean Marl
Op1
Black Rock Marl
Ovingdean Marl
Friars Bay Marls
Sheepcote Valley Flint
Kempton Marl
Brighton Marl
Brighton Five Marls
Hawks Brow Flint
Buckle Marls 1–4
Buckle Flint
Exceat Flint
palynomorph abundance minimum
increased P/G ratio
species richness maximum
increased P/G ratio
decreasing dominance of C-H assemblage
diversity minima
C33r
C34n
?
Senonensis
Meeching
Pilula
Rottingdean
'c'
LSE
b
a
FN3
FN2
FN1
Foreness CIEs
Hawks Brow
Buckle

5.1.1.8. Odontochitina porifera. At Seaford Head, *O. porifera* (Fig. 7K) is rare and sporadic from 99 m and above (Fig. 5). The LO occurs in the upper Santonian (*U. socialis* Zone), immediately below the Hawks Brow CIE.

5.1.1.9. Palaeohystrichophora infusorioides. A marked influx of peridinioid cysts, *Palaeohystrichophora infusorioides* (Fig. 8A) accompanied by *Subtilisphaera pontis-mariae*, occurs at 139 m in the lower Campanian (top of the *O. pilula* Zone) at Seaford Head. These two taxa dominate the palynological assemblages at the top of the study section (Figs. 5, 6).

5.1.1.10. Rhynchodiniopsis saliorum *and* Rhynchodiniopsis juneae *sp. nov.* At Seaford, the LO of *Rhynchodiniopsis saliorum* (Fig. 8D) occurs at 105 m in the upper Santonian (*Marsupites* Zone) between the Foreness FN1 and FN2 CIEs. It is rare and sporadic up section to 142 m in the lower Campanian (high *O. pilula* Zone) between the Meeching and Senonensis CIEs, where it is still rare but persistently recorded to the top of the section (Fig. 5). A similar distribution was observed with *Cordosphaeridium catherineae*. Distinctly foveolate specimens of *Rhynchodiniopsis* are encountered from 127 m (mid-*Offaster pilula* Zone) to the penultimate studied sample at 150 m (*G. quadrata* Zone). These are described as the new species *Rhynchodiniopsis juneae* sp. nov. (Figs. 8B–C) (see Appendix A and B Supplementary data Table 2). The LO of persistently recorded specimens is at 143 m (Fig. 5, uppermost *Offaster pilula* Zone).

5.1.1.11. Senoniasphaera macroreticulata. *Senoniasphaera macroreticulata* (Fig. 8F) is a distinctive taxon that occurs at the bottom of the *O. pilula* Zone for a short interval between Friar's Bay Marl 3 and the Ovingdean Marl, from 114.5 to 117 m at Seaford Head. This corresponds to an interval within the upper LSE between peaks b and 'c' (Figs. 5, 6).

5.1.1.12. Senoniasphaera protrusa. *Senoniasphaera protrusa* (Fig. 8G) constitutes a major component of the palynological assemblages throughout the Santonian–Campanian boundary interval at Seaford Head (Figs. 5, 6). The species dominates the dinocyst assemblages from the base of our study section at 92 m, upper Santonian (low *U. socialis* Zone), to 116 m in the basal *O. pilula* Zone. The established LO lies below the base of our current study, and preliminary data indicate that the LO of the species occurs immediately below the Horseshoe Bay CIE. It remains a significant component above this, through the *O. pilula* and lower *G. quadrata* zones. The HO occurs at 149 m, below the Castle Hill Marls, and immediately below the Senonensis CIE.

5.1.1.13. Surculosphaeridium longifurcatum.
Surculosphaeridium longifurcatum (Fig. 8H) occurs consistently through the Santonian–Campanian boundary interval at Seaford Head but in varying proportions (Figs. 5, 6). The species has a high relative abundance at the bottom of the study section, but has a conspicuous low abundance interval from 99 m in the upper Santonian *U. socialis* Zone (below the Hawks Brow CIE) to 115 m in the uppermost Santonian basal *O. pilula* Zone, the top of the LSE peak b. From 116 m (below the Ovingdean Marl) to 135 m (basal Meeching CIE) the species is relatively well represented but then it becomes rare up to its HO in the Arundel Sponge Bed at 147 m, the basal *G. quadrata* Zone below the Senonensis CIE.

5.1.1.14. Trimuridinium whitenessensee. *Trimuridinium whitenessense* (Fig. 8I) occurs only in two samples from Seaford Head (Fig. 5). The first lies at 97 m in the upper Santonian (mid-*U. socialis* Zone), a short distance above the Buckle CIE, the second was recovered from 115 m at the base of the *O. pilula* Zone within the upper LSE.

5.1.1.15. Whitecliffia spinosa. The questionable LO of *Whitecliffia spinosa* (Fig. 8J) at Seaford Head lies at 102 m in the upper Santonian (*M. laevigatus* Zone), between the Hawks Brow and Foreness FN1 CIEs. An isolated but confident specimen also occurs in the *M. testudinarius* Zone between the Foreness FN1 and FN3 CIEs at 105 m. Confident and persistently recorded specimens are observed up section from 109 m in the *M. testudinarius* Zone, between the Foreness FN3 and LSE CIEs. It becomes particularly common within the lower Campanian *G. quadrata* Zone (Figs. 5, 6).

5.1.1.16. Xenascus perforatus. A few records of *Xenascus perforatus* (Fig. 8K) occur in the *M. testudinarius* and *O. pilula* zones at Seaford Head, but the species occurs persistently in moderate numbers only for a short interval in the upper *O. pilula* Zone from above the Pilula CIE to immediately above the Meeching CIE, between 131 and 138 m (Figs. 5, 6). Its HO lies at the top of this interval.

A pulse of *X. perforatus* in the *O. pilula* Zone at Whitecliff IOW (Prince et al., 1999; compare our specimen with their plate II, fig. 19) may correspond to the same event, but the stratigraphy of this part of the section at Whitecliff is complicated by attenuation, with the presence of multiple hardgrounds and phosphatic chalks (Whitecliff Ledge Beds; Gale et al., 1987, 2013; Prince et al., 1999; Mortimore et al., 2001; Jarvis, 2006; Gale, 2018) making precise correlation uncertain.

5.2. Bocieniec

All palynological samples from Bocieniec quarry were productive and yielded well-preserved assemblages, although samples at the base and towards the top of the section commonly showed very poor to moderate recovery. Most samples are dominated by dinocysts (158 taxa) with a species richness per sample of 9–78 taxa. Other marine palynomorphs, including algal cysts, acritarchs and prasinophytes (23 taxa) and fungal hyphae are present throughout. Terrestrial palynomorphs (43 taxa), principally bisaccate pollen grains, occur consistently, with significant numbers in the bottom and highest samples. Note that taxa recorded to generic level (as spp.) are included in the counts.

The ranges of dinocyst taxa considered to be of wider stratigraphic significance are plotted in Fig. 10, the relative abundances of the main elements of the flora are shown in Fig. 11, and key taxa are figured in Figs. 8 and 12. Palynomorph assemblage composition data are summarised in Fig. 13. Appendix A provides a list of palynological taxa identified from the section; sample counts and statistics are contained in Appendix B Supplementary data Table 3.

Fig. 9. Palynomorph abundance and dinocyst assemblage parameter plots for the Santonian–Campanian boundary interval at Seaford Head. See Fig. 3 for stratigraphy abbreviations and data sources. P/G ratio = number of peridinioid/gonyaulacoid cysts obtained by the equation P/G = nP/(nP + nG), where n is the number of specimens counted, P are peridinioid (or protoperidinioid) dinocysts and G are gonyaulacoid dinocysts. C–H/S–P ratio = *Circulodinium–Heterosphaeridium/Spiniferites–Palaeohystrichophora* ratio (obtained by the equation nC–H/nC–H + nS–P where n is the number of specimens counted and C–H and S–P comprise taxa assigned to those associations, cf. Pearce et al., 2003). Highest palynological abundances are observed in marls (***M***), but not all marls (*M*) show anomalously high recovery. The P/G ratio exhibits a cyclic pattern with significant maxima within the LSE and at the correlated position of the C34n/C33r polarity reversal boundary. A large increase in peridinioid cysts and a decreased dominance of the C–H assemblage characterise the upper *O. pilula*–lower *G. quadrata* zones; red and purple curves highlight coherent trends in the P/G and C–H/S–P ratios, respectively. Fisher's α diversity correlates well with species richness, with diversity minima in the upper *U. anglicus* Zone and lower *O. pilula* Zone. (For interpretation of the references to colour in this figure legend, the reader is referred to the Web version of this article).

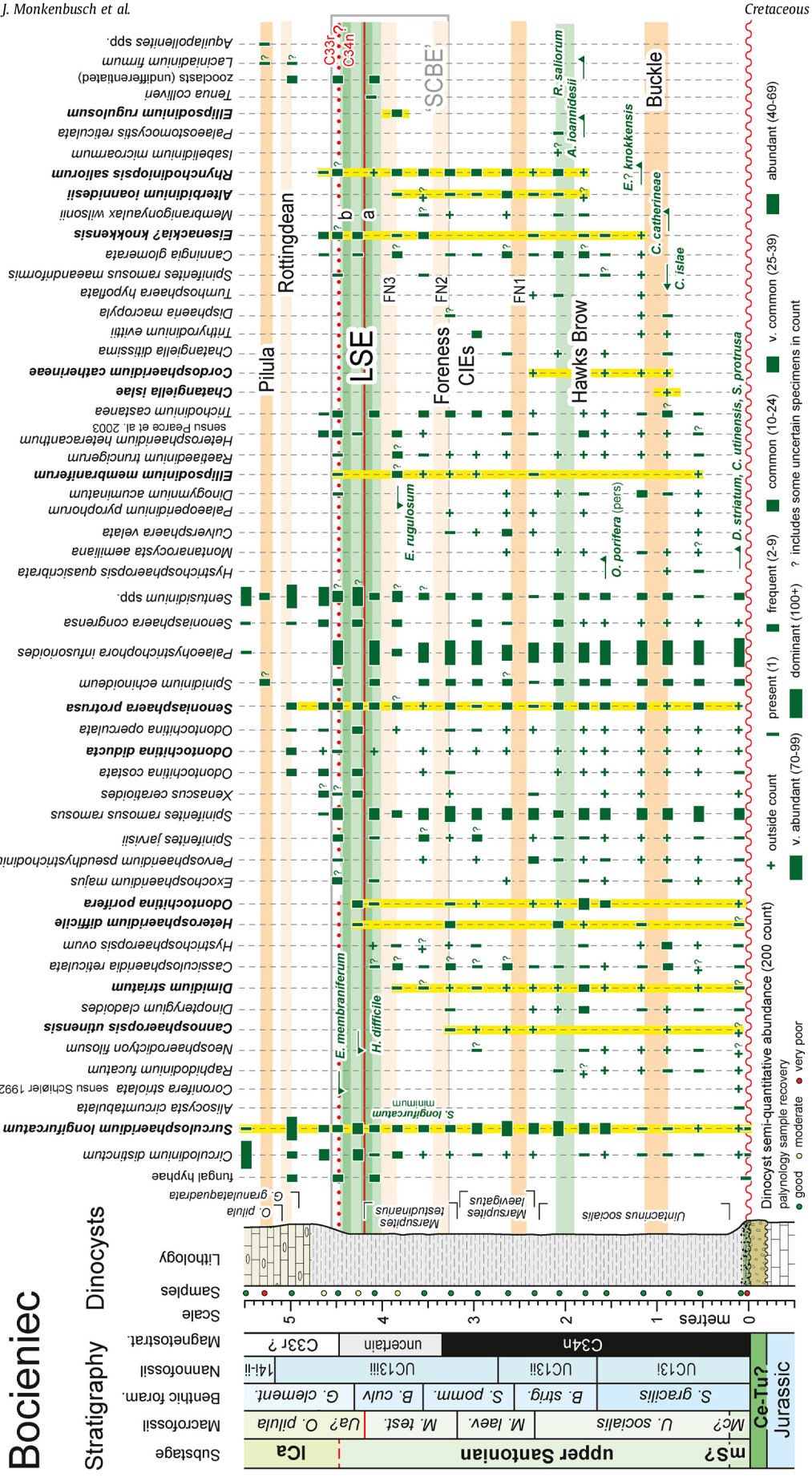

Fig. 10. Semi-quantitative range chart for stratigraphically significant dinocyst taxa recorded from the Santonian–Campanian boundary interval, Bocieniec. See Fig. 4 for stratigraphy abbreviations and data sources. Significant lowest occurrence (LO) and highest occurrence (HO) levels are shown for key taxa; pers = persistent. Yellow bars and bold text of species names highlight the ranges of the stratigraphically most significant taxa. Species counts are presented in Appendix B Supplementary data Table 3. (For interpretation of the references to colour in this figure legend, the reader is referred to the Web version of this article).

A very impoverished and very low abundance dinocyst assemblage characterises the lowest sample collected from the Santonian–Campanian boundary interval at Bocieniec, sampling the base of the glauconitic marl at 0.03 m, immediately above the Turonian/Santonian unconformity (Figs. 10, 11). Here, angiosperm pollen, bisaccate gymnosperm pollen, and fungal remains account for 75% of the total assemblage (Fig. 13, Appendix B Supplementary data Table 3). Dinocysts present comprise a very low diversity (9 species) assemblage that amongst the taxa common through the remainder of the section (Fig. 11), includes only *Circulodinium distinctum*, *Spiniferites twistringiensis* and *Surculosphaeridium longifurcatum* (Fig. 12L).

Samples from 0.10 to 3.83 m are dominated by *Palaeohystrichophora infusorioides*, with a broadly decreasing trend up section. In this interval, *Spiniferites ramosus* subsp. *ramosus, S. twistringiensis* and *Subtilisphaera pontis-mariae* are also well represented (Fig. 11). This assemblage is typical of the open shelf *Spiniferites–Palaeohystrichophora* (S–P) assemblage (Pearce et al., 2003, 2009; Prince et al., 2008; Jarvis et al., 2021).

Surculosphaeridium longifurcatum has a highly variable relative abundance but is particularly well represented between 1.56 and 2.96 m (Fig. 11). Above 3.83 m, a significant assemblage turnover occurs in the upper *M. testudinarius* Zone with a punctuated upwards decline in the abundance of S–P assemblage species and an increase in the relative abundance of *Circulodinium distinctum*, *Sentusidinium* spp., and *Surculosphaeridium longifurcatum*, typical of the marginal marine *Circulodinium–Heterosphaeridium* (C–H) assemblage (Pearce et al., 2003). This assemblage shift coincides with an increase in the relative abundance of angiosperm and bisaccate gymnosperm pollen, algae, and the occurrence of rare spores (Appendix B Supplementary data Table 3).

The initiation of the increase in the C–H assemblage appears to occur lower in the *M. testudinarius* Zone at 3.54 m, as evidenced by the slight increase in relative proportion of the areoligeracean dinocyst *Heterosphaeridium heteracanthum* and *Leiosphaeridia* prasinophyte algae (Fig. 11). Rare reworking of Devonian (*Densosporites*), Triassic (*Ovalipollis*), and Jurassic to mid-Cretaceous terrestrial palynomorph and dinocyst taxa (*Callialasporites*, *Chasmatosporites*, *Densoisporites*, *Litosphaeridium*, *Muderongia*, *Nannoceratopsis*) occurs from 0.10 m to 4.08 m.

5.2.1. Palynological bioevents

Several stratigraphic markers occur through the section and are described in stratigraphic order from the lowest upwards.

5.2.1.1. Alterbidinium ioannidesii. *Alterbidinium ioannidesii* (Fig. 8L) is a high-latitude species and is typically recorded from the upper Santonian? – lower Campanian of the North Sea, and the Norwegian Sea (MAP pers. obs.). The LO of *A. ioannidesii* at Bocieniec is questionable at 1.79 m in the upper Santonian (high *U. socialis* Zone) immediately below the Hawks Brow CIE, but confident at 2.07 m within the Hawks Brow CIE, and confirm here the occurrence in the upper Santonian (Figs. 10, 11). Specimens of *A. ioannidesii* are particularly difficult to identify at Bocieniec, being very thin, pale and usually fragmentary.

5.2.1.2. Cannosphaeropsis utinensis *and* Senoniasphaera protrusa. The LOs of *Cannosphaeropsis utinensis* (Figs. 10, 12A) and *Senoniasphaera protrusa* (Figs. 10, 11, 12J) are recorded from 0.10 m at Bocieniec. The FADs of both species co-occur in the middle Santonian upper (*Micraster coranguinum* Zone) between the Haven Brow and Horseshoe Bay CIEs (see Section 7.5.1), so the absence of these species in the lowermost sample at 0.01 m may suggest an age of early middle Santonian or older for the basal glauconitic marl, but alternatively may be a product of the poor recovery of dinocysts from that sample (Appendix B Supplementary data Table 3).

Cannosphaeropsis utinensis and *S. protrusa* are frequent through the section up to 3.23 m in the upper Santonian (uppermost *M. laevigatus* Zone) below the Foreness FN2 CIE, and up to 4.98 m in the lower Campanian (*O. pilula* Zone) below the Rottingdean CIE, respectively. The HO of *S. congrensa* (Fig. 8E) ranges higher to the top of the section and therefore, somewhere above the Pilula CIE.

5.2.1.3. Chatangiella islae. A specimen of *Chatangiella islae* occurs at 0.88 m (Figs. 10, 12B) in the upper Santonian (*Uintacrinus socialis* Zone) at the base of the Buckle CIE. The genus *Chatangiella* is considered here (MAP pers. obs.) to have been particularly adapted to distal water masses, the single recovered specimen is assumed therefore, to be a fortuitous occurrence of the species at the proximal edge of its ecological range.

5.2.1.4. Cordosphaeridium catherineae. At Bocieniec, the LO of *C. catherineae* (Fig. 12C) occurs at 0.88 m (Fig. 10) in the upper Santonian (*U. socialis* Zone), at the base of the Buckle CIE. The HO was recorded at 2.34 m in the upper Santonian (low *M. laevigatus* Zone), immediately below the Foreness FN1 CIE.

5.2.1.5. Dimidium striatum. The tentative LO of *Dimidium striatum* (Fig. 12D) lies at 0.10 m at Bocieniec, questionably within the middle Santonian. Confident specimens occur persistently upwards from 0.54 m in the upper Santonian (*U. socialis* Zone) and below the Buckle CIE to 3.83 m below the Foreness FN3 CIE (Fig. 10).

5.2.1.6. Eisenackia? knokkensis. The LO of *E? knokkensis* (Fig. 12E) at Bocieniec is recorded at 1.16 m the mid-*U. socialis* Zone, immediately above the Buckle CIE, but the species occurs most abundantly above the FN2 CIE and around the LSE, with a highest occurrence at 4.63 m (Figs. 10, 11).

5.2.1.7. Ellipsodinium *spp.* Frequent *Ellipsodinium rugulosum* are only recorded at Bocieniec in the sample at 3.83 m, while *E. membraniferum* (Fig. 12F) are sporadic to occasionally persistent though the section with an HO at 4.48 m (Fig. 10). The latter event occurs immediately above the LSE at level of the C34n/C33r boundary.

5.2.1.8. Heterosphaeridium difficile. *Heterosphaeridium difficile* is generally sporadic at Bocieniec, but is occasionally frequent up to 4.26 m in the upper Santonian (*U. anglicus*? Zone), within the LSE (Fig. 10). Specimens are smaller and more gracile than the type specimen, but otherwise conform to the species concept (Fig. 12G).

5.2.1.9. Odontochitina porifera. At Bocieniec, *O. porifera* (Fig. 12H) occurs persistently upwards from 1.56 m in the upper Santonian (mid-*U. socialis* Zone) (Figs. 10, 11) between the Buckle and Hawks Brow CIEs. A rare and isolated specimen was recorded at 0.10 m in the questionably middle Santonian interval.

5.2.1.10. Rhynchodiniopsis saliorum. The LO of *Rhynchodiniopsis saliorum* (Fig. 12I) occurs at 1.79 m at Bocieniec in the upper Santonian, towards the top of the *U. socialis* Zone, immediately below the Hawks Brow CIE (Figs. 10, 11). It is rare to frequent, but persistently recorded up to 4.63 m in the lowermost Campanian, between the LSE and the Rottingdean CIEs.

5.2.1.11. Palaeohystrichophora infusorioides. This species dominates the marl facies at Bocieniec and broadly decreases in relative abundance upwards from 0.10 m to 3.83 m in the upper Santonian (*M. testudinarius* Zone) below the Foreness FN3 CIE (Figs. 10, 11).

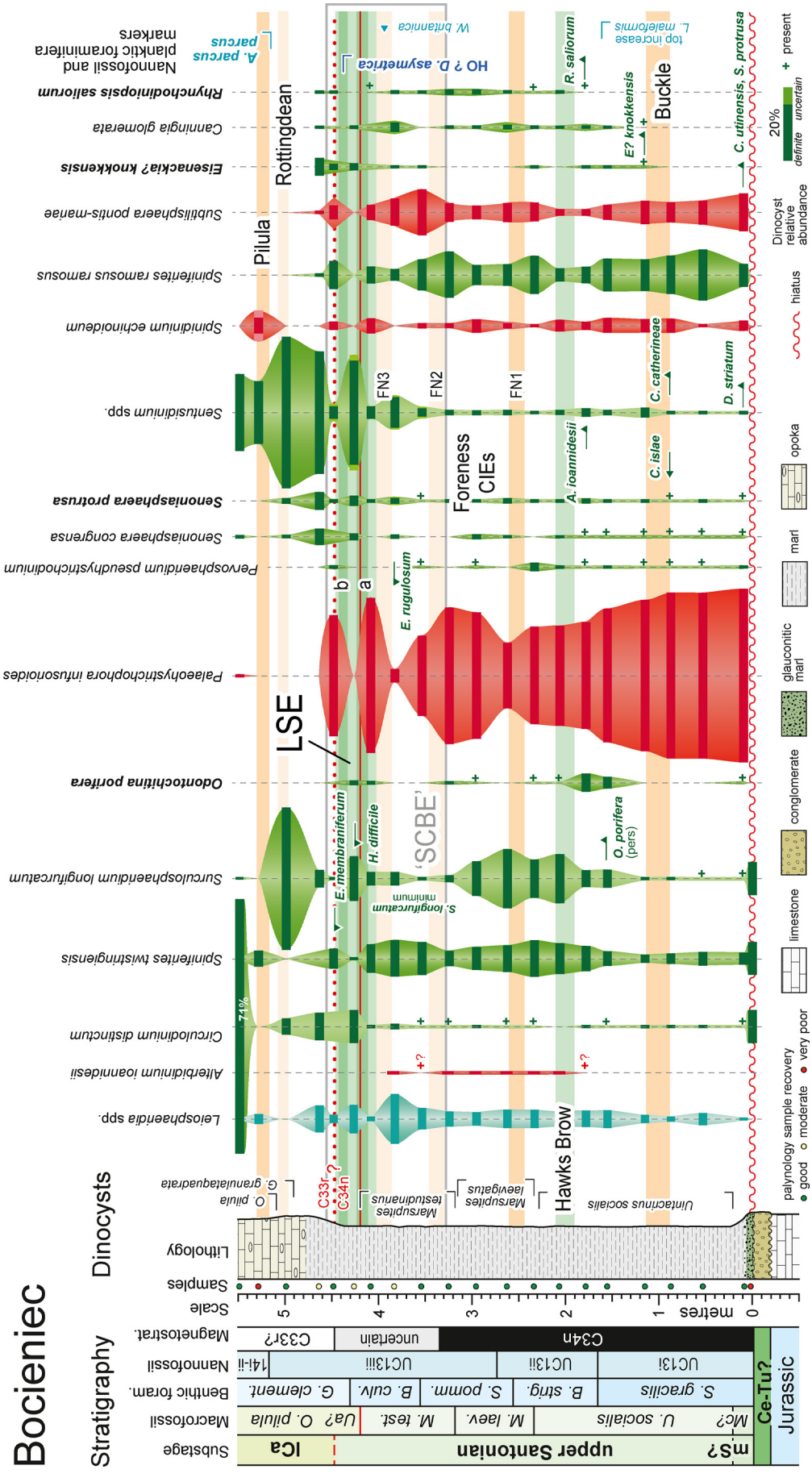
Bocieniec
Stratigraphy
Dinocysts
Jurassic
Ce-Tu?
mS?
upper Santonian
ICa
Substage
Macrofossil
Benthic foram.
Nannofossil
Magnetostrat.
Scale
Samples
Lithology
metres
M. socialis
U. socialis
S. gracilis
B. stria.
S. pomm.
B. culv.
G. clement.
O. pilula
M. test.
M. laev.
Ua?
UC13i
UC13ii
UC13iii
14i-ii
C34n
uncertain
C33r?
C33r
C34n
O. pilula
G. granulataquadrata
Marsupites testudinarius
Marsupites laevigatus
Hawks Brow
Uintacrinus socialis
Leiosphaeridia spp.
Alterbidinium ioannidesii
Circulodinium distinctum
Spiniferites twistringiensis
Surculosphaeridium longifurcatum
Odontochitina porifera
Palaeohystrichophora infusorioides
Pervosphaeridium pseudhystrichodinium
Senoniasphaera congrensa
Senoniasphaera protrusa
Sentusidinium spp.
Spiridinium echinoideum
Spiniferites ramosus ramosus
Subtilisphaera pontis-mariae
Eisenackia? knokkensis
Canningia glomerata
Rhynchodiniopsis sallorum
A. parcus
Nannofossil and planktic foraminifera markers
Pilula
Rottingdean
LSE
'SCBE'
FN3
FN2
FN1
Foreness CIEs
a
b
E. membranifertum
H. difficile
S. longifurcatum minimum
E. rugulosum
O. porifera (pers)
W. biannica
HO ? D. asymetrica
R. saliorum
top increase L. maleformis
A. ioannidesii
C. islae
C. catherineae
D. striatum
E? knokkensis
Buckle
C. utinensis, S. protrusa
71%
?
?
palynology sample recovery
good
moderate
very poor
limestone
conglomerate
glauconitic marl
marl
opoka
hiatus
Dinocyst relative abundance
20%
present
definite
uncertain

Conspicuously high abundances are recorded at the base and immediately above the top of the LSE, but the species is absent in the opoka facies at the top of the section.

5.2.1.12. Surculosphaeridium longifurcatum.
Surculosphaeridium longifurcatum (Fig. 12L) is one of the few dinocyst species observed in the poor recovery, lowermost sample at 0.03 m. The relative abundance increases to 2.96 m (apparently associated with declining *P. infusorioides*), marking the base of a low abundance interval from 3.25 m to 3.54 m within the upper Santonian (*Marsupites* Zone), around the Foreness FN2 CIE (Figs. 10, 11). Above 3.54 m, the species increases in relative abundance and is dominant at 4.98 m in the lower Campanian (*O. pilula* Zone), within the Rottingdean CIE, but is rare above.

6. Palynomorph assemblages and palaeoenvironments

Variations in palynological assemblage compositions spanning the Santonian–Campanian boundary at Seaford Head and Bocieniec are summarised in Figs. 9 and 13, respectively.

6.1. Seaford Head

Palynological assemblages at Seaford Head are overwhelming dominated by dinocysts throughout the Santonian–Campanian boundary interval. These are accompanied by a significant but subordinate proportion of prasinophycean algae (up to 25%), principally *Leiosphaeridia* spp. (Fig. 6, Appendix B Supplementary data Table 2), and smaller numbers of the acritarch *Paralecaniella indentata*, particularly in the upper Santonian, along with smooth algal cysts. The last of these become slightly more common in the upper half of the study interval. Terrestrial palynomorphs, represented by rare (<1%) bisaccate pollen, occur only sporadically through the section, together with occasional other pollen grains and very rare spores. They show no discernible stratigraphic trend.

6.1.1. Palynomorph abundance: chalks and marls

Palynomorph abundances at Seaford Head are generally low, averaging (with standard deviation) 310 ± 230 ppg, with lowest abundances (<100 ppg) observed in the mid-*O. pilula* Zone between the Pilula and Meeching CIEs (Fig. 9). The highest abundances are associated with marl seams: in additional to the regular metre-spaced sampling, samples of 4 prominent marl seams were taken: Friars Bay Marl 3, Saltdean Marl, Rottingdean Marl 2, and the Old Nore Marl, all of which yielded marginally higher palynomorph abundances than adjacent samples (up to 1400 ppg in the Old Nore Marl, Fig. 9). Many other marls sampled (e.g. Buckle Marl 3, Brighton Marl, Telscombe Marl 1) yielded low abundances, so palynomorph enrichment in marls is not universal and is associated with thicker, well-developed beds exhibiting elevated non-carbonate contents.

The mineralogy and chemistry of lower Campanian marl seams in East Sussex, have been studied principally from the Peacehaven Steps section (Old Nore Marl – Black Rabbit Marls succession, cf. Fig. 3), 7 km NW of Seaford Head, by Jeans et al. (2014) and Wray and Jeans (2014). All samples displayed a broadly similar <2 μm mineralogical composition consisting of smectite or smectite-rich illite-smectite with subordinate illite and minor amounts of talc. Typical sand and silt fractions of lower Campanian chalk residues consist mainly of chalcedonic and opaline silica, collophane, limonite and detrital quartz, together with authigenic apatite, quartz and alkali feldspar in the silt fraction (Weir and Catt, 1965; Jeans et al., 2014).

Most marl seams have elevated smectite contents and an acid-insoluble residue composition that is geochemically distinct from the over- and underlying white chalk. This indicates that marl seams are primary sedimentary features rather than being solely the products of pressure solution of carbonate along bedding planes during burial (cf. Garrison and Kennedy, 1977). Non-carbonate material found in white chalks and most marl seams is of detrital origin (Weir and Catt, 1965; Jeans et al., 2014; Wray and Jeans, 2014).

Higher palynomorph abundances in marl seams is likely a product of their lower carbonate contents. There is no increase in the relative proportion of terrestrial palynomorphs in any of the marls studied here (Appendix B Supplementary data Table 2). Most yielded no spores or pollen and none show anomalous dinocyst assemblages (e.g. P/G, C–H/S–P ratios, Section 6.1.3) compared to immediately under- or overlying white chalks (Figs. 6, 9). The different mineralogical composition of the marls must reflect differences in provenance and/or diagenesis that did not impact the palynology. Any environmental changes accompanying marl deposition had no discernible effect on the preserved organic-walled microbiota.

Uniquely in the lower Campanian, a negative europium anomaly and the associated trace-element geochemistry of the Old Nore Marl evidence a significant volcanically derived component in this marl. However, the proposed correlation of the Old Nore Marl (Wray and Jeans, 2014) with the M1 'bentonite' marl at Lägerdorf (Schönfeld et al., 1996) is challenged by our carbon isotope correlation (Section 7, Fig. 14), although the low-resolution of the Lägerdorf $\delta^{13}C_{carb}$ curve introduces some uncertainty.

6.1.2. Dinocyst species richness and diversity

Dinocyst species richness at Seaford Head varies between 30 and 64 per sample with no strong stratigraphic trend. A maximum of 64 species is observed above the Rottingdean Pair Marls in the lower part of the Rottingdean CIE, in the lower *O. pilula* Zone (Fig. 9). Diversity is similarly relatively stable throughout the succession with Shannon diversity *H* values of 1.7–3.4 and Fisher's α diversity values of 7–21. Stratigraphic diversity trends broadly track species richness and display no relationship to palynomorph abundance. Small diversity minima occur towards the top of the *U. anglicus* Zone within LSE peak b, and above the Saltdean Marl in the lower *O. pilula* Zone (Fig. 9).

6.1.3. Dinocyst assemblage composition

The ratio between peridinioid and gonyaulacoid dinocysts [P/G ratio: obtained by the equation P/G = nP/(nP + nG), where n is the number of specimens counted, P are peridinioid (or proto-peridinioid) dinocysts and G are gonyaulacoid dinocysts] shows significant changes through the succession (Fig. 9), driven principally by pulsed increases in the proportion of *Subtilisphaera pontis-mariae* in the upper Santonian, and *S. pontis-mariae* and

Fig. 11. Stratigraphic variation in the relative abundance of major palynological constituents through the Santonian–Campanian boundary interval, Bocieniec. See Fig. 4 for stratigraphy abbreviations and data sources. LOs, HOs and acmes of stratigraphically significant taxa are shown. Bold text of species names indicates the stratigraphically most significant taxa. Bars represent relative abundances determined in individual samples based on 200 dinocyst counts. Green, gonyaulacoid dinocysts; red, peridinioid dinocyst. Note the differentiation between definite (dark colour) and uncertain (pale colour) counts of specimens identified at specific level (Appendix B Supplementary data Table 3) contributing to the abundance bars. (For interpretation of the references to colour in this figure legend, the reader is referred to the Web version of this article).

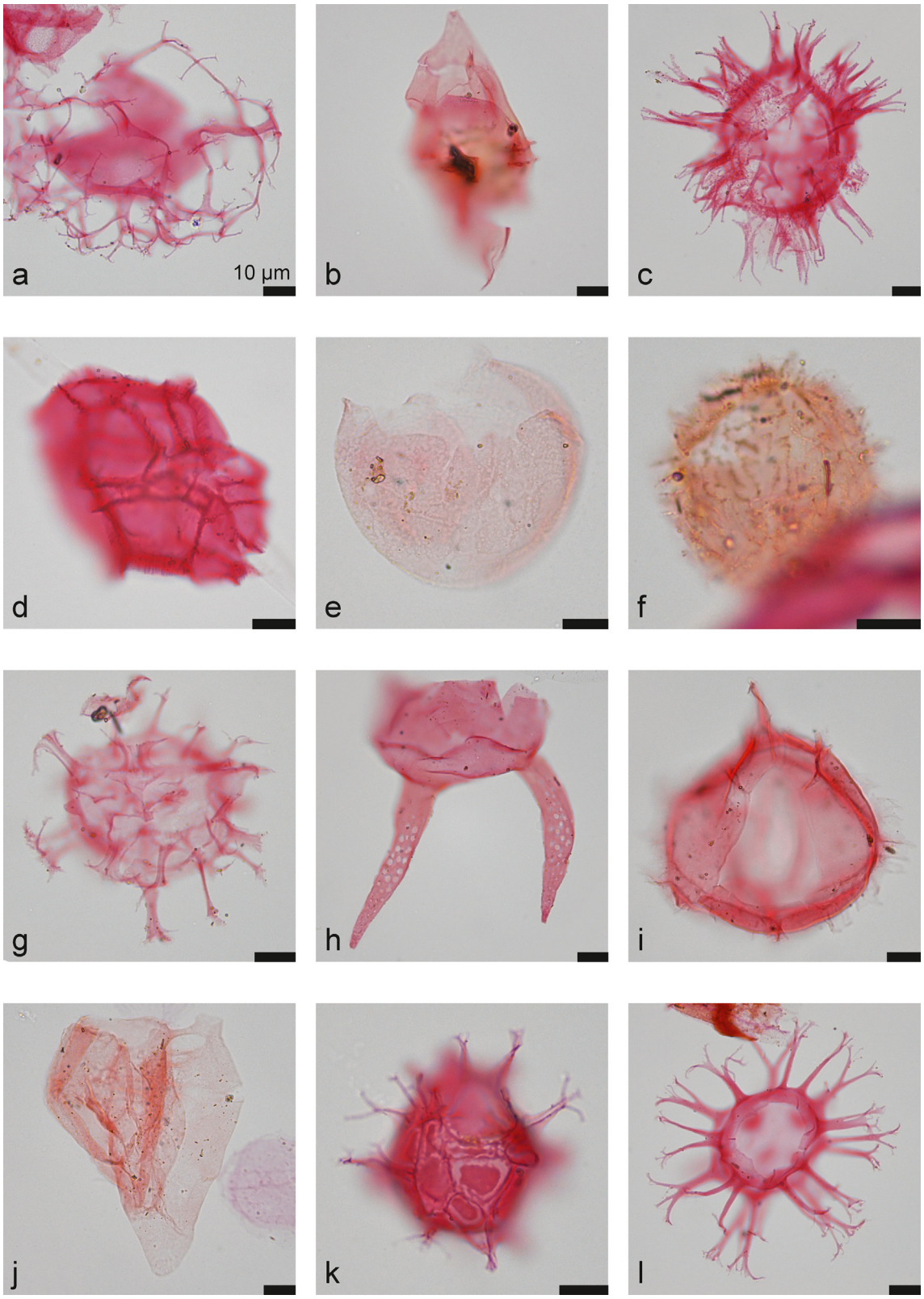

Fig. 12. Selected stratigraphically important dinocyst species from the Santonian–Campanian boundary interval, Bocieniec. **A**. *Cannosphaeropsis utinensis*, 0.88 m, EF: G44/1. **B**. *Chatangiella islae*, 0.88 m, EF: W32/4. **C**. *Cordosphaeridium catherineae*, 2.34 m, EF: L17. **D**. *Dimidium striatum*, 2.34 m, EF: G42/2. **E**. *Eisenackia*? *knokkensis*, 4.48 m, EF: L31/4. **F**. *Ellipsodinium membraniferum*, 2.96 m, EF: P23. **G**. *Heterosphaeridium difficile*, 4.62 m, EF: F34. **H**. *Odontochitina porifera*, 1.56 m, EF: G28. **I**. *Rhynchodiniopsis saliorum*, 4.08 m, EF: F19. **J**. *Senoniasphaera protrusa*, 4.48 m, EF: L33/1. **K**. *Spiniferites jarvisii*, 3.54 m, EF: L31. **L**. *Surculosphaeridium longifurcatum*, 2.63 m, EF: M43/2. Scale bars are 10 µm.

Palaeohystrichophora infusorioides in the lower Campanian (Fig. 6). P/G ratios range between 0.02 at 114 m and 123 m, and a maximum of 0.60 at 141–142 m. Marked P/G ratio increases occur in the lower part of the LSE, peaking around Friars Bay Marl 2 in the mid-*U. anglicus* Zone (Fig. 9), and at the level of the Op1 *Offaster pilula* band, coincident with the inferred position of the C34n/C33r boundary.

A marked shift in dinocyst assemblage composition is observed at the summit of the *O. pilula* Zone, with an influx in peridinioid cysts below the Meeching Pair Marls and a sharp increase in the P/G ratio from 0.07 at 138 m to 0.41 at 139 m (Fig. 9). A broad P/G acme in which peridinioid cysts predominate (P/G ratios 0.55–0.60) characterises the interval from below the Meeching Pair Marls to Telscombe Marls 1–3 between 140 and 143 m, and the P/G ratio remains high upwards to Castle Hill Flint 1, the top of our study section.

The *Circulodinium–Heterosphaeridium* (C–H)/*Spiniferites–Palaeohystrichophora* (S–P) assemblage ratio (Pearce et al., 2003, 2009; Prince et al., 2008; Jarvis et al., 2021) is less variable but displays a generally inverse pattern to the P/G ratio, with an overall falling (C–H)/(S–P) ratio [= nC–H)/n(C–H) + n(S–P), where n is the number of specimens counted] upwards (Fig. 9).

The P/G ratio is generally regarded as a proxy for nutrient availability and palaeoproductivity (Powell et al., 1992; Eshet et al., 1994; de Vernal and Marret, 2007; Pearce et al., 2009; Prauss, 2015; Tahoun et al., 2018; Amenábar et al., 2020; Leandro et al., 2020; Jarvis et al., 2021), based on observations of the distribution of living protoperidinioid dinoflagellates and their cyst records in associated sediments (e.g. Reichart and Brinkhuis, 2003). Application of the P/G ratio to the geological record assumes that extinct species of dinoflagellates generating P-cysts would have had the same heterotrophic habit as the living dinoflagellate genus *Protoperidinium*, while G-cysts would have originated from dinoflagellates with a phototrophic or mixotrophic behaviour (Sluijs et al., 2005; de Vernal and Marret, 2007; Esper and Zonneveld, 2007).

Protoperidinioid dinoflagellate species feed mainly on diatoms and other phytoplankton, so high relative abundances of P-cysts characterize areas of high organic productivity driven by elevated concentrations of dissolved nutrients in surface waters, such as upwelling zones, inner shelf environments, and estuaries (Powell et al., 1990; Sluijs et al., 2005; de Vernal and Marret, 2007). By contrast, a high relative abundance of G-cysts suggests nutrient-poor outer shelf or open ocean waters. However, it is known that some modern peridinioid dinoflagellates are phototrophic autotrophs (Dale and Fjellså, 1994; Sluijs et al., 2005), and no consensus exists on which Cretaceous peridinioid dinocysts are associated with heterotrophic dinoflagellates, which complicates the interpretation of the P/G ratio. However, evidence suggests (e.g. Eshet et al., 1994; Reichart and Brinkhuis, 2003) that although the inclusion of some peridinioid cysts from phototrophic dinoflagellate species in such a ratio will modify the palaeoenvironmental signal, but it should not obscure it.

The P/G acme at Seaford Head is driven principally by a marked influx of *P. infusorioides* (Fig. 6). This taxon is believed to be the cyst stage of a heterotrophic dinoflagellate that predominated at offshore sites of upwelling in Late Cretaceous epicontinental seas lacking significant terrestrial influence (Gedl, 2007; Pearce et al., 2009; Jarvis et al., 2021), or to be associated with episodes of increased runoff and supply of land-derived nutrients, with reduced salinity and stratified water masses (e.g. Van Helmond et al., 2014; Tahoun et al., 2018). Terrestrial palynomorphs are very minor constituents throughout the Santonian–Campanian boundary interval at Seaford Head and show no correlation to increases in P/G ratio (Appendix B Supplementary data Table 2). It is considered unlikely that an increased terrestrial nutrient supply was the mechanism driving phases of enhanced productivity, leaving pulsed marine upwelling events as the most likely potential cause.

It is notable that the P/G ratio increase and maximum spanning the *O. pilula–G quadrata* zone boundary at Seaford Head corresponds stratigraphically to the main phase of the "*pilula*-Transgression" of Niebuhr et al. (2000) [= "*senonensis* transgression" of Neumann et al. (2002)] in northern Germany; a NW European sea-level minimum and onset of sea-level rise at this level was proposed by Hancock (1993), arguably corresponding to the base of Sequence 3.5 of Haq et al. (1988). Our unpublished data from Trunch shows a marked P/G ratio increase at the same level as at Seaford Head. It may be speculated that sea-level rise and associated water mass reorganisation offer potential factors driving the productivity pulse identified at Seaford Head and Trunch, but additional records are required to test this further.

6.2. Bocieniec

With the exceptions of the lowest sample, a glauconitic marl taken from immediately above the Santonian unconformity, and a sample of chert at 5.28 m, palynological assemblages at Bocieniec are dominated by dinocysts throughout the Santonian–Campanian boundary succession (Fig. 13). These are accompanied by a significant but subordinate proportion of prasinophycean algae (up to 27%), principally *Leiosphaeridia* spp. (Fig. 11, Appendix B Supplementary data Table 3), and smaller numbers of the acritarch *Paralecaniella indentata*.

Terrestrial palynomorphs, represented principally by bisaccate pollen, occur in low numbers throughout the section, together with occasional other pollen grains and rare spores. However, they dominate the sample at the base of the Santonian section and, together with algae, they constitute a significant proportion of the assemblages spanning the stage boundary interval between 3.83 and 4.63 m (Fig. 13). The opoka sample at 5.28 m in the *O. pilula* Zone yielded 38% spores and pollen associated with 24% algal cysts and a low diversity dinocyst assemblage. The dinocyst assemblage changes to a dominance of C–H taxa in the upper beds with large sample-by-sample fluctuations in the proportions of *Circulodinium distinctum, Sentusidinium* spp. and *Surculosphaeridium longifurcatum*, the first of these constituting 71% of the assemblage in the uppermost sample (Fig. 11).

6.2.1. Dinocyst species richness and diversity

Dinocyst species richness at Bocieniec varies between 9 and 78 per sample, with a general trend of falling values upwards from the upper *U. socialis* Zone and Hawks Brow CIE towards *O. pilula* Zone at section top (Fig. 13, Appendix B Supplementary data Table 3). The lowest species richness was recorded in the lowest Santonian sample, which yielded only 9 dinocyst species, and values fall again in the lower Campanian opoka section above 4.80 m, where samples contained 10–14 species (Fig. 13). With the exception of the basal sample, diversity remains relatively constant throughout the Santonian section with an average species richness of 63 ± 15, Shannon diversity H values of 2.2–3.2, and Fisher's α values of 10–22. Lower diversity values characterise samples from the opoka facies of the *O. pilula* Zone (H = 0.8–1.9; α = 3–9), accompanying the significant fall in dinocyst species richness.

6.2.2. Palynological assemblage composition

The Santonian–Campanian boundary succession at Bocieniec is characterised by significant changes in the palynomorph assemblage composition (Fig. 13). The lowest sample, taken from the base of the glauconitic marl (0.03 m height) that immediately overlies the Santonian unconformity, yielded only a very low-abundance, low-diversity assemblage dominated by terrestrial palynomorphs,

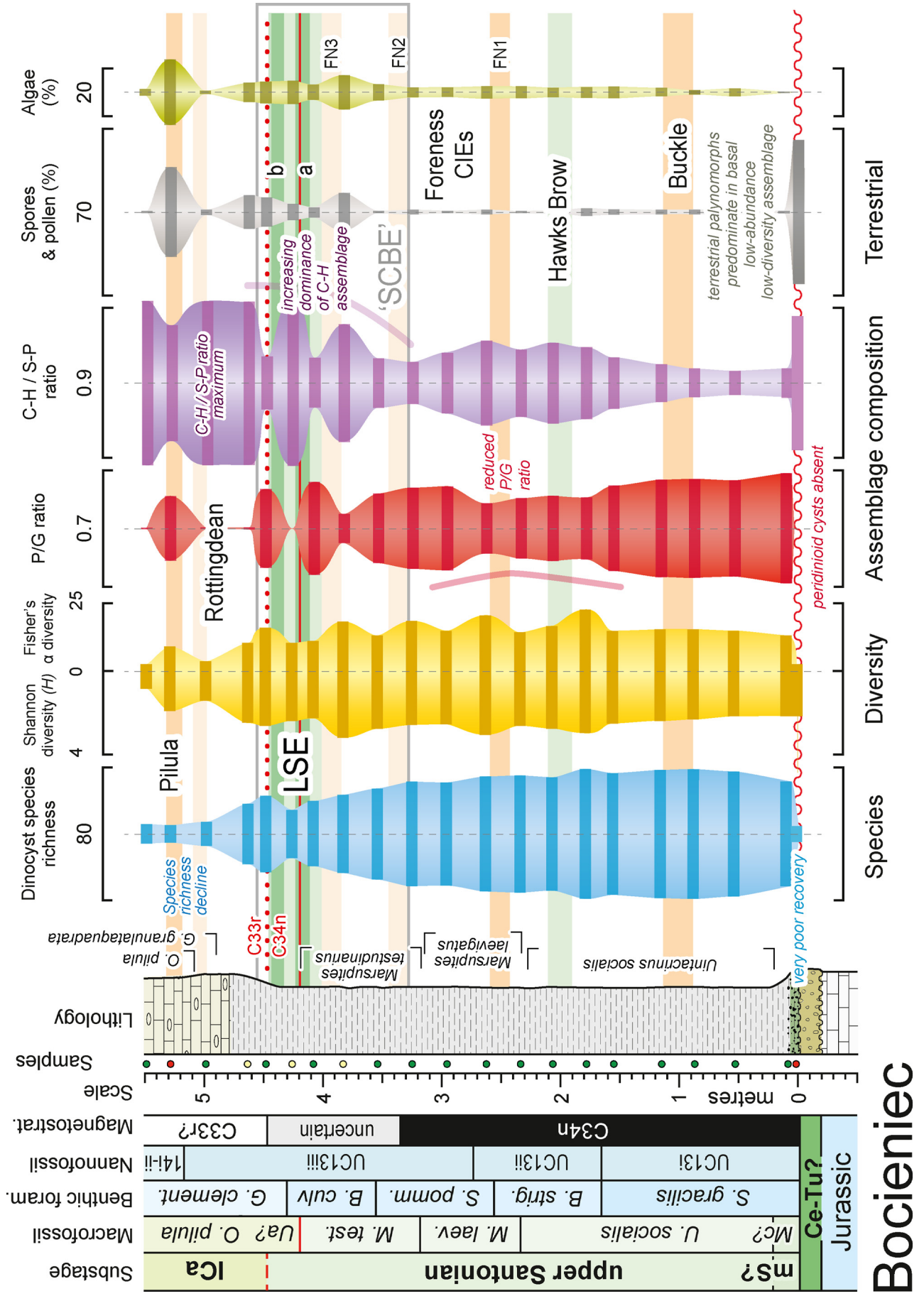
Substage
Macrofossil
Benthic foram.
Nannofossil
Magnetostrat.
Scale
Samples
Lithology
Dinocyst species richness
Shannon diversity (H)
Fisher's α diversity
P/G ratio
C-H / S-P ratio
Spores & pollen (%)
Algae (%)
Species
Diversity
Assemblage composition
Terrestrial
Jurassic
Ce-Tu?
mS?
upper Santonian
lCa
Mc?
U. socialis
M. laev.
M. test.
Ua?
O. pilula
S. gracilis
B. strig.
S. pomm.
B. cuv.
G. clement.
UC13i
UC13ii
UC13iii
14i-ii
C34n
uncertain
C33r?
meters
Pilula
Rottingdean
LSE
C33r
C34n
O. pilula
G. granulataquadrata
Species richness decline
Marsupites testudinarius
Marsupites laevigatus
Uintacrinus socialis
very poor recovery
peridinioid cysts absent
C-H/S-P ratio maximum
increasing dominance of C-H assemblage
'SCBE'
reduced P/G ratio
terrestrial palynomorphs predominate in basal low-abundance low-diversity assemblage
Foreness CIEs
Hawks Brow
Buckle
FN1
FN2
FN3
a
b
Bocieniec

principally bisaccate pollen together with *Deltoidospora* spp., *Tricolpites* spp., *Ericipites* spp. and *Monoporites* spp. These occur with 9 gonyaulacoid dinocyst species, fungal cell colonies and hyphae, and the acritarch *Paralecaniella indentata*.

An abundant and diverse assemblage with 64 species of dinocyst and dominated by peridinioid cysts (P/G ratio 0.66), principally *Palaeohystrichophora infusorioides* (48%), and only rare terrestrial palynomorphs (total count yields 1% spores and pollen) accompanies the change to marl facies at 0.10 m (Fig. 13). The high P/G ratio and the dominance of *P. infusorioides* continues upwards through the marl interval, falling slightly through the upper Santonian and showing a reduced P/G ratio (0.30) in the lower *M. laevigatus* Zone around the Foreness FN1 CIE.

A marked change in palynomorph assemblage composition is observed towards the top of the marls, in the *M. testudinarius* to *O. pilula* zones. A sharp decline in peridinioid dinocysts occurs above 3.54 m, with a fall in the proportion of *P. infusorioides* to 4% of the total count, which are replaced by typically nearshore dinocysts including *Circulodinium distinctum*, *Heterosphaeridium heteracanthum*, *Sentusidinium* spp. and *Surculosphaeridium longifurcatum* (see Pearce et al., 2003). Proportions of different dinocyst taxa fluctuate wildly across the stage boundary interval and in the overlying lower Campanian (Fig. 11). These produce variable P/G ratios of between 0 and 0.55 and a shift in the C–H/S–P ratio to values of between 0.30 and 0.99, but with an overall increasing dominance of the C–H assemblage towards the top of the section. These changes are accompanied by increases in the proportions of pollen, spores and prasinophycean algae.

These data suggest that relatively marginal marine conditions occurred immediately above the Santonian unconformity, with the deposition of glauconitic marl (cf. Wilmsen and Bansal, 2021). The transition to marls, above, reflects flooding with neritic and highly fertile surface waters which, due to the absence of terrestrial palynomorphs, likely received nutrients from coastal upwelling. A broadly regressive trend with decreasing distance to shoreline followed towards the top of the section, evidenced by the increasing proportion of spores and pollen, with a concomitant decline in surface water fertility, presumably due to an increasing distance from the upwelling source. Shoaling likely drove the transition from marls to opoka facies and silicisponge-dominated benthic communities (cf. Jurkowska et al., 2019a,b).

7. Towards a Santonian–Campanian boundary holostratigraphy for the Boreal and Tethyan realms

The upper Santonian–lower Campanian $\delta^{13}C_{carb}$ profiles for Seaford Head and Bocieniec are correlated to stratigraphically equivalent published curves for 3 Boreal Chalk successions in Fig. 14: the Trunch borehole eastern England (Jenkyns et al., 1994; Jarvis et al., 2002, 2006; Pearce et al., 2020); the Poigny borehole in the central Paris Basin (Chenot et al., 2016; Pearce et al., 2022); and Lägerdorf quarry north Germany (Voigt et al., 2010). The proposed correlation to a composite profile for the Tethyan limestone sections constituting the Campanian GSSP at Gubbio northern Italy (Thibault et al., 2016; Sabatino et al., 2018) is also shown (Fig. 14). This provides a basis for equating the Boreal and Tethyan biostratigraphic frameworks.

Key biostratigraphic datum levels, principally LOs and HOs derived from published macrofossil, microfossil, nannofossil and dinocyst records (see caption Fig. 14), and the new palynological data presented herein for Seaford Head and Bocieniec are plotted in Fig. 14. These may be used to better constrain isotope correlations based on $\delta^{13}C_{carb}$ profile values and morphology – the recognition of long-term trends and short-term positive and negative excursions (named CIEs), and to also test the regional synchroneity and reliability of the biotic markers. The integrated chemostratigraphy and biostratigraphy offers enhanced resolution and enables direct comparison between the stratigraphic positions of faunal and floral markers from different biotic provinces and/or different depositional environments and facies.

7.1. Macrofossil datum levels

Good consistency is observed between key macrofossil datum levels, where available, and the correlated CIEs in the five northern European sections, with the LO of *U. socialis* below the Buckle CIE, the LO of *Marsupites* (*M. laevigatus*) at the top of the Hawks Brow CIE, the LO of *M. testudinarius* below the Foreness FN2 CIE, the HO of *Marsupites* (*M. testudinarius*) at the top of LSE peak a, the LO of *O. pilula* towards the top of the LSE, and the HCO of *O. pilula* between the Pilula and Senonensis CIEs (Fig. 14). These placements are consistent with $\delta^{13}C_{carb}$ records from other European Chalk sections including Whitecliff IOW, Dover east Kent, and Danes Dyke east Yorkshire (Jarvis et al., 2006; Deville de Periere et al., 2019).

7.2. New carbon-isotope isotope events

The position of the upper Santonian Foreness negative CIE warrants further discussion. This was placed in the (undivided) mid-*Marsupites* Zone at Seaford Head, at the level of the Kempton Marl, by Jarvis et al. (2006), using the low-resolution $\delta^{13}C_{carb}$ data of Jenkyns et al. (1994). It is bounded by the "p1" and "q1" minor positive excursions below and above the event. This negative excursion lies in the basal *M. testudinarius* Zone of the current more refined stratigraphy (Fig. 3).

The new high-resolution $\delta^{13}C_{carb}$ profile presented here (Fig. 3) shows three distinct negative $\delta^{13}C_{carb}$ excursions within the *M. laevigatus–M. testudinarius* zones (equivalent to the undivided *Marsupites* Zone, i.e. the traditional '*M. testudinarius*' Zone of older literature, e.g. Mortimore et al., 2001). The most prominent $\delta^{13}C_{carb}$ minimum and turning point on the long-term profile spans the Brighton Five Marls in the mid-*M. laevigatus* Zone, below the Foreness CIE sensu Jarvis et al. (2006). A third negative excursion occurs in the mid-*M. testudinarius* Zone at the level of Sheepcote Valley Flint, immediately below the base of the LSE (Fig. 3).

The three negative excursions in the *M. laevigatus–M. testudinarius* zones are here designated the Foreness FN1–FN3 CIEs, with FN2 corresponding to the Foreness CIE as originally defined by Jarvis et al. (2006), but with FN1 representing a significant reversal point on the medium-term $\delta^{13}C_{carb}$ curve (= Foreness CIE sensu Thibault et al., 2016). These events may be problematic to differentiate in lower resolution isotope curves or in condensed sections, but they represent significant structure in the upper Santonian $\delta^{13}C_{carb}$ profile. The preferred correlation between our study sections is shown in Fig. 14.

Correlation of our new high-resolution $\delta^{13}C_{carb}$ profiles for Seaford Head to the other sections (Fig. 14) provides a basis to define 3 further new CIEs, based on the recognition of coherent structure within the different isotope profiles. These events are,

Fig. 13. Dinocyst assemblage parameter plots, with terrestrial palynomorphs (spores and pollen) and algae relative abundances for the upper Santonian–lower Campanian at Bocieniec. See Fig. 4 for stratigraphy abbreviations and data sources, and Fig. 9 for ratio definitions. Species richness and the P/G ratio decrease significantly at the top of the upper Santonian, with the stage boundary and LSE interval being characterised by a very low P/G ratio, a very high C–H/S–P ratio, and significantly increased numbers of spores, pollen and algae.

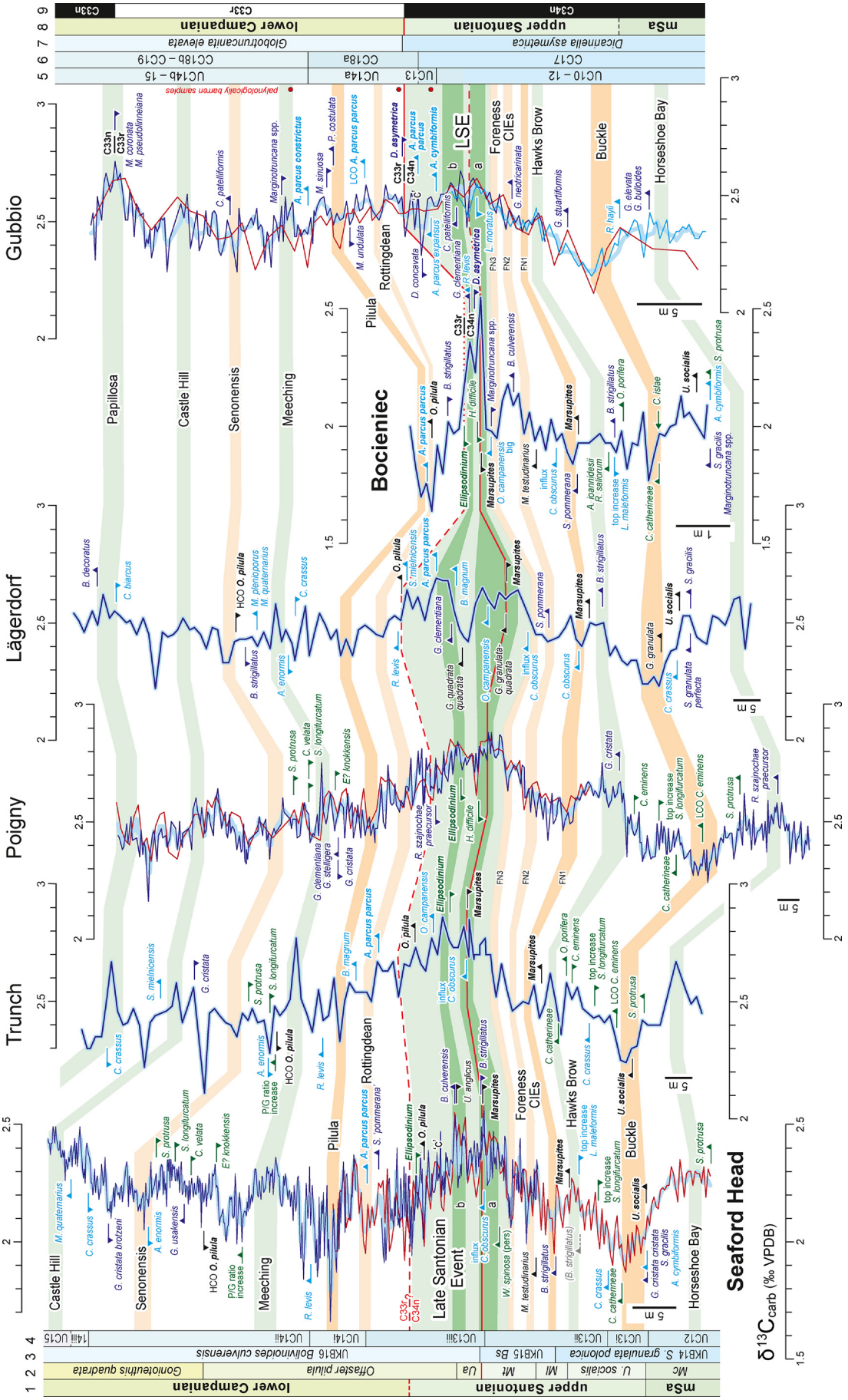
Gubbio
Lägerdorf
Poigny
Trunch
Seaford Head
Papillosa
Castle Hill
Senonensis
Meeching
Bocieniec
Pilula
Rottingdean
Foreness CIEs
Hawks Brow
Buckle
Horseshoe Bay
LSE
Late Santonian Event
lower Campanian
upper Santonian
mSa
Offaster pilula
Globotruncanita elevata
Dicarinella asymetrica
δ13Ccarb (‰ VPDB)

from base to summit, the: Rottingdean, Meeching, and Castle Hill CIEs, named after their proximity to key lithostratigraphic markers in the Seaford Head reference succession (Figs. 2, 3).

7.2.1. Rottingdean and Pilula CIEs

The Rottingdean CIE comprises a 0.2‰ low-amplitude short-term negative excursion with a 2.0‰ $\delta^{13}C_{carb}$ minimum situated between the Rottingdean Pair Marls and the Roedean Triple Marls, and incorporates the LO of *A. parcus parcus* at Seaford Head (Fig. 3). Significantly, it marks a distinct break in the long-term $\delta^{13}C_{carb}$ profile from falling values beginning above the top of the LSE to sharply rising values and a double peak above the Rottingdean CIE. The top of the CIE also corresponds to a sharp change in the $\delta^{18}O_{carb}$ profile from stable long-term values of around −2.5‰ through the upper Santonian and basal Campanian, to a steadily rising (i.e., cooling) trend above, reaching values higher than −1.5‰ $\delta^{18}O_{carb}$ at the section top (Fig. 3).

A larger amplitude (up to 0.5‰) negative $\delta^{13}C_{carb}$ excursion lying above the Rottingdean CIE, the Pilula CIE ("pillula Zone Event" of Thibault et al., 2016), is characterised by values falling to 1.8‰. This constitutes the ultimate minimum on the long-term falling trend above the base Campanian at Seaford Head, followed by rising values above.

7.2.2. Meeching CIE

The Meeching CIE is a well-developed broad maximum with values of up to 2.3‰ $\delta^{13}C_{carb}$ between the Meeching Flints and Meeching Triple Marl 3 (Fig. 3), in the upper part of the *O. pilula* Zone.

7.2.3. Senonensis and Castle Hill CIEs

The Castle Hill CIE comprises the $\delta^{13}C_{carb}$ maximum of around 2.5‰ occurring at the section top between Castle Hill Flints 8 and 9 and previously ascribed to the Papillosa CIE ("*papillosa* Zone Event") by Thibault et al. (2016). The Castle Hill CIE marks the top of a rising trend (albeit truncated by erosion at the section top) starting at a $\delta^{13}C_{carb}$ minimum at level of the Castle Hill Marls in the lower *G. quadrata* Zone that we correlate to the Senonensis CIE.

The placement of the Senonensis CIE in this study is 7 m higher at Seaford Head than that proposed by Thibault et al. (2016), based on new constraints provided herein by the HOs of the dinocysts *S. longifurcatum* and *S. protrusa* (Figs. 5, 14, Section 5.1.1) at Seaford Head and their equivalent positions in the Trunch and Poigny successions (Fig. 14; Pearce et al., 2022).

7.3. Utility of foraminifera markers

Benthic foraminifera have been widely used for stratigraphic purposes in most areas of the European epicontinental Upper Cretaceous (e.g. Vasilenko, 1961; Koch, 1977; Monciardini et al., 1980; Hart et al., 1989; Schönfeld, 1990; Wilkinson, 2011; Walaszczyk et al., 2016; Guzhikov et al., 2021). Their application for regional correlation is not without difficulties. Key biostratigraphic markers are provided principally by species of *Bolivinoides*, *Gavelinella* and *Stensioeina* (Hart and Swiecicki, 1987; Hart et al., 1989; Walaszczyk et al., 2016). Constituting part of the benthic epifauna and shallow infauna (e.g. Dubicka et al., 2018), these groups are sensitive to bottom water and sediment conditions and marker species may be rare, occur intermittently, or be entirely absent from some sections or stratigraphic intervals. Additionally, individual genera form evolutionary lineages of species that evolve from one to another, commonly with transitional forms and with overlapping ranges (e.g. Petters, 1977; Hart and Swiecicki, 1987; Dubicka and Peryt, 2014, 2016; Walaszczyk et al., 2016). Regional biostratigraphic correlation, based principally on the LO and HO datum levels of individual species within a lineage, is hampered by different morphological and nomenclatural interpretations made by different researchers.

The presence or absence and abundance of biostratigraphic marker species may show considerable differences between sections. It is regrettable that range charts showing sample-by-sample records and relative abundances of foraminifera are unavailable for Seaford Head (Hampton et al., 2007), Trunch (Wood et al., 1994) or Lägerdorf (Schönfeld, 1990), and no quantitative data have been published for Poigny (Robaszynski and Bellier, 2000; Robaszynski et al., 2005). This compromises the ability to critically assess the reliability of reported LO and HO datum levels in individual sections and precludes the use of more refined biostratigraphic criteria such as lowest and highest persistent or common occurrences.

Key Boreal benthic foraminifera taxa commonly used for zonation and correlation of Santonian–Campanian boundary intervals (e.g. Dubicka in Walaszczyk et al., 2016; Hart et al., 1989) include: *Stensioeina gracilis* Brotzen; *Gavelinella cristata* (Goel); *Bolivinoides strigillatus* (Cushman); *Bolivinoides culverensis* Barr; *Stensioeina pommerana* Brotzen; and *Gavelinella* ex gr. *clementiana* (d'Orbigny).

The LO of *Stensioeina gracilis* has been recorded along with the LO *G. cristata* (base BGS Subzone 18i) in Buckle Marl 1 at the base of the *U. socialis* Zone, below the Buckle CIE, at Seaford Head (Hampton et al., 2007). The LO of *S. gracilis* occurs at a comparable position at Lägerdorf (Fig. 11; Schönfeld, 1990); the species ranges upwards from the base of the marl section at Bocieniec (Dubicka et al., 2017). The appearance of *S. gracilis* has been interpreted to be a

Fig. 14. Carbon isotope stratigraphy and correlation of European Santonian–Campanian boundary successions. Carbon isotope events after Jarvis et al. (2006), Thibault et al. (2016) and this study. Biostratigraphic datum levels for key macrofossil (black), foraminifera (dark blue), calcareous nannofossil (pale blue) and dinocyst (green) taxa are shown. Stratigraphy: **1, 8**, substages, MSa, middle Santonian, with the base upper Santonian defined by the LO of *U. socialis* at the bottom of the Buckle CIE. The base of the lower Campanian is placed confidently at the base of Chron C33r for localities with magnetostratigraphy (solid horizontal red line, Bocieniec, Gubbio), with its inferred position (dashed red line) based on the carbon-isotope correlation elsewhere. The LAD *Marsupites* (traditional top of the Santonian in chalk facies) in the Boreal sections (solid red line within the LSE) is correlated to Gubbio (dashed red line) based on its position at the top of LSE peak a at Seaford Head. **2**, macrofossil zones: *Mc*, *Micraster coranguinum*; *U. socialis*, *Uintacrinus socialis*; *Ml*, *Marsupites laevigatus*; *Mt*, *Marsupites testudinarius*, *Ua*; *Uintacrinus anglicus*. **3**, UK benthic foraminifera zones (Hart et al., 1989): *Bs*, *Bolivinoides strigillatus*. **4**, UC calcareous nannofossil zones (Fritsen et al., 1999). **5**, UC calcareous nannofossil zones (Burnett et al., 1998). **6**, CC calcareous nannofossil zones (Sissingh, 1977; Perch-Nielsen, 1985). **7**, planktonic foraminifera zones (Coccioni and Premoli Silva, 2015). **8**, substages. **9**, chrons. Data sources – **Seaford Head**: carbon isotopes, dark blue (this study), red (Thibault et al., 2016), pale blue (3 point moving average, all data); macrofossils, Thibault et al. (2016), Mortimore (2021), this study; benthic foraminifera and nannofossils, Hampton et al. (2007); dinocysts, this study. **Trunch**: carbon isotopes, Jenkyns et al. (1994), Jarvis et al. (2006); macrofossils, Wood et al. (1994), Pearce et al. (2020); calcareous nannofossils, Burnett et al. (1998) plotted after Voigt et al. (2010), and Hampton et al. (2007); dinocysts, Pearce et al. (2020). **Poigny**: carbon isotopes, dark blue (Pearce et al., 2022), red (Chenot et al., 2016), pale blue (3 point moving average, all data); benthic foraminifera, Robaszynski and Bellier (2000), Robaszynski et al. (2005); dinocysts, Pearce et al. (2022). **Lägerdorf**: carbon isotopes, Voigt et al. (2010); macrofossils, Ernst and Schulz (1974); benthic foraminifera, Schönfeld (1990), calcareous nannofossils, Burnett et al. (1998) plotted after Voigt et al. (2010), and Hampton et al. (2007). **Bocieniec**: carbon isotopes, Dubicka et al. (2017); macrofossils, Dubicka et al. (2017), Gale et al. (in press); benthic foraminifera and calcareous nannofossils, Dubicka et al. (2017); dinocysts, this study. **Gubbio**: carbon isotopes, dark blue Bottaccione Road (Sabatino et al., 2018), medium blue Bottaccione River, lower section, red Bottaccione Road, low resolution (Thibault et al., 2016); planktonic foraminifera, calcareous nannofossils and magnetostratigraphy, Coccioni and Premoli Silva (2015), Miniati et al. (2020), Maron and Muttoni (2021). Preparation of three palynological test samples from the Bottaccione Road section (red-filled circles) for this study all proved to be barren. (For interpretation of the references to colour in this figure legend, the reader is referred to the Web version of this article).

relatively rapid event of speciation from the *Stensioeina exsculpta* lineage that provides a high stratigraphic value (see Dubicka and Peryt, 2014). The *S. gracilis* Zone is a partial range zone spanning the top middle Santonian–mid-upper Santonian (LO *S gracilis* to LO *B. strigillatus*) in Poland (Dubicka in Walaszczyk et al., 2016). The occurrence of the taxon at the base of the Bocieniec marls (Fig. 4) confirms that these are uppermost middle Santonian or higher.

Bolivinoides strigillatus is a key marker species for the Santonian–Campanian boundary interval in northern Europe constituting the index taxon of UKB15 *B. strigillatus* taxon range zone of Hart et al. (1989), British Geological Survey partial range Subzone 18iii (Wilkinson, 2011, 2013), and the *B. strigillatus* partial range zone in Poland (Dubicka in Walaszczyk et al., 2016). The species forms part of an evolutionary sequence of *B. strigillatus* to *B. culverensis* (Barr, 1966, 1967; Dubicka and Peryt, 2016). *Bolivinoides culverensis* has generally been regarded as a lower Campanian species (Bailey et al., 1983; Hart et al., 1989; Wilkinson, 2011, 2013; Walaszczyk et al., 2016) but ranges down to middle of the LSE (peak b) at Seaford Head and therefore occurs in the upper Santonian (Fig. 14). *Bolivinoides strigillatus* is rare and occurs sporadically in the Chalk of southern England (Hampton et al., 2007). Its LO at Seaford Head has been recorded in the mid-*M. laevigatus* Zone at the base of the Foreness FN1 CIE (Fig. 11). However, records from elsewhere in southern England indicate a FAD somewhat lower, below the Hawks Brow Flint (Wilkinson, 2013), i.e. below the Hawks Brow CIE at the summit of the *U. socialis* Zone (grey colour dashed LO marked in Fig. 14). This lower placement agrees well with its position at Lägerdorf (Schönfeld, 1990) and Bocieniec (Dubicka et al., 2017).

The LO of *S. pommerana* occurs towards the base of the *M. laevigatus* Zone at Bocieniec (Dubicka et al., 2017) and somewhat higher, in the middle of the undivided *Marsupites* Zone at Lägerdorf (Schönfeld, 1990). The species is considered to be a mid-*O. pilula* Zone species in southern England (Wilkinson, 2011): the LO of '*S. pommerana*' was recorded in the Rottingdean Pair Marls (Fig. 14), base of the Rottingdean CIE at Seaford Head by Hampton et al. (2007), but it was acknowledged that transitional species occur lower. The reliability of the LO of *S. pommerana* as a biostratigraphic datum level is therefore doubtful.

The LO of *B. culverensis* has been recorded immediately above the HO of *U. anglicus* (i.e. base of the *O. pilula* Zone), at the top of LSE peak b at Seaford Head (Fig. 14; Hampton et al., 2007), but it has been reported in the lower *M. testudinarius* Zone at Bocieniec (Dubicka et al., 2017). The HO of *B. strigillatus*, the ancestral species, occurs above the HO of *Marsupites* in the two sections, but is significantly higher at Bocieniec (Fig. 14). The HO of *B. strigillatus* at Lägerdorf has been placed close to the top of the *O. pilula* Zone (Schönfeld, 1990). The varying positions of these *Bolivinoides* datum levels may be due to variations in species concepts between authors.

The LO of *G.* ex gr. *clementiana* lies within LSE peak b both at Lägerdorf and Bocieniec (Schönfeld, 1990; Dubicka et al., 2017), marking the base of the *G. clementiana* partial range zone of Dubicka (in Walaszczyk et al., 2016; Fig. 4). The LO of *G. clementiana* has been recorded much higher at Poigny (Robaszynski and Bellier, 2000; Robaszynski et al., 2005), below the Meeching CIE (Fig. 14). The taxon is unrecorded at Seaford Head and occurs rarely in the upper *G. quadrata* Zone elsewhere in southern England (Wilkinson, 2011, 2013), so it has limited stratigraphic value. Published benthic foraminifera records from the higher *O. pilula* Zone and lowest *G. quadrata* Zone show poor consistency between our study sections.

Planktonic foraminifera generally show limited diversity, occur in low numbers, and offer poor stratigraphic resolution within Boreal Santonian–Campanian chalk sections (e.g. Dubicka in Walaszczyk et al., 2016; Hart et al., 1989; Peryt et al., 2022); key Tethyan marker species are exceedingly rare or absent. By contrast planktonic taxa, principally globotruncanids and heterohelicids, provide the main means for correlating and dating equivalent Tethyan successions (e.g. Robaszynski et al., 1984; Premoli Silva and Sliter, 1995; Robaszynski and Caron, 1995; Coccioni and Premoli Silva, 2015). The Santonian–Campanian stage boundary is near coincident with the *Dicarinella asymetrica–Globotruncanita elevata* zone boundary: this is defined by the HO (presumed LAD) of *D. asymetrica* (Sigal) (Robaszynski et al., 1984) which lies 20 cm above the base of Chron C33r in the Bottaccione GSSP at Gubbio (Miniati et al., 2020).

Many significant planktonic foraminifera LO and HO datum levels occur within the Santonian–Campanian boundary succession at Gubbio (Coccioni and Premoli Silva, 2015; Gale et al., in press), and the stratigraphic positions of these may be correlated to the northern European biostratigraphy using a combination of calcareous nannofossil biostratigraphy (Section 7.4, below) and carbon isotope stratigraphy (Figs. 14, 15). The Bocieniec succession (Dubicka et al., 2017) uniquely provides magnetostratigraphic and Tethyan planktonic foraminifera records in a succession yielding Boreal macrofossils and benthic foraminifera with a carbon isotope record that helps tie together the Boreal and Tethyan stratigraphic frameworks (Fig. 14).

7.4. Calcareous nannofossil events

The calcareous nannofossil biostratigraphy of the Santonian–Campanian boundary interval has been described from multiple sections, including Boreal chalks and marls (Burnett et al., 1998; Fritsen et al., 1999; Hampton et al., 2007; Dubicka et al., 2017; Guzhikov et al., 2021), Tethyan carbonates (Gardin et al., 2001; Tremolada, 2002; Wolfgring et al., 2018a,b; Miniati et al., 2020), US Western Interior and Gulf Coast localities (Gale et al., 2008; Kita et al., 2017), and ocean drilling sites (Stradner and Steinmetz, 1984; Bralower and Siesser, 1992; Petrizzo, 2000). The fossil group provides the main means for biostratigraphic correlation of the boundary interval on a global scale (cf. Sissingh, 1977; Roth, 1978; Perch-Nielsen, 1985; Bralower et al., 1995; Burnett et al., 1998), as reviewed recently by Dubicka et al. (2017 fig. 14), Miniati et al. (2020 fig. 6) and Gale et al. (in press).

The LO of *Arkhangelskiella cymbiformis* Vekshina, the basal marker of nannofossil Zone UC13, was interpreted by Burnett et al. (1998) to be a lower Campanian marker. However, the species first appears at the base of the upper Santonian *U. socialis* Zone, immediately below the Buckle CIE at Seaford Head (Hampton et al., 2007), and ranges up from the base of the marls at Bocieniec (Dubicka et al., 2017). The species first occurs in the middle Santonian upper *M. coranguinum* Zone and below the Horseshoe Bay CIE at Trunch and Lägerdorf (Hampton et al., 2007), short distances below the bases of our study intervals. Similarly, the LO of *A. cymbiformis* occurs below the LO *U. socialis* in Texas (Gale et al., 2008). Kita et al. (2017) reported the species ranging well down into the upper Santonian, to the base of their study sections in the Western Interior. By contrast, the LO of *A. cymbiformis* at Gubbio (Coccioni and Premoli Silva, 2015; Miniati et al., 2020) lies considerably higher, above peak b of the LSE (Fig. 14). This diachroneity of the datum level shows that it cannot be used as a reliable stage boundary marker, and this severely compromises the stratigraphic utility of the UC13 Zone (Fig. 14).

The LO of *Cylindralithus crassus* Stover, the taxon used to define the base of UC13ii in the North Sea (Fritsen et al., 1999), occurs in the mid-*U. socialis* Zone at Seaford Head (Hampton et al., 2007). This event appears to correlate regionally, occurring at an equivalent level in the Trunch borehole and slightly lower in the *U. socialis* Zone at Lägerdorf (Fig. 14). By contrast the HO of *C. crassus* reported by Hampton et al. (2007), the marker for the base of Zone UC14iii,

shows significant diachroneity between Seaford Head, Trunch and Lägerdorf (Fig. 14). The species is unrecorded from the other sections.

Lucianorhabdus maleformis Reinhardt shows similar distributions at Seaford Head and Bocieniec. It occurs frequently in the interval between the top *M. coranguinum* to upper *U. socialis* zones (top of the Horseshoe Bay to base of the Hawks Brow CIEs) at Seaford Head. At Bocieniec it is common from the base of the marls to the upper *U. socialis* Zone (immediately below the Hawks Brow CIE) (Hampton et al., 2007; Dubicka et al., 2017).

Calculites obscurus (Deflandre) Prins and Sissingh is another nannofossil showing comparable distributions in multiple sections (Fig. 14). The LO of this taxon is used to place the base of Zones CC17 and NC17 (Sissingh, 1977; Roth, 1978; Perch-Nielsen, 1985; Burnett et al., 1998), and the LO has generally been regarded as an upper Santonian marker. However, the LO of the taxon has been reported in the middle Coniacian *M. coranguinum* Zone at Seaford Head (Hampton et al., 2007), below the Kingsdown CIE, although its occurrence here is sporadic. The abundance of *C. obscurus* increases upwards at Seaford Head towards the top of the middle Santonian above the Horseshoe Bay CIE, coincident with an increase in *L. maleformis* (Hampton et al., 2007). This is likely equivalent to the position of the LO of *C. obscurus* recorded elsewhere, used to place the base of the CC17 and NC17 Zones. The species was noted as being common in the *Marsupites* Zone at Lägerdorf by Burnett (1990). A significant influx of *C. obscurus*, used to mark the base of Subzone 13iii, has been recorded at the top of the *M. testudinarius* Zone at both Seaford Head and at Trunch (Hampton et al., 2007), and somewhat lower in the *Marsupites* Zone at Lägerdorf (Fig. 14). An influx of *C. obscurus* occurs in the mid-*M. laevigatus* Zone at Bocieniec, where the taxon is also common in the lower *U. socialis* Zone (Fig. 4; Dubicka et al., 2017).

Orastrum campanensis (Cepek) Wind & Wise was originally considered to be a Campanian species (Wise and Wind, 1977; Perch-Nielsen, 1985), although the taxon is now known to range down to the Coniacian–Santonian boundary in the Western Interior (Blair and Watkins, 2009). Nonetheless, the LO of consistent *O. campanensis* occurs within the LSE at Trunch and Lägerdorf (Fig. 14) based on the records of Burnett (1990) and Burnett et al. (1998), as plotted by Voigt et al. (2010 fig. 3). This event was not identified at Seaford Head by Hampton et al. (2007), but the LO of large *O. campanensis* occurs near the top of the *M. testudinarius* Zone at Bocieniec (Fig. 4), coincident with the lowest consistent occurrence of the species. The LO of consistent *O. campanensis* has been recorded also in the lowest *U. anglicus* Zone in Texas (Gale et al., 2008), confirming a close association of the nannofossil event with the level of the LSE, albeit with minor differences in stratigraphic level reported from different sections.

The LO of *Aspidolithus parcus parcus* (Stradner) Noël, the basal marker of the CC18, NC18 and UC14 Zones (Sissingh, 1977; Roth, 1978; Perch-Nielsen, 1985; Burnett et al., 1998), occurs immediately below the Roedean Triple Marls in the lower *O. pilula* Zone (Hampton et al., 2007), at the base of the Rottingdean CIE at Seaford Head (Fig. 3). The stratigraphic positions of the LOs of *A. parcus parcus* at Trunch and Lägerdorf, as reported by Hampton et al. (2007 p. 52), are closely comparable to this (Fig. 14).

It should be noted that there are different taxonomic views regarding the generic assignment and subspecies definition of *Aspidolithus* species and subspecies. Boreal workers typically ascribe the taxon to *Broinsonia* Bukry. This genus was published slightly before *Aspidolithus* and Noël (1970) placed the genera in synonymy. *Broinsonia* has been used by some authors for forms with an axial cross, and *Aspidolithus* for those with a central plate, and Perch-Nielsen (1979, 1985) suggested to retain the two distinct genus names. These issues were reviewed by Miniati et al. (2020) who published a taxonomic revision formalising the two-fold generic classification.

Within the *Aspidolithus* lineage, the sequential appearances of *A. parcus expansus*, *A. parcus parcus* and *A. parcus constrictus* are marked by a gradual reduction of the central area/margin ratio, as described by Wise (1983). Subspecies assignments require careful biometric analysis, and different criteria for the definition of subspecies have been employed by different workers (e.g. Wise, 1983; Gardin et al., 2001; Wolfgring et al., 2018b), so stratigraphic comparisons between studies by different groups must be treated with caution.

In the Bottaccione GSSP at Gubbio, *A. parcus parcus* is extremely rare and discontinuous at the base of its range (Miniati et al., 2020), only becoming continuous and frequent above the Rottingdean CIE, plotted as the lowest common occurrence of the subspecies in Fig. 14. Nannofossil preservation at Gubbio is moderate to poor, but the LO of common *A. parcus parcus* there compares well with the stratigraphic position of the LO recorded in the other sections, although the bases of Zones UC14a and CC18a at Gubbio are placed at the FAD of *A. parcus parcus* in Fig. 14, following Coccioni and Premoli Silva (2015) and Miniati et al. (2020).

The LO of *Reinhardtites levis* Prins and Sissingh occurs in the mid-*O. pilula* Zone a short distance above the Pilula CIE at both Seaford Head and Trunch but is recorded lower, coincident with the LO of *A. parcus parcus*, at Lägerdorf (Fig. 14; Hampton et al., 2007). The HO of *Aspidolithus enormis* (Shumenko) lies in the basal *G. quadrata* Zone below the Senonensis CIE at Seaford Head and at a comparable level at Trunch. The HO of *Cylindralithus crassus* has been recorded near the top of our study sections in both cases (Hampton et al., 2007).

The relationships between the inception (FAD) of *A. parcus parcus*, the extinction level (LAD) of *M. testudinarius*, the LAD of *U. anglicus*, and the FAD of *O. pilula*, together with the position of the C34n/C33r palaeomagnetic reversal and the FAD of *D. asymetrica* (see Fig. 14), are of key importance for defining the Santonian–Campanian stage boundary (Gale et al., in press).

7.5. Dinocyst events

Key stratigraphically significant dinocyst events at Seaford Head and Bocieniec have been discussed in Sections 5.1.1 and 5.2.1, respectively. A selection of these events may be used to further constrain correlations between the two GSSP auxiliary sections and the Chalk sections at Trunch and Poigny (Fig. 14). Palynological data are currently lacking from Lägerdorf. Sadly, a pilot study of 3 samples from the Santonian–Campanian stage boundary interval in the Gubbio GSSP (Fig. 14) indicates that this part of the section is effectively barren of palynomorphs.

Integration of the new dinocyst records presented in this paper with published results from complementary Chalk studies provides a basis for defining a series of biostratigraphic datum level considered to define the Santonian–Campanian boundary interval. These are summarised below and plotted in Fig. 15.

7.5.1. Principal dinocyst events

Seventeen stratigraphically important events (Fig. 15, events in green) are described in sequential order, with the oldest first.

7.5.1.1. FAD of Senoniasphaera protrusa. The LO of *Senoniasphaera protrusa* (Figs. 8G, 12J) occurs in the middle Santonian between the Horseshoe Bay and Buckle CIEs at Trunch and Poigny (Pearce et al., 2020, 2022), and ranges to the base of the marls at Bocieniec (Fig. 14).

As discussed by Pearce et al. (2020 p. 50), the LO of *S. protrusa* has stratigraphic value, although the FAD of the taxon in

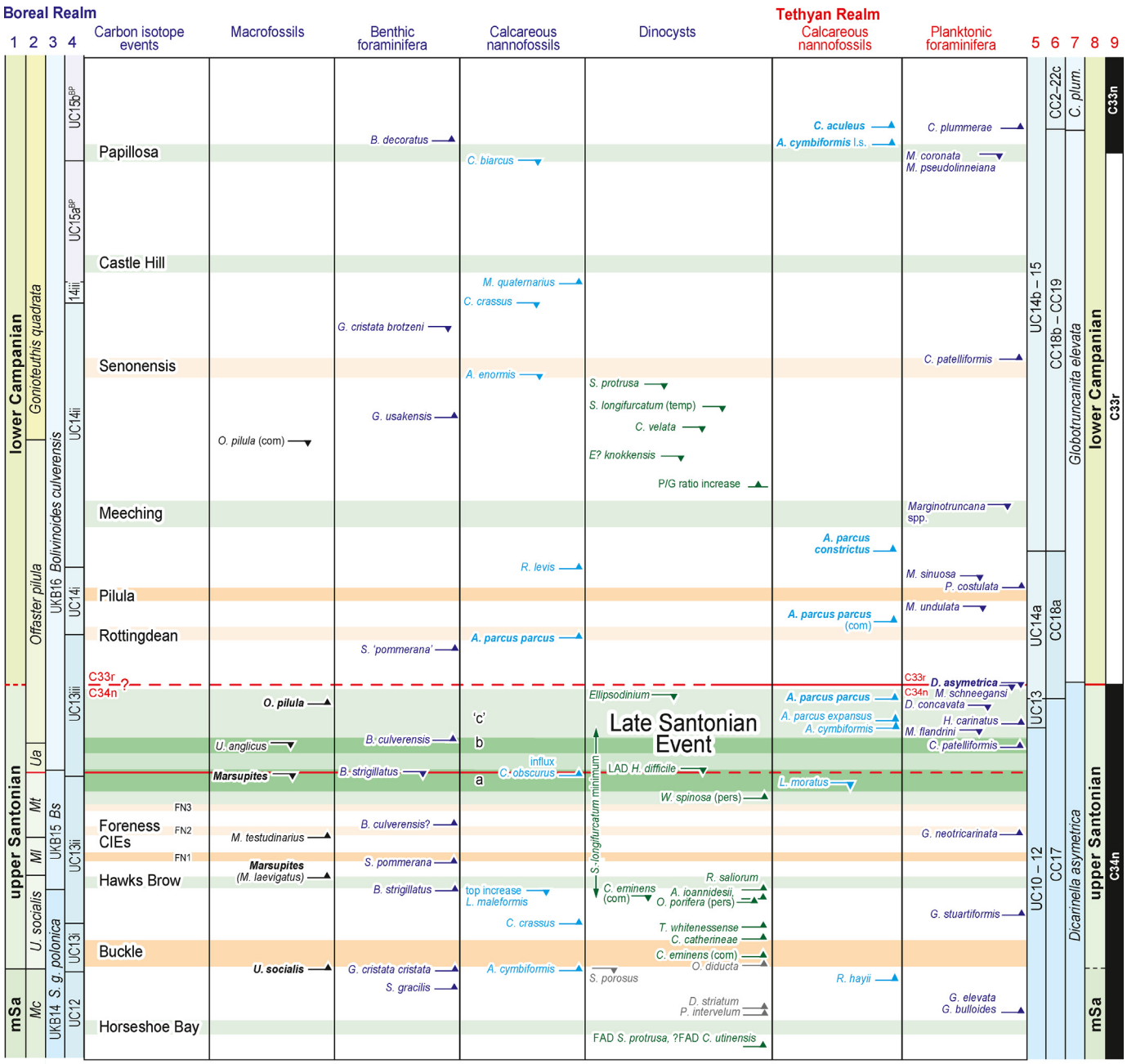

Fig. 15. Holostratigraphy of the Santonian–Campanian boundary interval in Europe showing the carbon isotope event stratigraphy and the relative positions of key biostratigraphic marker taxa, standard regional biozones, and the C34n/C33r magnetic reversal. The placement of markers is derived from the regional chemo- and biostratigraphic correlation (Fig. 14). Primary events are in bold. Stratigraphy: **1, 8**, substages, with the base upper Santonian defined by the LO of *U. socialis* and the base lower Campanian placed at the C34n/C33r boundary; mSa, middle Santonian; **2**, macrofossil zones – *Mc*, *Micraster coranguinum*, *U. socialis*, *Uintacrinus socialis*, *Ml*, *Marsupites laevigatus*, *Mt*, *Marsupites testudinarius*, *Ua*, *Uintacrinus anglicus*; **3**, UK benthic foraminifera zones (Hart et al., 1989), *Bs*, *Bolivinoides strigillatus*; **4**, UC calcareous nannofossil zones (Fritsen et al., 1999); **5**, UC calcareous nannofossil zones (Burnett et al., 1998); **6**, CC calcareous nannofossil zones (Sissingh, 1977; Perch-Nielsen, 1985); **7**, planktonic foraminifera zones (Coccioni and Premoli Silva, 2015) – *C. plum.*, *Contusotruncana plummerae*; **8**, substages; **9**, chrons (Miniati et al., 2020). The HO of *Marsupites*, the previously favoured position of the Santonian–Campanian boundary in Boreal sections, is highlighted (solid red horizontal line) for the Boreal Realm and correlated (dashed red line) to the Gubbio GSSP and Tethyan Realm based on $\delta^{13}C$ chemostratigraphy (Fig. 14). The Campanian stage boundary is placed at the base of Chron C33r (solid red line) with its chemostratigraphic correlation to the Boreal stratigraphy indicated by the dashed red line. Data sources for datum levels: macrofossils, Thibault et al. (2016), Mortimore (2021), this study; benthic foraminifera and calcareous nannofossils, Hampton et al. (2007); dinocysts, this study with additional Chalk datum levels (in grey) after Prince et al. (1999), Pearce et al. (2020, 2022); Tethyan calcareous nannofossils and planktonic foraminifera, Coccioni and Premoli Silva (2015), Miniati et al. (2020). (For interpretation of the references to colour in this figure legend, the reader is referred to the Web version of this article).

the middle Santonian (between the Haven Brow and Horseshoe CIEs) was not captured by the present study at Seaford Head. However, preliminary data from the section indicate that the species does extend downwards in the *M. coranguinum* Zone to the Horseshoe Bay CIE. The LO of *S. protrusa* has been recorded slightly higher, between the Horseshoe Bay and Buckle CIEs at Trunch (Pearce et al., 2020) and in the Poigny borehole (Pearce et al., 2022) (Fig. 14).

Slimani (2001) recorded rare and sporadic specimens of *S. protrusa* in the upper Campanian of Beutenaken quarry (The Netherlands) and rare to common specimens in the upper Campanian of Hallembaye quarry (Belgium). However, according to the emended species description (Prince et al., 1999 p. 162): "*Senoniasphaera protrusa* differs from all other *Senoniasphaera* species by having an elongated inner and outer body which possess two antapical horns of unequal size, giving the cyst its characteristic elongate and asymmetrical shape". Photographs of *S. protrusa* from Hallembaye (Slimani, 2000 plate 5, figures 9, 10) that conform to the original description of the species illustrate a bilaterally symmetrical specimen of subequal width and length that we would now include in *Canningia glomerata*. We therefore exclude records of *S. protrusa* by Slimani (2001), as he may have been unaware of the emendation. It is notable that *S. protrusa* has not been recorded from the upper Campanian of the Meer borehole (northern Belgium; Slimani et al., 2011) or Tercis (western France; Antonescu et al., 2001a,b; Schiøler and Wilson, 2001).

With very few exceptions, specimens conforming to the latest emendation of *S. protrusa* are not known from the Southern Hemisphere; therefore, the FAD in the middle Santonian (Fig. 15) is useful for the Northern Hemisphere only (Pearce et al., 2020).

7.5.1.2. FAD of Cannosphaeropsis utinensis. Based on the lowest coincident occurrence of both *Cannosphaeropsis utinensis* (Fig. 12A) and *S. protrusa* in the Duttières 3 borehole, Vendée, western France (Azema et al., 1981), Pearce et al. (2020, see also their fig. 18) suggested that these species have a similar FAD (i.e in the middle Santonian, between the Haven Brow and Horseshoe CIEs). Subsequently, Pearce et al. (2022) recognised that from $\delta^{13}C$ calibrated sections, the LO of *C. utinensis* appears to have a diachronous northward migration, possibly associated with progressive Late Cretaceous cooling. They noted that it appears in the uppermost middle Santonian, immediately below the Buckle CIE at Poigny, in the upper Santonian, *Uintacrinus socialis* Zone at Whitecliff, and in the *Marsupites* Zone, at the base of the LSE at Trunch. *Cannosphaeropsis utinensis* was not recorded at Seaford; however, it is interesting that the LO at Bocieniec is apparently synchronous with Poigny.

7.5.1.3. LCO of Chatangiella eminens. *Chatangiella eminens* was not encountered in the present study. However, it has proven to have some stratigraphically important events in the Anglo-Paris and southern North Sea basins and is briefly discussed here. The likely inception of *C. eminens* is probably in the middle Santonian. Specifically, the LO of *C. eminens* has been recorded within the Haven Brow CIE at Poigny (Pearce et al., 2022 fig. 3), slightly higher within the Horseshoe Bay CIE at Trunch and between Horseshoe Bay and Buckle CIEs at Whitecliff IOW (Pearce et al., 2020; Fig. 15). The variability is attributable to the generally rare and sporadic occurrence of the species. The LCO appears to be a much more reliable event and lies in the upper Santonian, lower *U. socialis* Zone within or immediately above the Buckle CIE at Poigny, Whitecliff IOW and Trunch (Figs. 14, 15). Both events have been proposed as correlatable datum levels (Pearce et al., 2020, 2022).

7.5.1.4. LO of Cordosphaeridium catherineae. This relatively new species (Pearce, 2010; Figs. 7C, 12C) is currently only known from NW Europe; Pearce et al. (2020) recorded a LO in the upper Santonian at the base of the Hawks Brow CIE, at the top of the *U. socialis* Zone in the Trunch borehole (Fig. 14). Recent work on the Poigny borehole (Pearce et al., 2022) extended the LO slightly lower, in the lower *U. socialis* Zone between the Buckle and Hawks Brow CIEs (Fig. 14). Results from Seaford and Bocieniec suggest a still lower LO, within the Buckle CIE (Fig. 14) at the base of the *U. socialis* Zone, but highlight its usefulness as an upper Santonian marker event (Fig. 15). At Bocieniec and Seaford, the species is rare and was only recorded outside of the main count of 200 dinocyst specimens, only Seaford had occurrences in the Campanian.

7.5.1.5. LO of Trimuridinium whitenessense. The LO of *Trimuridinium whitenessense* (Fig. 8I) was proposed as a late Santonian marker event situated immediately above the Buckle CIE by Pearce et al. (2020), based primarily on records from east Kent (Prince et al., 2008). The species was not recorded at Bocieniec, and occurs in only two samples from Seaford, which provide a range of mid-*U. socialis* Zone (above the Buckle CIE) to the base of the *O. pilula* Zone (mid-LSE). The range of *T. whitenessense* is confined to the lowest *O. pilula* Zone in the Trunch borehole (Pearce et al., 2020). Thus, despite the very sparse record at Seaford, the LO of *T. whitenessense* (Fig. 15) is consistent with the event stratigraphy of Pearce et al. (2020). The full stratigraphic range of the species remains uncertain.

7.5.1.6. LO of persistent Odontochitina porifera. Pearce et al. (2020) reported a LO (a likely FAD) of *Odontochitina porifera* (Figs. 7K, 9H) in the lower Santonian as a near globally synchronous event, while noting that a delayed LO in the upper Santonian is typical in NW Europe. They considered that the LO of *O. porifera* at Whitecliff IOW (Prince et al., 1999) in the *U. socialis* Zone between the Buckle and Hawks Brow CIEs to be representative. This is also closely comparable with the results from Trunch (Pearce et al., 2020). The record of the species at Poigny is poor; although it has been persistently recorded (Pearce et al., 2022), it is a rare component of the assemblages and the LO is recorded higher, within the LSE. Results from Bocieniec (Fig. 14) indicate the LO of persistent *O. porifera* is essentially synchronous with the LO at Whitecliff IOW and Trunch, between the Buckle and Hawks Brow CIEs. The rare and isolated specimen in the middle Santonian at Bocieniec corresponds to an older FAD suggested by Pearce et al. (2020). Given the possibility of rare *O. porifera* in the lower and middle Santonian, a LO of persistent specimens is coined here (Fig. 15).

7.5.1.7. LO of Alterbidinium ioannidesii. The LO of the confidently identified specimens (Fig. 8L) is observed at Bocieniec in the upper Santonian, *U. socialis* Zone immediately below the Hawks Brow CIE (although questionable specimens are recorded below this). Nøhr-Hansen et al. (2020) used the LO of *A. ioannidesii* to define the base of their late Santonian *Alterbidinium ioannidesii* (XI) Zone in NE Greenland. This Boreal species has been recovered from the Western Interior Seaway, Davies Strait, North Sea, and Norwegian–Greenland seas (see Pearce et al., 2020), but is apparently absent from the Anglo-Paris Basin (Poigny, Whitecliff IOW, Seaford). The LO at Bocieniec may represent the FAD of the species (Fig. 15).

7.5.1.8. HCO of Chatangiella eminens. The HCO of the species consistently lies in the upper Santonian, a short distance below the Hawks Brow CIE within the *U. socialis* Zone at Poigny, Whitecliff IOW and Trunch (Figs. 14, 15), and this event has been proposed as a correlatable datum level (Pearce et al., 2020, 2022). The species was not recorded at Bocieniec or Seaford Head, and it also appears to be absent from Santonian–Campanian sections in Kent (Prince et al., 2008). It has however, been observed in multiple Santonian intervals from exploration wells on the offshore Norwegian continental shelf (MAP pers. obs.).

7.5.1.9. FAD of Rhynchodiniopsis saliorum. The LO of *R. saliorum* (Figs. 8D, 12I) at Trunch (Pearce et al., 2020) and the LO of persistent specimens at Poigny in northern France (Pearce et al., 2022) occurs in the upper Santonian above the Foreness CIE, while in southern

England, it is recorded slightly stratigraphically lower (Prince, 1997, I.M. Prince pers. comm., 2021) at the Hawks Brow Flint (and therefore, within the Hawks Brow CIE). At Seaford Head, the LO of *R. saliorum* occurs above the Foreness FN1 CIE (Fig. 5), while at Bocieniec, the LO occurs immediately below the Hawks Brow CIE (Figs. 10, 11) and is apparently synchronous with southern England and is suggested to represent the FAD (Fig. 15). Since the observations from southern England are unpublished, the position of this FAD event can now be exemplified at Bocieniec (Fig. 14).

The conspicuously foveolate *Rhynchodiniopsis juneae* sp. nov. (Figs. 8B–C; Appendix A) encountered at Seaford Head (which has a similar distribution to *R. saliorum*) was also recorded by Pearce et al. (2022) as *Rhynchodiniopsis* sp. F at Poigny. The occurrences at Poigny appears to be correlatable with the persistently occurring specimens at Seaford.

7.5.1.10. Low abundance interval of Surculosphaeridium longifurcatum. The conspicuous decrease in relative numbers of *S. longifurcatum* (Figs. 8H, 12L) in the upper Santonian at Bocieniec and subsequent recovery into the lower Campanian has enabled the recognition of a low abundance interval that apparently also occurs at Poigny, Seaford, Whitecliff IOW and Trunch. At Poigny, Seaford and Trunch, the low abundance interval broadly spans the Hawks Brow to mid-LSE. At Whitecliff IOW, the low abundance interval spans the upper Santonian, mid-*U. socialis* to *G. quadrata* zones and a CIE correlation is required. The precise stratigraphic development of the low abundance interval varies between sections, and is presumably palaeoenvironmentally controlled; however, it is remarkable in being consistently symmetrical about a level that lies between the Hawks Brow and LSE (Fig. 15).

7.5.1.11. LO of persistent Whitecliffia spinosa. The LO of persistent *W. spinosa* (Fig. 8J) at Seaford Head in the *M. testudinarius* Zone (Fig. 5), at the base of the LSE, is marginally lower than the datum level proposed by Pearce et al. (2020) in the middle of the LSE, above the FAD of *U. anglicus*. However, placement of the datum level (Fig. 15) is somewhat subjective since the species is recorded more persistently and occurs in larger proportions upwards through its range to the top of the study section at Seaford Head. *Whitecliffia spinosa* was not documented at Bocieniec.

7.5.1.12. LAD of Heterosphaeridium difficile. *Heterosphaeridium* (Fig. 12G) is generally rare in the Santonian, typically the species is only relatively numerous or persistent in the lower Santonian and below (Pearce et al., 2020). The species was not recorded from the Santonian–Campanian boundary intervals at Seaford Head or Trunch. Pearce et al. (2020, see their fig. 18) suggested that *H. difficile* has a worldwide LAD in the 'lower' upper Santonian mid-*U. socialis* Zone, below the Hawks Brow CIE. However, at Poigny, rare to frequent *H. difficile* have been subsequently recorded within the lower LSE (Pearce et al., 2022), which is apparently synchronous with the HO of 4.26 m observed at Bocieniec, and taken to represent the LAD of the species (Fig. 10). Interestingly, the oldest specimens of *H. difficile* tend to be relatively large and robust, but become relatively small and gracile towards the top of their range: compare the robust holotype (Manum and Cookson, 1964 pl. III, fig. 1) and a typical Turonian specimen (Pearce et al., 2003 pl. I, fig. 9), with the gracile specimen figured here (Fig. 12G).

7.5.1.13. HO of Ellipsodinium *spp.* The HO of *Ellipsodinium* spp. appears to be a particularly significant, albeit currently regional European marker for the Santonian–Campanian boundary interval (Pearce et al., 2022; Gale et al., in press). Early studies by Clarke and Verdier (1967) placed the HO of *E. rugulosum* in their sample 26 from the lower *M. testudinarius* Zone of the CulverWhitecliff section IOW, but their stratigraphy is now believed to be flawed (see below). Foucher (1976a,b, 1979) placed the HO in the middle Santonian of the Paris Basin. In their synthesis of the known range of Mesozoic and Cenozoic dinocysts, Williams and Bujak (1985) and Stover et al. (1996) both placed the HO of *E. rugulosum* in the mid-Santonian. The event was also questionably plotted in the middle Santonian in the 'Cretaceous biostratigraphy' chart of Hardenbol et al. (1998). In the last major synthesis of dinocyst ranges, Williams et al. (2004) placed the HO in the lowermost Campanian, based on unpublished data in Pearce (2000; see below).

In his PhD thesis on the Chalk of southern England, Prince (1997) identified *E. membraniferum* (Figs. 7G, 12F) at Whitecliff IOW (the section studied previously by Clarke and Verdier, 1967) low in the *O. pilula* Zone, but he did not include the species in his formally published results of that section (Prince et al., 1999). Prince et al. (1999) demonstrated that the stratigraphy employed by Clarke and Verdier (1967) was flawed, resulting in their HO of *E. rugulosum* actually occurring very close to the Santonian–Campanian boundary. The results from Prince (1997) indicate that at Whitecliff, the HO of *E. membraniferum* occurs in sample c7 of Prince et al. (1999; I.M. Prince pers. comm. 2021). According to Jarvis et al. (2006 fig. 11), this lies a few metres above the "SCBE" which may correspond to the upper part of the LSE as defined herein.

Ellipsodinium membraniferum was formally described by Prince et al. (2008) who recorded the HO in the uppermost *M. testudinarius* Zone at Foreness Point, Kent. The data from the Trunch borehole (Pearce, 2000; used by Williams et al., 2004) was published by Pearce et al. (2020) and the HO of *Ellipsodinium rugulosum* was demonstrated to occur within the LSE (Fig. 14). Most recently, the HO of *E. membraniferum* was recorded at Poigny by Pearce et al. (2022), also within the LSE (Fig. 14).

The HO of *Ellipsodinium membraniferum* appears to closely approximate the correlated position of the C34n/C33r boundary and the corresponding Santonian–Campanian boundary at Seaford Head (Figs. 5, 14). At Bocieniec, the HO of *E. membraniferum* occurs at the top of the LSE at level of the C34n/C33r boundary (Figs. 10, 14).

Excluding *E. tenuicinctum* He Chengquan from the Eocene of NW China (He Chengquan, 1991), and as we are unaware of any other occurrences of this species, the HO of *Ellipsodinium* spp. therefore, appears to offer an excellent palynological proxy for the base of the Campanian, at least in NW Europe (Fig. 12). However, this event may extend into North America based on the results of an 89 samples study from the Horton River section, District of Mackenzie, NW Canada by McIntyre (1974), although the chronostratigraphic calibration of the section was not adequately demonstrated. McIntyre (1974) showed that the HO of *E. rugulosum* occurs within the "Bituminous Zone" (now the Smoking Hills Formation, Yorath and Norris, 1975), a unit that he stated was provisionally dated as 'late' Late Cretaceous, Campanian, and late Santonian to early Campanian by previous workers. Dixon (1999) subsequently noted that there are no definitive data to indicate an age any older than Santonian.

McIntyre (1974) observed that significant microfloral changes occur within the "Bituminous Zone", with the first (stratigraphically lowest) change characterised by the HO of *Dorocysta litotes* (known to occur in the mid-Santonian) and *Ellipsodinium rugulosum*. McIntyre (1974) referred specifically to the Santonian occurrence of *E. rugulosum* by Clarke and Verdier (1967) and apparently used the HO event to tentatively place the Santonian–Campanian boundary. This appears to have been prophetic given that we now consider the HO of *Ellipsodinium* to be the closest palynological event for the boundary in the GSSP auxiliary sections.

The Smoking Hills Formation comprises highly organic-rich shales, and organic matter can constitute up to 12% (by weight) of the rock (Dixon et al., 1992; Dixon, 1999). This may be significant,

as the HO of *Ellipsodinium* spp. in NW Europe occurs within latest Santonian chalks with high $\delta^{13}C$ values. It is speculated here that the Smoking Hills Formation may have provided a sink of ^{12}C, supplementing that in other areas of organic matter accumulation such as the lacustrine oil shales (Nenjiang Formation) in the Songliao Basin of NE China (Liu et al., 2022), and thereby contributing to the positive $\delta^{13}C$ excursion of the LSE.

7.5.1.14. HO of Eisenackia*?* knokkensis*. Eisenackia? knokkensis* (Figs. 7F, 12E) was first described from the 'lower' lower Campanian of Belgium (Louwye, 1992), and a comparable occurrence was noted from a single sample at Poigny between the Pilula and Senonensis CIEs (Pearce et al., 2022). The combined data from Bocieniec (Fig. 10) and Seaford (Fig. 5) indicates a total range of upper Santonian, mid-*U. socialis* Zone immediately above the Buckle CIE to the lower Campanian, high *O. pilula* Zone, between the Meeching and Senonensis CIEs (Fig. 15).

7.5.1.15. HO of Culversphaera velata*.* The HO of confident specimens of *C. velata* (Fig. 7D) occurs at Seaford within the lower Campanian, low *G. quadrata* Zone, below the Senonensis CIE, a short distance below the temporary HO of *S. longifurcatum* (Figs. 5, 14). A synchronous pattern has been recorded at Poigny (Pearce et al., 2022 fig. 3; Fig. 14). In both sections, rare questionable specimens occur above but no higher than the mid-lower Campanian, Papillosa CIE. The HO is also broadly comparable with the records from Whitecliff IOW (Prince et al., 1999) and Trunch (MAP pers. obs.) in the upper *O. pilula* Zone, and indicates that this may be a useful marker (Fig. 15).

7.5.1.16. Temporary HO of Surculosphaeridium longifurcatum*.* The HO of *S. longifurcatum* (Figs. 8H, 12L) is recorded in the basal *G. quadrata* Zone between the Meeching and Senonensis CIEs at Seaford Head (Figs. 5, 6), and at a comparable level at Whitecliff IOW (Prince et al., 1999), Trunch (Pearce et al., 2020) and Poigny (Pearce et al., 2022; Fig. 14). It was recorded to the section top at Bocieniec (Fig. 10). A clear HO of *S. longifurcatum* occurs also in the low Campanian of southern Germany (Kirsch, 1991). Elsewhere, *S. longifurcatum* is well distributed through the upper Campanian at Beutenaken quarry in The Netherlands and occurs as high as the upper Maastrichtian in Hallembaye quarry, Belgium (Slimani, 2001). It was recorded in a single sample from the upper Campanian at Tercis southwest France by Schiøler and Wilson (2001) and occurs in the lower Maastrichtian of the Middle Vistula River area in central Poland (Dziurków; Niechwedowicz and Walaszczyk, 2022). The HO of *S. longifurcatum* in the *G. quadrata* Zone, therefore, represents a local temporary disappearance event that, nonetheless, may provide a useful local marker in the lower Campanian of the Anglo-Paris Basin and southern North Sea Basin (Fig. 15).

7.5.1.17. LAD of Senoniasphaera protrusa*.* The HO of *S. protrusa* (Figs. 8G, 12J) at Seaford Head (Figs. 5, 14) lies in the basal *G. quadrata* Zone immediately below the Senonensis CIE. At Poigny, the HO of the species occurs above the HO of *S. longifurcatum*, between the Meeching and Senonensis CIEs (Pearce et al., 2022; see Section 7.2 for revised CIE stratigraphy) (Fig. 14). Pearce et al. (2020) recorded the HO of *S. protrusa* in their highest sample from the Trunch borehole, from the bottom of the *G. quadrata* Zone. However, our unpublished data indicate that specimens of the taxon continue higher in the Zone (Fig. 14), with an HO at a comparable level to that at Seaford Head and Poigny, between the Meeching and Senonensis CIEs. The HO of *S. protrusa* at Seaford Head, which is coincident with the HO of *S. congrensa* (Figs. 5, 6), would appear to be a useful datum level and the likely LAD of the former species (Fig. 15).

7.5.2. Additional dinocyst marker taxa

A number of other stratigraphically significant dinocyst datum levels were considered by Pearce et al. (2020) to characterise the Santonian–Campanian stage boundary interval, and are briefly discussed here from the stratigraphically lowest upward. The HO of *Renidinium rigidum* was proposed as a mid-middle Santonian marker. The species was not observed in either section in this study. The reappearance of *Coronifera striolata* sensu Schiøler (1992) was also considered to be a possible marker for the middle Santonian (Pearce et al., 2020). In this study, a single specimen observed at the base of the marls at Bocieniec, and sporadic records from within the upper *O. pilula* Zone at Seaford Head, offer no additional stratigraphic constraints (Appendix B Supplementary data Tables 2 and 3).

Pervosphaeridium intervelum and *Dimidium striatum* (Figs. 7E, 12D) were considered to have NW Europe-wide FADs in the top middle Santonian *M. coranguinum* Zone, above the Horseshoe Bay CIE, by Pearce et al. (2020), based on records from Trunch and Whitecliff IOW (Prince et al., 1999). These taxa occur very infrequently at Seaford Head with lowest records in the mid-upper Santonian (Appendix B Supplementary data Table 2). *Dimidium striatum* occurs more consistently at Bocieniec but remains uncommon and ranges down below the LO of *U. socialis* at the site; *P. intervelum* was not recorded from Bocieniec (Appendix B Supplementary data Table 3). The new records here are consistent with the established FADs but offer no better constraints (Fig. 15). The LAD of *Spiniferites porosus* has been suggested to lie in the mid-Santonian in the Northern Hemisphere (Williams and Bujak, 1985). The species was not recorded at Seaford Head or Bocieniec but it ranges upwards to immediately below the Buckle CIE at Poigny (Pearce et al., 2022) (Fig. 15).

The LO of *Odontochitina diducta* (Fig. 7J) occurs at the base of the Buckle CIE at Seaford Head in agreement with the position of this regional datum level and potential FAD reported by Pearce et al. (2020), although the species is recorded sporadically towards the base of its range at Seaford. The species is uncommon but occurs consistently to the base of the marls at Bocieniec, although the stratigraphic position of these remains uncertain (Fig. 4). *Spiniferites jarvisii* (Fig. 12K) similarly ranges to the base of the marls at Bocieniec but is unrecorded at Seaford Head. Its LO was placed in the middle Santonian immediately above the Haven Brow CIE at Poigny by Pearce et al. (2022).

The LADs of *Kleithriasphaeridium readei* and *Scriniodinium campanula* were considered to be mid-upper Santonian Northern Hemisphere wide datum levels by Pearce et al. (2020). Neither species was observed at Seaford Head or Bocieniec. *Spiniferites ramosus* subsp. *maeandriformis* first appears in the lowest Santonian but the taxon has a lowest persistent occurrence in the lower Campanian (Pearce et al., 2020). The subspecies is unrecorded at Seaford Head and occurs very infrequently at Bocieniec. The HO of *Dinopterygium alatum* typically occurs in the upper Santonian in the Northern Hemisphere but it may range into the low lower Campanian elsewhere (Pearce et al., 2020). It occurs infrequently in the *U. socialis* Zone at Bocieniec and there is one uncertain record from the *M. laevigatus* Zone at Seaford Head (Appendix B Supplementary data Tables 2 and 3).

Senoniasphaera macroreticulata (Fig. 8F) was described by Prince et al. (2008) from the basal lower Campanian, *O. pilula* Zone, base of the Whitecliff Ledge Beds, Isle of Wight (sample c1 of Prince et al., 1999). In the type material, it has a LO in the middle Santonian (upper *M. coranguinum* Zone) sample 90 of Prince et al. (1999) (I.M. Prince pers. comm.), but it is rare and sporadic until sample c1 within the lower *Offaster pilula* Zone close to the base of the Whitecliff Ledge Beds, where it has an average abundance of 12%. From here, it occurs consistently in significant numbers upwards,

reaching a maximum of 25% of the dinocyst assemblage in sample c6. Sporadic occurrences with low numbers are recorded again from the upper Whitecliff Ledge Beds, also within the lower *O. pilula* Zone.

At Whitecliff the LO of common *S. macroreticulata* was recorded 25 cm above the HO of *Marsupites testudinarius*, in a sample taken from immediately above a glauconitised hardground (Prince et al., 1999). The HO of *Marsupites testudinarius* itself lies immediately above another glauconitised hardground, and it is likely that the top Santonian is either missing or highly condensed in the section (Jarvis et al., 2006). At Seaford Head the LO of common *S. macroreticulata* occurs from 114.5 to 116 m within the Old Nore Beds, lowermost *O. pilula* Zone, within LSE b and 'c', with an average abundance of 9%.

The absence of hardgrounds (and therefore, the Whitecliff Ledge Beds) in the lower Campanian at Seaford Head indicates that the section is relatively more expanded than at Whitecliff. This makes a direct lithological correlation between Whitecliff and Seaford impossible. *Senoniasphaera macroreticulata* has also been recorded over the Santonian–Campanian boundary interval in Kent (Prince et al., 1999) and at Poigny (Pearce et al., 2022). It was not found in significant numbers in Kent, while at Poigny, the lowest occurrence at 275.75 m immediately above the LSE b appears to be synchronous with the LCO at Seaford Head.

The LO of *Spiniferites multispinulus* was proposed as an *O. pilula* Zone marker at Trunch (Pearce et al., 2020). A single specimen was recovered from the Old Nore Marl in the mid-*O. pilula* Zone at Seaford Head; we have no records from Bocieniec. The LO of persistent *Chatangiella manumii* is also considered to occur in the *O. pilula* Zone, although the species ranges down into the middle Santonian *M. coranguinum* Zone at Trunch (Pearce et al., 2020). A single uncertain record occurs towards the top of the *O. pilula* Zone at Seaford Head (Appendix B Supplementary data Table 2); we have no records of the species from Bocieniec. A LAD of *Chatangiella eminens* in the lower Campanian was proposed by Pearce et al. (2020), based on unpublished records of infrequent specimens from Whitecliff IOW (Prince, 1997). Additional lower Campanian studies are required to test this.

The HO of *Cordosphaeridium catherineae* (Figs. 7C, 12C) may also have regional stratigraphic value. The event is observed in the lower Campanian, *G. quadrata* Zone at Trunch (Pearce, 2010) and confidently between the Pilula and Senonensis CIEs at Poigny (Pearce et al., 2022; questionable specimens may range slightly higher to between Senonensis and Papillosa CIEs). *Cordosphaeridium catherineae* was not recorded in the Campanian at Bocieniec, but despite occurring at the top of the Seaford study interval (within the Senonensis CIE, Fig. 5), this HO is consistent with its recorded range at Trunch. Additional lower Campanian studies are also required to test the upper range of the species.

Locally, similarities exist between Whitecliff and Seaford, with increased relative numbers of *Canningia glomerata* (Fig. 7A) generally occurring below the upper Santonian, Hawks Brow CIE. An influx of *Xenascus perforatus* (Fig. 8K) also exists in the *O. pilula* Zone at Whitecliff and Seaford, but a $\delta^{13}C$ calibration is required at the former locality to test its synchronicity. The conspicuous increase in the abundance of *Palaeohystrichophora infusorioides* in the upper *O. pilula* Zone at Seaford is also apparent at Whitecliff, immediately above the published data of Prince et al. (1999) (I.M. Prince pers. comm. 2022). The stratigraphic level of this influx appears to be above the studied interval at Bocieniec. Multiple influxes of *P. infusorioides* (and other peridinioid dinocysts) noted from personal observation of the Campanian section at Trunch suggest that these influxes may be correlatable and related to major sea-level fluctuations.

Finally, *Chatangiella islae* (Fig. 12B) is a very important species in the Norwegian–Greenland Sea with a probable range of intra-lower Coniacian to Santonian (Pearce et al., 2019), and where it is very abundant in the Coniacian. A rare specimen was recorded at Bocieniec at the base of Buckle CIE in the upper Santonian *U. socialis* Zone. It has also been recorded as rare in the Coniacian–Santonian boundary sample at Poigny (Pearce et al., 2022). The occurrence at Bocieniec is the highest stratigraphically calibrated occurrence known.

8. Magnetostratigraphy and age of the base Campanian

The palaeomagnetic record of the Seaford section has been reviewed in Section 2.1.5. Previously proposed, widely different, placements of the C34n/C33r polarity reversal boundary (Barchi, 1995; Montgomery et al., 1998) are inconsistent with our carbon isotope correlation to the magnetostratigraphic reference section at Gubbio, northern Italy (Sabatino et al., 2018; Miniati et al., 2020; Maron and Muttoni, 2021), which places the boundary midway between the LSE and the Rottingdean CIEs (Fig. 14).

Following a review of the proposed ages of the C34n/C33r boundary, Maron and Muttoni (2021) derived a preferred age of 83.06 ± 0.18 Ma based on the astrochronological tuning of Bottaccione $\delta^{13}C_{carb}$ data from the literature. This compares favourably to the astronomically tuned age of 82.875 Ma calculated by Wu et al. in Ogg (2020), the age of 82.7 ± 0.6 Ma derived by Shen et al. (2022), and the superspline age of 82.8 Ma adopted by Gradstein and Agterberg (2022), but is younger than the base Campanian age of 83.65 Ma assigned by Gale et al. (2020).

9. Holostratigraphy of the Santonian–Campanian boundary interval

Results of our palynological and chemostratigraphic study of the Campanian–Santonian boundary interval in the Campanian auxiliary reference sections at Seaford Head and Bocieniec, integrated with published macrofossil, foraminifera and calcareous nannofossil data, are summarised in Fig. 15. Vertical scaling is based on the sediment thickness at Seaford Head. Placement of zones and key biostratigraphic datum levels is modified where necessary to take account of lower or higher positions indicated by correlation to other Boreal sections (Fig. 15). Placement of corresponding Tethyan zones and datum levels data is derived principally from the carbon isotope correlation to the Gubbio Campanian GSSP (Fig. 14).

10. Conclusions

Bottaccione (Gubbio, Italy) is the GSSP for the Campanian Stage with the C34n/C33r geomagnetic reversal (top of the Cretaceous Long Normal Superchron) as the primary stratigraphic marker. This is closely associated with the first appearance datum (FAD) level of the calcareous nannofossil *Aspidolithus parcus parcus*, below, and the last appearance datum (LAD) of the planktonic foraminifera *Dicarinella asymetrica*, immediately above the boundary. This contrasts to the established placement of the Santonian–Campanian boundary in Boreal sections, where the LAD of the crinoid *Marsupites* spp. has been the favoured primary marker. Here, reliable palaeomagnetic records are lacking, *D. asymetrica* is absent, and the lowest occurrence (LO) of *A. parcus parcus* occurs significantly above the LAD of *Marsupites*.

Carbon isotope stratigraphy applied to the Gubbio GSSP and two auxiliary GSSP sections, Seaford Head, England and Bocieniec, Poland, provides a means to determine the equivalence between the Tethyan and Boreal stratigraphic schemes and place the palaeomagnetically defined stage boundary within Boreal

successions. Of particular significance is the relative position of potential boundary markers in relation to a major widely developed long-term positive $\delta^{13}C$ excursion, the Late Santonian Event (LSE), previously referred to as the Santonian–Campanian Boundary Event (SCBE).

The auxiliary Campanian GSSP section at Seaford Head yields low abundance but well-preserved and diverse palynological assemblages throughout the Santonian–Campanian stage boundary interval, top *Micraster coranguinum*–lowest *Gonioteuthis quadrata* macrofossil zones. The assemblages are overwhelmingly dominated by organic-walled dinoflagellate cysts (dinocysts) comprising 147 taxa. The ranges of key taxa, variations in species abundance, and comparison with published records elsewhere, provide the basis to define 27 datum levels that are considered to have biostratigraphic significance. The dinocyst biostratigraphy is placed in a high-resolution lithostratigraphic framework of >40 regional marker beds, calibrated using macrofossil, benthic foraminifera (UKB14 *Stensioeina granulata polonica*–UKB16 *Bolivinoides culverensis* zones) and calcareous nannofossil records (UC12–UC14ii zones).

Palynological assemblages spanning the boundary interval at Seaford Head display significant changes with prasinophytes *Leiosphaeridia* spp. and the gonyaulacoid dinocysts *Senoniasphaera protrusa* being the most prominent taxa in the upper Santonian. Pulses of the peridinioid dinocyst *Subtilisphaera pontis-mariae* occur within the LSE, at the correlated position of the C34n/C33r palaeomagnetic reversal, and within the upper *Offaster pilula*–lower *G. quadrata* zones. Large increases in the proportions of *Canningia senonica* occur either side of the C34n/C33r boundary. An influx of *Palaeohystrichophora infusorioides* with *S. pontis-mariae* in the upper *O. pilula* Zone marks a significant change upwards to assemblages dominated by peridinioid cysts. The high P/G ratio is indicative of increased surface water productivity.

A new high-resolution (10-cm spacing) bulk carbonate C-isotope ($\delta^{13}C_{carb}$) reference curve for Seaford Head has enabled refinement of the carbon isotope event (CIE) stratigraphy of the stage boundary interval with 10 named events: the Buckle; Hawks Brow; Foreness FN1–FN3; the Late Santonian Event LSE, with peaks a and b; Rottingdean; Pilula; Meeching; and Senonensis CIEs. The Foreness FN1–FN3 CIEs in the *Marsupites laevigatus–M. testudinarius* zones and the Rottingdean and Meeching CIEs in the *O. pilula* Zone are newly defined. Carbon isotope curves and their constituent CIEs constrained by biostratigraphy, including the new palynological records reported in this paper, provide a basis for correlation between Seaford Head and coeval Chalk sections at Trunch eastern England, Poigny northern France, and Lägerdorf north Germany.

The auxiliary Campanian GSSP section at Bocieniec yields well-preserved and diverse palynological assemblages from the Santonian–Campanian stage boundary interval, *Uintacrinus socialis–O. pilula* zones. The assemblages are generally dominated by dinocysts comprising 158 taxa, with 11 datum levels considered to have stratigraphic significance. Terrestrial palynomorphs dominate a basal glauconitic marl sample overlying the Santonian unconformity of possible middle Santonian age, and also form an increasingly significant component of assemblages towards the section top. Additional stratigraphic constraints at Bocieniec are provided by benthic foraminifera (*Stensioeina gracilis–Gavelinella clementiana* zones) and calcareous nannofossil (UC13i–UC14i-ii) zonations, supplemented by records of the highest occurrence, and likely LAD, of the planktonic foraminifera *Dicarinella asymetrica*, and the palaeomagnetic C34n/C33r boundary.

Palaeohystrichophora infusorioides dominates palynological assemblages through the upper Santonian *U. socialis*–upper *M. testudinarius* zones at Bocieniec but is replaced by *Sentusidinium* spp. at the top of the *M. testudinarius* Zone and into the lower *O. pilula* Zone, accompanied by falling dinocyst species richness, an increased proportion of terrestrial palynomorphs and algae. This precedes a lithological change from marls to opoka and is interpreted to indicate regional shoaling.

Newly published macrofossil records from Bocieniec, together with our dinocyst data, require significant revision of the C-isotope stratigraphy of the section, including a substantial reduction in the thickness of the LSE interval. The age of sediments at the base of the marl succession at Bocieniec remains uncertain but may extend into the uppermost middle Santonian. The revised stratigraphy has been successfully correlated to Seaford Head and other NW European Chalk sections. The Bocieniec section uniquely provides a direct means of correlation between the Tethyan and Boreal stratigraphic schemes by including records of the LAD *D. asymetrica* and the C34n/C33r geomagnetic reversal in a Boreal biostratigraphic framework of benthic foraminifera, calcareous nannofossils, and dinocysts.

Combining our new dinocyst records from Seaford Head and Bocieniec with published data enables the recognition of 20 dinocyst datum levels spanning the Santonian–Campanian boundary interval that have at least regional biostratigraphic utility. These are, from bottom to top:

(1) FAD *Senoniasphaera protrusa*; (2) FAD *Cannosphaeropsis utinensis*; (3) LO of *Pervosphaeridium intervelum*; (4) LO of *Dimidium striatum*; (5) HO of *Spiniferites porosus* in the middle Santonian *M. coranguinum* Zone;
(6) LO of *Odontochitina diducta*; (7) LO of common *Chatangiella eminens*; (8) LO of *Cordosphaeridium catherineae*; (9) LO of *Trimuridinium whitenessense*; (10) top increase of *Surculosphaeridium longifurcatum*; (11) LO of *Odontochitina porifera*; (12) LO of *Alterbidinium ioannidesii*; (13) HO of common *Chatangiella eminens*; (14) LO of persistent *Rhynchodiniopsis saliorum* in the low upper Santonian *U. socialis* Zone;
(15) LO of persistent *Whitecliffia spinosa* in the high upper Santonian *M. testudinarius* Zone; (16) LAD of *Heterosphaeridium difficile* close to the base of the *U. anglicus* Zone and immediately above the LAD *Marsupites* spp. and the top of LSE peak a;
(17) LAD of *Ellipsodinium* spp. in the lower *O. pilula* Zone, at the top of the LSE and immediately below the correlated position of the C34n/C33r palaeomagnetic reversal boundary, the base of the Campanian;
(18) a marked increase in the peridinioid/gonyaulacoid dinocyst ratio; (19) the HO of *Eisenackia*? *knokkensis* at the top of the lower Campanian *O. pilula* Zone;
(20) the temporary disappearance of *Surculosphaeridium longifurcatum*; (21) HO of *Senoniasphaera protrusa* in the lower Campanian basal *G. quadrata* Zone.

Dinocyst datum levels are consistent between sections within a correlation framework provided by the carbon isotope stratigraphy and other biostratigraphic marker taxa. The lower Campanian dinocyst events in particular offer improved stratigraphic resolution for correlation within the upper *O. pilula*–lower *G. quadrata* zones where other biostratigraphic markers are limited. *Rhynchodiniopsis juneae* sp. nov. is described from the lower Campanian at Seaford Head.

Sadly, palynological analysis of 3 pilot samples from the Santonian–Campanian boundary interval at Gubbio showed all samples to be barren of palynomorphs. The carbon isotope correlation between Gubbio and the Boreal sections demonstrates that the extinction level of *Marsupites* lies in the upper *D. asymetrica* Zone, a significant distance below the C34n/C33r palaeomagnetic reversal. The base Campanian as defined by the chron boundary correlates to the lower *O. pilula* Zone (the base of which is defined

by the LAD of *U. anglicus*) in Boreal Chalk sections, and close to the LO of *O. pilula* and the LAD of *Ellipsodinium* spp.

It is notable that although the FAD of *A. parcus parcus* occurs below the C34n/C33r boundary and the LAD of *D. asymetrica* at Gubbio, the LO of the nannofossil (base marker of zones UC14 and CC18) consistently occurs significantly above the palaeomagnetic reversal level at Bocieniec and its correlatives, close to the Rottingdean CIE in all Boreal sections. The LO of the taxon here approximates to the LO of common *A. parcus parcus* in the proposed boundary stratotype, generating basal diachroneity in UC14 and CC18. Significantly, the LO of *Arkhangelskiella cymbiformis*, the basal index of nannofossil zone UC13, is markedly diachronous, occurring at the base of the upper Santonian Buckle CIE at Seaford Head and at the top of the upper Santonian (upper LSE interval) at Gubbio.

The holostratigraphy developed here provides an improved calibration of Boreal and Tethyan biostratigraphic schemes that is essential to refine the existing Late Cretaceous time scale, and to test the synchroneity of climate, sea-level and other palaeoenvironmental changes within the different biotic provinces.

Data availability

Stable isotope data and palynology counts are provided in Appendix B Supplementary data Tables 1 - 3.

Acknowledgements

Field assistance at Seaford Head was ably provided by Kevin Attree, Tara Brodie, Simon Crust, Delano Henry (Kingston University London), Kresten Anderskouv, Toms Buls (University of Copenhagen) and Madeleine Vickers (University of Oslo). Malcolm Jones (Palynological Laboratory Services Limited, PLS) is thanked for the preparation of the palynological samples. Iain Prince (Shell USA) provided unpublished data from his palynological study of Whitecliff, IOW. IJ was funded by UK Natural Environment Research Council (NERC) grant NE/H020756/1. Support by Evolution Applied Limited to MAP and Equinor Energy AS (previously Statoil ASA) to IJ (contract 4502311303) is gratefully acknowledged. Preparation of palynological samples from Bocieniec was funded by the National Science Centre of Poland (grant 2020/37/B/ST10/00287 to AJ). NT and JM acknowledge Carlsbergfondet CF16-0456 for funding travel expenses, sampling, and geochemical analysis. Poul Schiøler, Irek Walaszczyk and editor Eduardo Koutsoukos are thanked for their careful reviews and suggestions for improving the manuscript.

References

Amenábar, C.R., Montes, M., Nozal, F., Santillana, S.N., 2020. Dinoflagellate cysts of the La Meseta Formation (middle to late Eocene), Antarctic Peninsula: implications for biostratigraphy, palaeoceanography and palaeoenvironment. Geological Magazine 157, 351–366.

Ando, A., Woodard, S.C., Evans, H.F., Littler, K., Herrman, S., Macleod, K.G., Kim, S., Khim, B.K., Robinson, S.A., Huber, B.T., 2013. An emerging palaeoceanographic 'missing link': multidisciplinary study of rarely recovered parts of deep-sea Santonian–Campanian transition from Shatsky Rise. Journal of the Geological Society 170, 381–384.

Antonescu, E., Foucher, J.-C., Odin, G.S., 2001a. Les kystes de dinoflagellés de la carrière de Tercis les Bains (Landes, France). In: Odin, G.S. (Ed.), The Campanian–Maastrichtian Boundary. Characterisation at Tercis les Bains (France) and Correlation with Europe and other Continents. Elsevier, Amsterdam, pp. 235–252.

Antonescu, E., Foucher, J.-C., Odin, G.S., Schiøler, P., Siegl-Farkas, A., Wilson, G.J., 2001b. Dinoflagellate cysts in the Campanian–Maastrichtian succession of Tercis les Bains (Landes, France), a synthesis. In: Odin, G.S. (Ed.), The Campanian–Maastrichtian Boundary. Characterisation at Tercis les Bains (France) and Correlation with Europe and other Continents. Elsevier, Amsterdam, pp. 253–264.

Azema, C., Fauconnier, D., Viaud, J.M., 1981. Microfossils from the Upper Cretaceous of Vendée (France). Review of Palaeobotany and Palynology 35, 237–281. https://doi.org/10.1016/0034-6667(81)90111-1.

Bailey, H.W., Gale, A.S., Mortimore, R.N., Swiecicki, A., Wood, C.J., 1983. The Coniacian–Maastrichtian stages of the United Kingdom, with particular reference to southern England. Newsletters on Stratigraphy 12, 29–42.

Bailey, H.W., Gale, A.S., Mortimore, R.N., Swiecicki, A., Wood, C.J., 1984. Biostratigraphical criteria for the recognition of the Coniacian to Maastrichtian stage boundaries in the Chalk of North West Europe, with particular reference to southern England. Bulletin of the Geological Society of Denmark 33, 31–39.

Barchi, P., 1995. Géochimie et Magnetostratigraphie du Campanien de l'Europe Nord–Ouest (Unpublished PhD thesis). Pierre et Marie Curie Paris VI, Paris, p. 288.

Barr, F.T., 1966. The foraminiferal genus *Bolivinoides* from the Upper Cretaceous of the British Isles. Palaeontology 9, 220–243.

Barr, F.T., 1967. *Bolivinoides culverensis*, new name for the Campanian foraminifer *B. hiltermanni* Barr. Contributions from the Cushman Foundation for Foraminiferal Research 18, 136.

Barrois, C., 1876. Recherches sur le terrain Crétacé Supérieur de l'Angleterre et de l'Irlande. In: Mémoires de la Société géologique du Nord 1. Imprimerie et Librairie Six-Horemans, Lille, p. 232.

Batten, D.J., Morrison, L., 1983. Methods of palynological preparation for palaeoenvironmental, source potential and organic maturation studies. Norwegian Petroleum Directorate Bulletin 2, 35–53.

Birkelund, T., Hancock, J.M., Hart, M.B., Rawson, P.F., Remane, J., Robaszynski, F., Schmid, F., Surlyk, F., 1984. Cretaceous stage boundaries - proposals. Bulletin of the Geological Society of Denmark 33, 3–20.

Blair, S.A., Watkins, D.K., 2009. High-resolution calcareous nannofossil biostratigraphy for the Coniacian/Santonian Stage boundary, Western Interior Basin. Cretaceous Research 30, 367–384.

Blakey, R., 2012. Paleogeography of Europe Series, Cretaceous ca. 75 Ma. Colorado Plateau Geosystems (now DeepTimeMapsTM), Flagstaff AZ.

Bralower, T.J., Siesser, W.G., 1992. Cretaceous calcareous nannofossil biostratigraphy of Sites 761, 762 and 763, Exmouth and Wombat Plateaus, Northwest Australia. Proceedings of the Ocean Drilling Program. Scientific Results 122, 529–556.

Bralower, T.J., Leckie, R.M., Sliter, W.V., Thierstein, H.R., 1995. An integrated Cretaceous microfossil biostratigraphy. In: Berggren, W.A., Kent, D.V., Aubry, M.-P., Hardenbol, J. (Eds.), Geochronology, Time Scales and Global Stratigraphic Correlation. SEPM (Society for Sedimentary Geology), Tulsa, pp. 65–79.

Bristow, C.R., Mortimore, R.N., Wood, C.J., 1997. Lithostratigraphy for mapping the Chalk of southern England. Proceedings of the Geologists' Association 108, 293–315.

Brydone, R.M., 1912. The Stratigraphy of the Chalk of Hants. Dulau and Co. Ltd, London, p. 116.

Brydone, R.M., 1914. The zone of *Offaster pilula* in the south English Chalk. Geological Magazine 6, 359–369, 405–411, 449–457, 509–513.

Brydone, R.M., 1939. The Chalk Zone of *Offaster pilula*. Dulau and Co. Ltd, London, p. 8.

Burnett, J.A., 1990. A new nannofossil zonation scheme for the Boreal Campanian. International Nannofossil Association Newsletter 12, 67–70.

Burnett, J.A., Whitham, F., 1999. Correlation between the nannofossil and macrofossil biostratigraphies and the lithostratigraphy of the Upper Cretaceous of NE England. Proceedings of the Yorkshire Geological Society 52, 371–381.

Burnett, J.A., Gallagher, L.T., Hampton, M.J., 1998. Upper Cretaceous. In: Bown, P.R. (Ed.), Calcareous Nannofossil Biostratigraphy. Kluwer, Dordrecht, pp. 132–199.

Chenot, E., Pellenard, P., Martinez, M., Deconinck, J.F., Amiotte-Suchet, P., Thibault, N., Bruneau, L., Cocquerez, T., Laffont, R., Puceat, E., Robaszynski, F., 2016. Clay mineralogical and geochemical expressions of the "Late Campanian Event" in the Aquitaine and Paris basins (France): palaeoenvironmental implications. Palaeogeography, Palaeoclimatology, Palaeoecology 447, 42–52.

Chenot, E., Deconinck, J.F., Puceat, E., Pellenard, P., Guiraud, M., Jaubert, M., Jarvis, I., Thibault, N., Cocquerez, T., Bruneau, L., Razmjooei, M.J., Boussaha, M., Richard, J., Sizun, J.P., Stemmerik, L., 2018. Continental weathering as a driver of Late Cretaceous cooling: new insights from clay mineralogy of Campanian sediments from the southern Tethyan margin to the Boreal realm. Global and Planetary Change 162, 292–312.

Clarke, R.F.A., Verdier, J.P., 1967. An investigation of microplankton assemblages from the Chalk of the Isle of Wight, England. Verhandelingen der Koninklijke Nederlandse Akademie van Wetenschappen, Afdeling Natuurkunde, Eerste Reeks 24, 1–96, 17 Plates.

Cobban, W.A., 1995. Occurrences of the free-swimming Upper Cretaceous crinoids *Uintacrinus* and *Marsupites* in the Western Interior of the United States. US Geological Survey Bulletin 2113-C, C1–C6.

Coccioni, R., Premoli Silva, I.P., 2015. Revised Upper Albian–Maastrichtian planktonic foraminiferal biostratigraphy and magnetostratigraphy of the classical Tethyan Gubbio section (Italy). Newsletters on Stratigraphy 48, 47–90.

Cramer, B.S., Jarvis, I., 2020. Carbon isotope stratigraphy. In: Gradstein, F., Ogg, J.G., Ogg, G. (Eds.), The Geologic Time Scale 2020. Elsevier, Amsterdam, pp. 309–343.

Dale, B., Fjellså, A., 1994. Dinoflagellate cysts as paleoproductivity indicators: state of the art, potential and limits. In: Zahn, R., Pedersen, T.F., Kaminiski, M., Lebeyrie, L. (Eds.), Carbon Cycling in the Glacial Ocean: Constraints on the Ocean's Role in Global Change. Springer, Berlin, Heidelberg, pp. 521–537.

de Vernal, A., Marret, F., 2007. Chapter Nine. Organic-Walled Dinoflagellate Cysts: Tracers of Sea-Surface Conditions. In: Developments in Marine Geology 1. Elsevier, Amsterdam, pp. 371–408.

Deville de Periere, M.D., Pellenard, P., Thibault, N., 2019. The Santonian–Campanian Boundary Event (SCBE) in Boreal Basins: new geochemical and mineralogical

data from the Northern Chalk Province (East Yorkshire, UK). Cretaceous Research 95, 61–76.
Dixon, J., 1999. Mesozoic–Cenozoic stratigraphy of the Northern Interior Plains and Plateaux, Northwest Territories. Geological Survey of Canada Bulletin 536, 1–62.
Dixon, J., Dietrich, J.R., McNeil, D.H., 1992. Upper Cretaceous to Pleistocene sequence stratigraphy of the Beaufort-Mackenzie and Banks Island areas, Northwest Canada. Geological Survey of Canada Bulletin 407, 1–100.
Dubicka, Z., Peryt, D., 2014. Classification and evolutionary interpretation of late Turonian–early Campanian *Gavelinella* and *Stensioeina* (Gavelinellidae, benthic foraminifera) from western Ukraine. Journal of Foraminiferal Research 44, 151–176.
Dubicka, Z., Peryt, D., 2016. *Bolivinoides* (benthic foraminifera) from the Upper Cretaceous of Poland and western Ukraine - Taxonomy, evolutionary changes and stratigraphic significance. Journal of Foraminiferal Research 46, 75–94.
Dubicka, Z., Jurkowska, A., Thibault, N., Razmjooei, M.J., Wojcik, K., Gorzelak, P., Felisiak, I., 2017. An integrated stratigraphic study across the Santonian/Campanian boundary at Bocieniec, southern Poland: a new boundary stratotype candidate. Cretaceous Research 80, 61–85.
Dubicka, Z., Wierzbowski, H., Wierny, W., 2018. Oxygen and carbon isotope records of Upper Cretaceous foraminifera from Poland: vital and microhabitat effects. Palaeogeography, Palaeoclimatology, Palaeoecology 500, 33–51.
Eldrett, J.S., Vieira, M., Gallagher, L., Hampton, M.J., Blaauw, M., Swart, P.K., 2021. Late Cretaceous to Palaeogene carbon isotope, calcareous nannofossil and foraminifera stratigraphy of the Chalk Group, Central North Sea. Marine and Petroleum Geology 124, 1–15, 104789.
Ernst, G., 1972. Grundfragen der Stammesgeschichte bei irregulären Echiniden der norwesteuropäischen Oberkreide. Geologisches Jahrbuch A4, 63–175.
Ernst, G., Schulz, M.-G., 1974. Stratigraphie und Fauna des Coniac und Santon im Schreibkreide-Richtprofil von Lägerdorf (Holstein). Mitteilungen des Geologisch-Paläontologischen Institutes der Universität Hamburg 43, 5–50.
Eshet, Y., Almogilabin, A., Bein, A., 1994. Dinoflagellate cysts, paleoproductivity and upwelling systems - a Late Cretaceous example from Israel. Marine Micropaleontology 23, 231–240.
Esper, O., Zonneveld, K.A.F., 2007. The potential of organic-walled dinoflagellate cysts for the reconstruction of past sea-surface conditions in the Southern Ocean. Marine Micropaleontology 65, 185–212.
Fensome, R.A., Taylor, F.J.R., Norris, G., Sarjeant, W.A.S., Wharton, D.I., Williams, G.L., 1993. A Classification of Living and Fossil Dinoflagellates. In: American Museum National History. Micropaleontology Press, Special Publication 7. Sheridan Press, Hanover, p. 351.
Fensome, R.A., Williams, G.L., MacRae, R.A., 2019a. The Lentin and Williams index of fossil dinoflagellates 2019 edition. American Association of Stratigraphic Palynologists Contribution Series 50, 1–1173.
Fensome, R.A., Williams, G.L., Wood, S.E.L., Riding, J.B., 2019b. A review of the areoligeracean dinoflagellate cyst *Cyclonephelium* and morphologically similar genera. Palynology 43 (Suppl. 1), 1–71.
Foucher, J.-C., 1976a. Les Dinoflagellés des silex et la stratigraphie du Crétacé supérieur français. Revue de Micropaléontologie 18, 213–220.
Foucher, J.-C., 1976b. Microplancton des silex crétacés du Beauvaises. Cahiers de Micropaléontologie 2, 1–28.
Foucher, J.-C., 1979. Distribution stratigraphique des kystes de Dinoflagellés et des Acritarches dans le Crétacé supérieur du Bassin de Paris et de l'Europe septentrionale. Palaeontographica, Abteilung B 169 (1–3), 78–105.
Fritsen, A., Bailey, H., Gallagher, L., Hampton, M., Krabbe, H., Jones, B., Jutson, D., Moe, A., Nielsen, E.B., Petersen, N.W., Riis, F., Sawyer, D., Sellwood, B., Strand, T., Øverli, P.E., Øxnevad, I., 1999. A Joint Chalk Stratigraphic Framework, Joint Chalk Research Program Topic V. Norwegian Petroleum Directorate, Stavanger, pp. 1–206.
Gale, A.S., 2015. Origin and phylogeny of verrucomorph barnacles (Crustacea, Cirripedia, Thoracica). Journal of Systematic Palaeontology 13, 753–789.
Gale, A.S., 2018. An integrated microcrinoid zonation for the lower Campanian chalks of southern England, and its implications for correlation. Cretaceous Research 87, 312–357.
Gale, A.S., 2019. Microcrinoids (Echinodermata, Articulata, Roveacrinida) from the Cenomanian–Santonian chalk of the Anglo-Paris Basin: taxonomy and biostratigraphy. Revue de Paléobiologie, Genève 38, 397–533.
Gale, A.S., Wood, C.J., Bromley, R.G., 1987. The lithostratigraphy and marker bed correlation of the White Chalk (Late Cenomanian – Campanian) in southern England. Mesozoic Research 1, 107–118.
Gale, A.S., Montgomery, P., Kennedy, W.J., Hancock, J.M., Burnett, J.A., McArthur, J.M., 1995. Definition and global correlation of the Santonian–Campanian boundary. Terra Nova 7, 611–622.
Gale, A.S., Kennedy, W.J., Lees, J.A., Petrizzo, M.R., Walszczyk, I., 2007. An integrated study (inoceramid bivalves, ammonites, calcareous nannofossils, planktonic foraminifera, stable carbon isotopes) of the Ten Mile Creek section, Lancaster, Dallas County, north Texas, a candidate Global boundary Stratotype Section and Point for the base of the Santonian Stage. Acta Geologica Polonica 57, 113–160.
Gale, A.S., Hancock, J.M., Kennedy, W.J., Petrizzo, M.R., Lees, J.A., Walaszczyk, I., Wray, D.S., 2008. An integrated study (geochemistry, stable oxygen and carbon isotopes, nannofossils, planktonic foraminifera, inoceramid bivalves, ammonites and crinoids) of the Waxahachie Dam Spillway section, north Texas: a possible boundary stratotype for the base of the Campanian Stage. Cretaceous Research 29, 131–167.
Gale, A.S., Surlyk, F., Anderskouv, K., 2013. Channelling versus inversion: origin of condensed Upper Cretaceous chalks, eastern Isle of Wight, UK. Journal of the Geological Society 170, 281–290.
Gale, A.S., Mutterlose, J., Batenburg, S., Gradstein, F.M., Agterberg, F.P., Ogg, J.G., Petrizzo, M.R., 2020. Chapter 27 - The Cretaceous Period. In: Gradstein, F.M., Ogg, J.G., Schmitz, M.D., Ogg, G.M. (Eds.), Geologic Time Scale 2020. Elsevier, Amsterdam, pp. 1023–1086.
Gale, A.S., Batenburg, S., Coccioni, R., Dubicka, Z., Erba, E., Falzoni, F., Haggart, J., Hasegawa, T., Ifrim, C., Jarvis, I., Jenkyns, H., Jurkowska, A., Kennedy, W.J., Maron, M., Muttoni, G., Pearce, M., Petrizzo, M.R., Premoli-Silva, I., Thibault, N., Voigt, S., Wagreich, M., Walaszczyk, I., (in press). The Global Boundary Stratotype Section and Point (GSSP) of the Campanian Stage at Bottaccione (Gubbio, Italy) and its auxiliary sections: Seaford Head (U.K.); Bocieniec (Poland); Postalm (Austria); Smoky Hill, Kansas (U.S.A.); Tepayac (Mexico).
Gardin, S., Del Panta, F., Monechi, S., Pozzi, M., 2001. A Tethyan reference record for the Campanian and Maastrichtian stages: the Bottaccione section (Central Italy); review of data and new calcareous nannofossil results. In: Odin, G.S. (Ed.), The Campanian–Maastrichtian Boundary. Characterisation at Tercis les Bains (France) and Correlation with Europe and other Continents. Elsevier, Amsterdam, pp. 745–757.
Garrison, R.E., Kennedy, W.J., 1977. Origin of solution seams and flaser structures in the Upper Cretaceous chalks of southern England. Sedimentary Geology 19, 107–137.
Gaster, C.T.A., 1924. The Chalk of the Worthing District of Sussex. Proceedings of the Geologists' Association 35, 89–110.
Gaster, C.T.A., 1937. The stratigraphy of the Chalk of Sussex. Part I. West Central area – Arun Gap to Valley of the Adur, with zonal map. Proceedings of the Geologists' Association 48, 356–373.
Gedl, P., 2007. Dinocysts from Upper Cretaceous deep-water marine variegated facies (Malinowa Shale Formation), Pieniny Klippen Belt, Poland: example from the Potok Trawne creek. In: Birkemajer, K. (Ed.), Geology of the Pieniny Klippen Belt and the Tatra Mts, Carpathians. Institute of Geological Sciences, Polish Academy of Sciences, Warsaw, pp. 139–152.
Gradstein, F.M., Agterberg, F.P., 2022. Application of supersplining to the Mesozoic and Paleozoic geologic time scales. Mathematical Geosciences 54, 1207–1226.
Griffith, C., Brydone, R.M., 1911. The Zones of the Chalk in Hants. Dulau and Company, London, p. 36.
Guzhikov, A.Y., Baraboshkin, E.Y., Aleksandrova, G.N., Ryabov, I.P., Ustinova, M.A., Kopaevich, L.F., Mirantsev, G.V., Kuznetsov, A.B., Fokin, P.A., Kosorukov, V.L., 2021. New bio-, chemo-, and magnetostratigraphy of the Santonian–Campanian Boundary in the Kudrino and Aksu-Dere Sections (SW Crimea): problems of global correlation and selection of the lower boundary stratotype of the Campanian. 1. Geological framework, sedimentology, biostratigraphy. Stratigraphy and Geological Correlation 29, 450–494.
Haggart, J.W., Graham, R., 2018. The crinoid *Marsupites* in the Upper Cretaceous Nanaimo Group, British Columbia: Resolution of the Santonian–Campanian boundary in the North Pacific Province. Cretaceous Research 87, 277–295.
Hampton, M.J., Bailey, H.W., Gallagher, L.T., Mortimore, R.N., Wood, C.J., 2007. The biostratigraphy of Seaford Head, Sussex, southern England; an international reference section for the basal boundaries for the Santonian and Campanian Stages in chalk facies. Cretaceous Research 28, 46–60.
Hancock, J.M., 1993. Transatlantic correlations in the Campanian–Maastrichtian stages by eustatic changes of sea-level. In: Hailwood, E.A., Kidd, R.B. (Eds.), High Resolution Stratigraphy, Geological Society of London Special Publication, vol. 30, pp. 241–256.
Hancock, J.M., Gale, A.S., 1996. The Campanian Stage. In: Rawson, P.F., Dhondt, A.V., Hancock, J.M., Kennedy, W.J. (Eds.), Proceedings "Second International Symposium on Cretaceous Stage Boundaries" Brussels 8–16 September 1995. l'Institut Royal des Sciences Naturelles de Belgique, pp. 103–109.
Haq, B.U., Hardenbol, J., Vail, P., 1988. Mesozoic and Cenozoic chronostratigraphy and cycles of sea-level change. In: Wilgus, C.K., Hastings, B.S., Ross, C.A., Posamentier, H., Van Wagoner, J., Kendall, C.G.S.C. (Eds.), Sea-Level Changes - An Integrated Approach. SEPM, Tulsa, pp. 71–108.
Hardenbol, J., Thierry, J., Farley, M.B., Jacquin, T., Graciansky, P.-C.d., Vail, P.R., 1998. Mesozoic and Cenozoic sequence chronostratigraphic framework in European basins. In: Graciansky, P.-C.d., Hardenbol, J., Jacquin, T., Vail, P.R. (Eds.), Mesozoic and Cenozoic Sequence Stratigraphy of European Basins, SEPM Special Publication, vol. 60, pp. 3–13.
Hart, M.B., Swiecicki, A., 1987. Foraminifera of the chalk facies. In: Hart, M.B. (Ed.), Micropaleontology of Carbonate Environments. Ellis Horwood for the British Micropalaeontological Society, Chichester, pp. 121–137.
Hart, M.B., Bailey, H.W., Crittenden, S., Fletcher, B.N., Price, R.J., Swiecicki, A., 1989. Cretaceous. In: Jenkins, D.G., Murray, J.W. (Eds.), Stratigraphical Atlas of Fossil Foraminifera, second ed. Ellis Horwood for the British Micropalaeontological Society, Chichester, pp. 273–371.
He Chengquan, H., 1991. Late Cretaceous–Early Tertiary Microphytoplankton from the Western Tarim Basin in Southern Xinjiang, China (in Chinese with English summary). Nanjing Institute of Geology and Palaeontology, Academia Sinica, Nanjing.
Hopson, P.M., 2005. A Stratigraphical Framework for the Upper Cretaceous Chalk of England and Scotland with Statements on the Chalk of Northern Ireland and the UK Offshore Sector. British Geological Survey Research Report RR/05/01, p. 102.

Hurst, M.D., Rood, D.H., Ellis, M.A., Anderson, R.S., Dornbusch, U., 2016. Recent acceleration in coastal cliff retreat rates on the south coast of Great Britain. Proceedings of the National Academy of Sciences 113, 13336–13341.
Ifrim, C., Stinnesbeck, W., 2021. Ammonoids and their biozonation across the Santonian–Campanian boundary in north-eastern Coahuila, Mexico. Palaeontologia Electronica 24, 1–62.
Ifrim, C., Stinnesbeck, W., Gonzáles Gonzáles, A.H., Schorndorf, N., Gale, A.S., 2021. Ontogeny, evolution and palaeogeographic distribution of the world's largest ammonite *Parapuzosia (P.) seppenradensis* (Landois, 1895). PLoS One 16, e0258510.
Jagt, J.W.M., Jaskuła, I., Witek, A., Jagt-Yazykova, E.A., 2008. A new record of the Late Cretaceous cirripede *Eoverruca hewitti* (Verrucomorpha, Proverrucidae) from southern Poland. Zootaxa 1671, 59–68.
Jarvis, I., 2006. The Santonian–Campanian phosphatic chalks of England and France. Proceedings of the Geologists' Association 117, 219–237.
Jarvis, I., Mabrouk, A., Moody, R.T.J., De Cabrera, S., 2002. Late Cretaceous (Campanian) carbon isotope events, sea-level change and correlation of the Tethyan and Boreal realms. Palaeogeography, Palaeoclimatology, Palaeoecology 188, 215–248.
Jarvis, I., Gale, A.S., Jenkyns, H.C., Pearce, M.A., 2006. Secular variation in Late Cretaceous carbon isotopes: a new $\delta^{13}C$ carbonate reference curve for the Cenomanian–Campanian (99.6–70.6 Ma). Geological Magazine 143, 561–608.
Jarvis, I., Pearce, M., Püttman, T., Voigt, S., Walaszczyk, I., 2021. Palynology and calcareous nannofossil biostratigraphy of the Turonian–Coniacian boundary: the proposed boundary stratotype at Salzgitter-Salder, Germany and its correlation in NW Europe. Cretaceous Research 123, 1–32.
Jeans, C.V., Tosca, N.J., Hu, X.F., Boreham, S., 2014. Clay mineral-grain size-calcite cement relationships in the Upper Cretaceous Chalk, UK: a preliminary investigation. Clay Minerals 49, 299–325.
Jenkyns, H.C., Gale, A.S., Corfield, R.M., 1994. Carbon- and oxygen-isotope stratigraphy of the English Chalk and Italian Scaglia and its palaeoclimatic significance. Geological Magazine 131, 1–34.
Joo, Y.J., Sageman, B.B., 2014. Cenomanian to Campanian carbon isotope chemostratigraphy from the Western Interior Basin, U.S.A. Journal of Sedimentary Research 84, 529–542.
Jurkowska, A., 2022. The biotic-abiotic control of Si burial in marine carbonate systems of the pre-Eocene Si cycle. Global Biogeochemical Cycles 36, 1–20.
Jurkowska, A., Świerczewska-Gładysz, E., 2020. Evolution of Late Cretaceous Si cycling reflected in the formation of siliceous nodules (flints and cherts). Global and Planetary Change 195, 1–26.
Jurkowska, A., Barski, M., Worobiec, E., 2019a. The relation of a coastal environment to early diagenetic clinoptilolite (zeolite) formation - new data from the Late Cretaceous European Basin. Palaeogeography, Palaeoclimatology, Palaeoecology 524, 166–182.
Jurkowska, A., Swierczewska-Gladysz, E., Bak, M., Kowalik, S., 2019b. The role of biogenic silica in the formation of Upper Cretaceous pelagic carbonates and its palaeoecological implications. Cretaceous Research 93, 170–187.
Kennedy, W.J., 2019. The Ammonoidea of the Upper Chalk. Part 1. Monographs of the Palaeontographical Society 173, 1–112.
Kirsch, K.-H., 1991. Dinoflagellatenzysten aus der Oberkreide des Helvetikums und Nordultrahelvetikums von Oberbayern. Munchner Geowissenschaftliche Abhandlungen - Reihe A: Geologie und Palaontologie 22, 1–306.
Kita, Z.A., Watkins, D.K., Sageman, B.B., 2017. High-resolution calcareous nannofossil biostratigraphy of the Santonian/Campanian Stage boundary, Western Interior Basin, USA. Cretaceous Research 69, 49–55.
Koch, W., 1977. Biostratigraphie in der Oberkreide und Taxonomie von Foraminiferen. Geologisches Jahrbüch A38, 11–123.
Lamolda, M.A., Hancock, J.M., 1996. The Santonian Stage and substages. In: Rawson, P.F., Dhondt, A.V., Hancock, J.M., Kennedy, W.J. (Eds.), Proceedings "Second International Symposium on Cretaceous Stage Boundaries" Brussels 8–16 September 1995. l'Institut Royal des Sciences Naturelles de Belgique, pp. 95–102.
Lamolda, M.A., Paul, C.R.C., Peryt, D., Pons, J.M., 2014. The Global Boundary Stratotype and Section Point (GSSP) for the base of the Santonian Stage, "Cantera de Margas", Olazagutia, northern Spain. Episodes 37, 2–13.
Leandro, L.M., Santos, A., Carvalho, M.d.A., Fauth, G., 2020. Middle to late Miocene Caribbean dinoflagellate assemblages and palynofacies (DSDP Leg 15 Site 153). Marine Micropaleontology 160, 101898.
Lignum, J., Jarvis, I., Pearce, M.A., 2008. A critical assessment of standard processing methods for the preparation of palynological samples. Review of Palaeobotany and Palynology 149, 133–149.
Liu, W., Liu, M., Yang, T., Liu, X., Them II, T.R., Wang, K., Bian, C., Meng, Q., Li, Y., Zeng, X., Zhao, W., 2022. Organic matter accumulations in the Santonian–Campanian (Upper Cretaceous) lacustrine Nenjiang shale (K2n) in the Songliao Basin, NE China: terrestrial responses to OAE3? International Journal of Coal Geology 260, 1–14.
Louwye, S., 1992. Dinoflagellate cyst stratigraphy of the Upper Cretaceous of western Belgium. Bulletin de la Société belge de Géologie 101, 255–275.
Lowrie, W., Alvarez, W., 1977. Late Cretaceous geomagnetic polarity sequence: detailed rock and palaeomagnetic studies of the Scaglia Rossa limestone at Gubbio, Italy. Geophysical Journal International 51, 561–581.
Manum, S., Cookson, I.C., 1964. Cretaceous microplankton in a sample from Graham Island, Arctic Canada, collected during the second "Fram" expedition (1898–1902). Schrifter utgitt av Det Norsk Videnskaps-Akademi 17, 1–35.
Marks, P., 1984. Proposal for the recognition of boundaries between Cretaceous stages by means of planktonic foraminiferal biostratigraphy. Bulletin of the Geological Society of Denmark 33, 163–169.
Maron, M., Muttoni, G., 2021. A detailed record of the C34n/C33r magnetozone boundary for the definition of the base of the Campanian Stage at the Bottaccione section (Gubbio, Italy). Newsletters on Stratigraphy 54, 107–122.
McIntyre, D.J., 1974. Palynology of an Upper Cretaceous Section, Horton River, District of Mackenzie, N.W.T. Geological Survey of Canada Paper 74-14, pp. 1–56.
Miniati, F., Petrizzo, M.R., Falzoni, F., Erba, E., 2020. Calcareous plankton biostratigraphy of the Santonian–Campanian boundary interval in the Bottaccione section (Umbria-Marche Basin, central Italy). Rivista Italiana di Paleontologia e Stratigrafia 126, 771–789.
Moffat, C., Richardson, H., Roberts, G., 2020. Natural England Marine Chalk Characterisation Project. Natural England Research Report 080, p. 117.
Monciardini, C., Alcaydé, G., Robaszynski, F., 1980. Sénonien. In: Mégnien, C., Mégnien, F. (Eds.), Synthèse Géologique du Bassin de Paris. BRGM, Orléans, pp. 302–309.
Montgomery, P., Hailwood, E.A., Gale, A.S., Burnett, J.A., 1998. The magnetostratigraphy of Coniacian–Late Campanian chalk sequences in southern England. Earth and Planetary Science Letters 156, 209–224.
Mortimore, R.N., 1986. Stratigraphy of the Upper Cretaceous White Chalk of Sussex. Proceedings of the Geologists' Association 97, 97–139.
Mortimore, R.N., 2021. The Chalk of the South Downs of Sussex and Hampshire and the North Downs of Kent. In: Geologists' Association Guide 74, vol. 1, p. 284.
Mortimore, R.N., Pomerol, B., 1987. Correlation of the Upper Cretaceous White Chalk (Turonian to Campanian) in the Anglo-Paris Basin. Proceedings of the Geologists' Association 98, 97–143.
Mortimore, R.N., Wood, C.J., Gallois, R.W., 2001. British Upper Cretaceous Stratigraphy. In: Geological Conservation Review Series 23. Joint Nature Conservation Committee, Peterborough, p. 558.
Neumann, C., Jagt, J.W.M., van der Ham, R.W.J.M., 2002. Rare Campanian echinoids from Hover and Misburg (Hannover area, Lower Saxony, Germany). Mitteilungen aus dem Museum für Naturkunde in Berlin, Geowissenschaftliche Reihe 5, 121–139.
Niebuhr, B., Wood, C.J., Ernst, G., 2000. Isolierte Oberkreide - vorkommen zwischen Wiehengebirge und Harz. In: Hiss, M., Schönfeld, J., Thiermann, A. (Eds.), Stratigraphie von Deutschland III. Die Kreide der Bundesrepublik Deutschland, Frankfurt am Main, pp. 101–109.
Niechwedowicz, M., 2022. Dinoflagellate cysts from the Upper Cretaceous (upper Campanian to lowermost Maastrichtian) of the Middle Vistula River section, Poland. Palynology 46, 1–37.
Niechwedowicz, M., Walaszczyk, I., 2022. Dinoflagellate cysts of the upper Campanian – basal Maastrichtian (Upper Cretaceous) of the Middle Vistula River section (central Poland): stratigraphic succession, correlation potential and taxonomy. Newsletters on Stratigraphy 55, 21–67.
Niechwedowicz, M., Walaszczyk, I., Barski, M., 2021. Phytoplankton response to palaeoenvironmental changes across the Campanian–Maastrichtian (Upper Cretaceous) boundary interval of the Middle Vistula River section, central Poland. Palaeogeography, Palaeoclimatology, Palaeoecology 577, 19.
Noël, D., 1970. Coccolithes Crétacés: la Craie Campanienne du Bassin de Paris. Éditions du Centre national de la recherche scientifique, Paris, p. 129.
Nøhr-Hansen, H., Piasecki, S., Alsen, P., 2020. A Cretaceous dinoflagellate cyst zonation for NE Greenland. Geological Magazine 157, 1658–1692. https://doi.org/10.1017/S0016756819001043.
Ogg, J.G., 2020. Geomagnetic polarity time scale. In: Gradstein, F., Ogg, J.G., Ogg, G. (Eds.), The Geologic Time Scale 2020. Elsevier, Amsterdam, pp. 159–192.
Pearce, M.A., 2000. Palynology and Chemostratigraphy of the Cenomanian to Lower Campanian Chalk of Southern and Eastern England (Unpublished PhD thesis). Department of Geography, Geology and the Environment, Kingston University London, Kingston upon Thames, p. 432.
Pearce, M.A., 2010. New organic-walled dinoflagellate cysts from the Cenomanian to Maastrichtian of the Trunch borehole, UK. Journal of Micropalaeontology 29, 51–72.
Pearce, M.A., 2018. Additional new organic-walled dinoflagellate cysts from two onshore UK Chalk boreholes. Journal of Micropalaeontology 37, 73–86.
Pearce, M.A., Jarvis, I., Swan, A.R.H., Murphy, A.M., Tocher, B.A., Edmunds, W.M., 2003. Integrating palynological and geochemical data in a new approach to palaeoecological studies: Upper Cretaceous of the Banterwick Barn Chalk borehole, Berkshire, UK. Marine Micropaleontology 47, 271–306.
Pearce, M.A., Jarvis, I., Tocher, B.A., 2009. The Cenomanian–Turonian boundary event, OAE2 and palaeoenvironmental change in epicontinental seas: new insights from the dinocyst and geochemical records. Palaeogeography, Palaeoclimatology, Palaeoecology 280, 207–234.
Pearce, M.A., Stickley, C.E., Johansen, L.M., 2019. *Chatangiella islae* and *Trithyrodinium zakkii*, new species of peridinioid dinoflagellate cysts (Family Deflandreoideae) from the Coniacian and Campanian (Upper Cretaceous) of the Norwegian Sea. Review of Palaeobotany and Palynology 271, 104080.
Pearce, M.A., Jarvis, I., Ball, P.J., Laurin, J., 2020. Palynology of the Cenomanian to lowermost Campanian (Upper Cretaceous) Chalk of the Trunch Borehole (Norfolk, UK) and a new dinoflagellate cyst bioevent stratigraphy for NW Europe. Review of Palaeobotany and Palynology 278, 104188.
Pearce, M.A., Jarvis, I., Monkenbusch, J., Thibault, N., Ullmann, C.V., Martinez, M., 2022. Coniacian–Campanian palynology, carbon isotopes and clay mineralogy

of the Poigny borehole (Paris Basin) and its correlation in NW Europe. Comptes Rendus Geoscience 354. https://doi.org/10.5802/crgeos.118.
Perch-Nielsen, K., 1979. Calcareous nannofossils from the Cretaceous between the North Sea and the Mediterranean. In: Wiedmann, J. (Ed.), Aspecte der Kriede Europas. International Union of Geological Sciences, Stuttgart, pp. 223–272.
Perch-Nielsen, K., 1985. Mesozoic calcareous nannofossils. In: Bolli, H.M., Saunders, J.B., Perch-Nielsen, K. (Eds.), Plankton Stratigraphy. Cambridge University Press, pp. 329–426.
Peryt, D., Dubicka, Z., Wierny, W., 2022. Planktonic foraminiferal biostratigraphy of the Upper Cretaceous of the Central European Basin. Geosciences 12, 1–24.
Petrizzo, M.R., 2000. Upper Turonian–lower Campanian planktonic foraminifera from southern mid-high latitudes (Exmouth Plateau, NW Australia): biostratigraphy and taxonomic notes. Cretaceous Research 21, 479–505.
Petrizzo, M.R., Falzoni, F., Silva, I.P., 2011. Identification of the base of the lower-to-middle Campanian *Globotruncana ventricosa* zone: comments on reliability and global correlations. Cretaceous Research 32, 387–405.
Petrizzo, M.R., Huber, B.T., Falzoni, F., MacLeod, K.G., 2020. Changes in biogeographic distribution patterns of southern mid-to high latitude planktonic foraminifera during the Late Cretaceous hot to cool greenhouse climate transition. Cretaceous Research 115, 104547.
Petters, S.W., 1977. *Bolivinoides* evolution and Upper Cretaceous biostratigraphy of the Atlantic Coastal Plain of New Jersey. Journal of Paleontology 51, 1023–1036.
Powell, A.J., Dodge, J.D., Lewis, J., 1990. Late Neogene to Pleistocene palynological facies of the Peruvian continental margin upwelling, Leg 112. Proceedings of the Ocean Drilling Project Scientific Results 112, 297–321.
Powell, A.J., Lewis, J., Dodge, J.D., 1992. The palynological expressions of post-Palaeogene upwelling: a review. In: Summerhayes, C.P., Prell, W.L., Emeis, K.C. (Eds.), Upwelling Systems: Evolution Since the Early Miocene, Geological Society Special Publication, vol. 64, pp. 215–226.
Prauss, M.L., 2015. Marine palynology of the Oceanic Anoxic Event 3 (OAE3, Coniacian–Santonian) at Tarfaya, Morocco, NW Africa - transition from preservation to production controlled accumulation of marine organic carbon. Cretaceous Research 53, 19–37.
Premoli Silva, I., 1977. Upper Cretaceous—Paleocene magnetic stratigraphy at Gubbio, Italy II. Biostratigraphy. Geological Society of America Bulletin 88, 371–374.
Premoli Silva, I., Sliter, W.V., 1995. Cretaceous planktonic foraminiferal biostratigraphy and evolutionary trends from the Bottaccione section, Gubbio, Italy. Palaeontographia Italica 82, 1–89.
Prince, I.M., 1997. Palynology of the Upper Turonian to Lower Campanian Chalks of Southern England (Unpublished PhD thesis). Institute of Earth Studies, University of Wales, Aberystwyth, p. 334.
Prince, I.M., Jarvis, I., Tocher, B.A., 1999. High-resolution dinoflagellate cyst biostratigraphy of the Santonian–basal Campanian (Upper Cretaceous): new data from Whitecliff, Isle of Wight, England. Review of Palaeobotany and Palynology 105, 143–169.
Prince, I.M., Jarvis, I., Pearce, M.A., Tocher, B.A., 2008. Dinoflagellate cyst biostratigraphy of the Coniacian–Santonian (Upper Cretaceous): new data from the English Chalk. Review of Palaeobotany and Palynology 150, 59–96.
Rawson, P.F., Allen, P., Gale, A.S., 2001. The Chalk Group - a revised lithostratigraphy. Geoscientist 11, 21.
Reichart, G.-J., Brinkhuis, H., 2003. Late Quaternary *Protoperidinium* cysts as indicators of paleoproductivity in the northern Arabian Sea. Marine Micropaleontology 49, 303–315.
Robaszynski, F., Bellier, J.P., 2000. Biostratigraphie de Crétacé avec les foraminifères dans les forages de Poigny et de Sainte-Coulombe. Bulletin d'Information des Géologues du Bassin de Paris 37, 59–65.
Robaszynski, F., Caron, M., 1995. Foraminifères planctoniques du Crétacé: commentaire de la zonation Europe - Méditerranée zonation. Bulletin de la Société géologique de France 166, 681–692.
Robaszynski, F., Caron, M., Gonzáles Donso, J.M., Wonders, A.A.H., the European Working Group on Planktonic Foraminifera, 1984. Atlas of Late Cretaceous globotruncanids. Revue de Micropaléontologie 26, 145–305.
Robaszynski, F., Pomerol, B., Masure, E., Bellier, J.P., Deconinck, J.F., 2005. Stratigraphy and stage boundaries in reference sections of the Upper Cretaceous Chalk in the east of the Paris Basin: the “Craie 700” Provins boreholes. Cretaceous Research 26, 157–169.
Robinson, D.A., 2020. The Chalk coast of Sussex. In: Goudie, A., Migoń, P. (Eds.), Landscapes and Landforms of England and Wales. Springer, Cham, pp. 119–143.
Roth, P.H., 1978. Cretaceous nannoplankton biostratigraphy and oceanography of the northwestern Atlantic Ocean. Initial Reports of the Deep Sea Drilling Project 44, 731–760.
Rowe, A.W., 1900. The zones of the White Chalk of the English coast I. Kent and Sussex. Proceedings of the Geologists' Association 16, 289–368.
Rutkowski, J., 1965. Senonian in the area of Miechów, southern Poland (in Polish). Rocznik Polskiego Towarzystwa Geologicznego - Annales de la Société Géologique de Pologne 35, 3–53.
Sabatino, N., Meyers, S.R., Voigt, S., Coccioni, R., Sprovieri, M., 2018. A new high-resolution carbon-isotope stratigraphy for the Campanian (Bottaccione section): its implications for global correlation, ocean circulation, and astrochronology. Palaeogeography, Palaeoclimatology, Palaeoecology 489, 29–39.
Schiøler, P., 1992. Dinoflagellate cysts from the Arnager Limestone Formation (Coniacian, Late Cretaceous), Bornholm, Denmark. Review of Palaeobotany and Palynology 72, 1–25.
Schiøler, P., Wilson, G.J., 2001. Dinoflagellate biostratigraphy around the Campanian–Maastrichtian boundary at Tercis les Bains, southwest France. In: Odin, G.S. (Ed.), The Campanian–Maastrichtian Boundary. Characterisation at Tercis les Bains (France) and Correlation with Europe and other Continents. Elsevier, Amsterdam, pp. 221–234.
Scholle, P.A., Arthur, M.A., 1980. Carbon isotope fluctuation in Cretaceous pelagic limestones: potential stratigraphic and petroleum exploration tool. American Association of Petroleum Geologists Bulletin 64, 67–87.
Schönfeld, J., 1990. Zur stratigraphie und ökologie benthischer foraminiferen im Schreibkreide – Richtprofil von Lägerdorf/Holstein. Geologisches Jahrbüch A 117, 3–151.
Schönfeld, J., Schulz, M.-G., McArthur, J.M., Burnett, J.A., Gale, A.S., Hambach, U., Hansen, H.J., Kennedy, W.J., Rasmussen, K.L., Thirlwall, M.F., Wray, D., 1996. New results on biostratigraphy, palaeomagnetism, geochemistry and correlation from the standard section for the Upper Cretaceous White Chalk of northern Germany (Lägerdorf - Kronsmoor - Hemmoor). Mitteilungen aus dem Geologisch - Paläontologischen Institut der Universitat Hamburg 77, 545–575.
Schulz, M.G., Ernst, G., Ernst, H., Schmid, F., 1984. Coniacian to Maastrichtian stage boundaries in the standard sections for the Upper Cretaceous white chalk of N.W. Germany (Lägerdorf - Kronsmoor - Hemmoor): definitions and proposals. Bulletin of the Geological Society of Denmark 33, 203–215.
Shen, Z., Yu, Z., Ye, H., Deng, C., He, H., 2022. Magnetostratigraphy of the Upper Cretaceous Nenjiang Formation in the Songliao Basin, northeast China: implications for age constraints on terminating the Cretaceous Normal Superchron. Cretaceous Research 135, 105213.
Sissingh, W., 1977. Biostratigraphy of Cretaceous nannoplankton. Geologie en Mijnbouw 56, 37–65.
Slimani, H., 2000. Nouvelle zonation aux kystes de dinoflagellés du Campanien au Danien dans le nord et l'est de la Belgique et dans le sud-est des Pays-Bas. Memoirs of the Geological Survey of Belgium 46, 1–88.
Slimani, H., 2001. Les kystes de dinoflagellés du Campanien au Danien dans la région de Maastricht (Belgique, Pays-Bas) et de Turnhout (Belgique): biozonation et corrélation avec d'autres régions en Europe occidentale. Geologica et Palaeontologica 35, 161–201.
Slimani, H., Louwye, S., Dusar, M., Lagrou, D., 2011. Connecting the Chalk Group of the Campine Basin to the dinoflagellate cyst biostratigraphy of the Campanian to Danian in borehole Meer (northern Belgium). Netherlands Journal of Geosciences - Geologie en Mijnbouw 90, 129–164.
Sluijs, A., Pross, J., Brinkhuis, H., 2005. From greenhouse to icehouse; organic-walled dinoflagellate cysts as paleoenvironmental indicators in the Paleogene. Earth-Science Reviews 68, 281–315.
Smith, A.B., Wright, C.W., 2003. British Cretaceous Echinoids. Part 7, Atelostomata I. Holasteroidea. Monograph of the Palaeontological Society 166, 440–568.
Stover, L.E., Evitt, W.R., 1978. Analysis of Pre-Pleistocene Organic Walled Dinoflagellates. In: Stanford University Publications, Geological Sciences, vol. 15, pp. 1–300.
Stover, L.E., Brinkhuis, H., Damassa, S.P., Verteuil, L.D., Helby, R.J., Monteil, E., Partridge, A.D., Powell, A.J., Riding, J.B., Smelror, M., Williams, G.L., 1996. Mesozoic–Tertiary dinoflagellates, acritarchs and prasinophytes. In: Jansonius, J., McGregor, D.C. (Eds.), Palynology: Principles and Applications, vol. 2. American Association of Stratigraphic Palynologists Foundation, College Station TX, pp. 641–750.
Stradner, H., Steinmetz, J., 1984. Cretaceous calcareous nannofossils from the Angola Basin, Deep Sea Drilling Project Site 530. Initial Reports of the Deep Sea Drilling Project 75, 565–649.
Surlyk, F., Rasmussen, S.L., Boussaha, M., Schioler, P., Schovsbo, N.H., Sheldon, E., Stemmerik, L., Thibault, N., 2013. Upper Campanian–Maastrichtian holostratigraphy of the eastern Danish Basin. Cretaceous Research 46, 232–256.
Tahoun, S.S., Deaf, A.S., Ied, I.M., 2018. The use of cyclic stratigraphic pattern of peridinioid and gonyaulacoid dinoflagellate cysts in differentiating potential thick monotonous carbonate reservoirs: a possible ecostratigraphic tool under test. Marine and Petroleum Geology 96, 240–253.
Takashima, R., Nishi, H., Yamanaka, T., Orihashi, Y., Tsujino, Y., Quidelleur, X., Hayashi, K., Sawada, K., Nakamura, H., Ando, T., 2019. Establishment of Upper Cretaceous bio- and carbon isotope stratigraphy in the northwest Pacific Ocean and radiometric ages around the Albian/Cenomanian, Coniacian/Santonian and Santonian/Campanian boundaries. Newsletters on Stratigraphy 52, 341–376.
Thibault, N., Jarvis, I., Voigt, S., Gale, A.S., Attree, K., Jenkyns, H.C., 2016. Astronomical calibration and global correlation of the Santonian (Cretaceous) based on the marine carbon isotope record. Paleoceanography 31, 847–865.
Tremolada, F., 2002. Aptian to Campanian calcareous nannofossil biostratigraphy from the Bottaccione section, Gubbio, Central Italy. Rivista Italiana di Paleontologia e Stratigrafia 108, 441–455.
Ullmann, C.V., Boyle, R., Duarte, L., Hesselbo, S., Kasemann, S.A., Klein, T., Lenton, T.M., Piazza, V., Aberhan, M., 2020. Warm afterglow from the Toarcian Oceanic Anoxic Event drives the success of deep-adapted brachiopods. Scientific Reports 10, 11.
Van Helmond, N.A.G.M., Sluijs, A., Reichart, G.-J., Sissingh Damsté, J.S., Slomp, C.P., Brinkhuis, H., 2014. A perturbed hydrological cycle during Oceanic Anoxic Event 2. Geology 42, 123–126.
Vasilenko, V.P., 1961. Upper Cretaceous Foraminifera from the Mangyshlak Peninsula (in Russian). Trudy Vsesoyuznogo Neftyanogo Nauchno-Issledovatel'skogo Issledovatel'skogo Geologo-Razvedochnogo Instituta (VNIGRI) 171, 3–390.

Voigt, S., Friedrich, O., Norris, R.D., Schönfeld, J., 2010. Campanian–Maastrichtian carbon isotope stratigraphy: shelf-ocean correlation between the European shelf sea and the tropical Pacific Ocean. Newsletters on Stratigraphy 44, 57–72.
Walaszczyk, I., Kennedy, W.J., Dembicz, K., Gale, A.S., Praszkier, T., Rasoamiaramanana, A.H., Randrianaly, H., 2014. Ammonite and inoceramid biostratigraphy and biogeography of the Cenomanian through basal Middle Campanian (Upper Cretaceous) of the Morondava Basin, western Madagascar. Journal of African Earth Sciences 89, 79–132.
Walaszczyk, I., Dubicka, Z., Olszewska-Nejbert, D., Remin, Z., 2016. Integrated biostratigraphy of the Santonian through Maastrichtian (Upper Cretaceous) of extra-Carpathian Poland. Acta Geologica Polonica 66, 313–350.
Wang, T., Ramezani, J., Wang, C., Wu, H., He, H., Bowring, S.A., 2016. High-precision U–Pb geochronologic constraints on the Late Cretaceous terrestrial cyclostratigraphy and geomagnetic polarity from the Songliao Basin, Northeast China. Earth and Planetary Science Letters 446, 37–44.
Weir, A.H., Catt, J.A., 1965. The mineralogy of some Upper Chalk samples from the Arundel area, Sussex. Clay Minerals 6, 97–110.
Wilkinson, I.P., 2011. Foraminiferal biozones and their relationship to the lithostratigraphy of the Chalk Group of southern England. Proceedings of the Geologists' Association 122, 842–849.
Wilkinson, I.P., 2013. A Preliminary Foraminiferal Biozonation of the Chalk Group. British Geological Survey Internal Report IR/00/13, p. 21.
Willcox, N.R., 1953. Zonal variations in selected morphological features of *Echinocorys scutata* Leske. Geological Magazine 90, 83–96.
Williams, G.L., Bujak, J.P., 1985. Mesozoic and Cenozoic dinoflagellates. In: Bolli, H.M., Saunders, J.B., Perch-Nielsen, K. (Eds.), Plankton Stratigraphy, Cambridge Earth Science Series, Cambridge, pp. 847–964.
Williams, G.L., Brinkhuis, H., Weegink, J.W., Bujak, J.P., 1998. A Classification of Living and Fossil Dinoflagellates: update, 1st November, 1998. Mesozoic–Cenozoic Dinoflagellate Cyst Course 17–22 May 1998. University of Urbino, Urbino, pp. 1–32.
Williams, G.L., Brinkhuis, H., Pearce, M.A., Fensome, R.A., Weegink, J.W., 2004. Southern Ocean and global dinoflagellate cyst events compared: index events for the Late Cretaceous–Neogene. Proceedings of the Ocean Drilling Program, Scientific Results 189, 1–98.
Wilmsen, M., Bansal, U., 2021. Depositional setting and limiting factors of early Late Cretaceous glaucony formation: implications from Cenomanian glauconitic strata (Elbtal Group, Germany). Facies 67, 24.
Wise, S.W., 1983. Mesozoic and Cenozoic calcareous nannofossils recovered by Deep Sea Drilling Project Leg 71 in the Falkland Plateau region, south-west Atlantic Ocean. Initial Reports of the Deep Sea Drilling Project 71, 481–550.
Wise, S.W., Wind, F.H., 1977. Mesozoic and Cenozoic calcareous nannofossils recovered by DSDP Leg 36 drilling on the Falkland Plateau, southwest Atlantic sector of the Southern Ocean. Initial Reports of the Deep Sea Drilling Project 36, 269–491.
Wolfgring, E., Wagreich, M., Dinares-Turell, J., Gier, S., Bohm, K., Sames, B., Spotl, C., Popp, F., 2018a. The Santonian–Campanian boundary and the end of the Long Cretaceous Normal Polarity-Chron: isotope and plankton stratigraphy of a pelagic reference section in the NW Tethys (Austria). Newsletters on Stratigraphy 51, 445–476.
Wolfgring, E., Wagreich, M., Dinares-Turell, J., Yilmaz, I.O., Bohm, K., 2018b. Plankton biostratigraphy and magnetostratigraphy of the Santonian–Campanian boundary interval in the Mudurnu-Goynuk Basin, northwestern Turkey. Cretaceous Research 87, 296–311.
Wood, C.J., Mortimore, R., 1988. Biostratigraphy of the Newhaven and Culver Members. In: Young, B., Lake, R.D. (Eds.), Geology of the Country around Brighton and Worthing. HMSO, London, pp. 58–64.
Wood, C.J., Morter, A.A., Gallois, R.W., 1994. Appendix 1. Upper Cretaceous stratigraphy of the Trunch borehole. TG23SE8. In: Arthurton, R.S., Booth, S.J., Morigi, A.N., Abbott, M.A.W., Wood, C.J. (Eds.), Geology of the Country around Great Yarmouth. Memoir for 1:50,000 Sheet 162 (England and Wales) with an Appendix on the Trunch Borehole by Wood and Morter. HMSO, London, pp. 105–110.
Wood, G.D., Gabriel, A.M., Lawson, J.C., 1996. Chapter 3. Palynological techniques - processing and microscopy. In: Jansonius, J., McGregor, D.C. (Eds.), Palynology: Principles and Applications. American Association of Stratigraphic Palynologists Foundation, Dallas, pp. 29–50.
Wray, D.S., Jeans, C.V., 2014. Chemostratigraphy and provenance of clays and other non-carbonate minerals in chalks of Campanian age (Upper Cretaceous) from Sussex, southern England. Clay Minerals 49, 327–340.
Yorath, C.J., Norris, D.K., 1975. The tectonic development of the southern Beaufort Sea and its relationship to the origin of the Arctic Ocean Basin. In: Yorath, C.J., Parker, E.R., Glass, D.J. (Eds.), Canada's Continental Margins and Offshore Petroleum Exploration, Canadian Society of Petroleum Geologists Memoir, vol. 4, pp. 589–611.

Appendix A. List of palynological taxa with taxonomy of *Rhynchodiniopsis juneae* sp. nov.

A complete list of organic-walled dinoflagellate cyst taxa and associated palynomorphs identified in this study of the Santonian–Campanian boundary sections at Seaford Head (SH) and Bocieniec (BC) are provided below. The classification of Fensome et al. (1993) with updates of Williams et al. (1998) is followed here, with references cited therein. The taxonomy of Fensome et al. (2019a) is employed and taxa are cited as they appear in that work, with additional updates from Pearce (2018), Fensome et al. (2019b), Pearce et al. (2019) and Niechwedowicz (2022).

Stratigraphically significant species and selected other taxa marked with an asterisk (*) are plotted on the Seaford Head and Bocieniec range charts (Figs. 5, 10); double dagger (‡) indicates taxa included on the assemblage plots (Figs. 6, 11). The species *Rhynchodiniopsis juneae* sp. nov. is described. Selected stratigraphically significant species are illustrated in Figs. 7, 8 and 12. Sample records of all taxa are listed in Appendix B Supplementary data Tables 2 and 3.

Division DINOFLAGELLATA (Bütschli 1885) Fensome et al., 1993		
Subdivision DINOKARYOTA Fensome et al., 1993		
Class DINOPHYCEAE Pascher, 1914		
Subclass GYMNODINIPHYCIDAE Fensome et al., 1993		
Order PTYCHODISCALES Fensome et al., 1993		
Family PTYCHODISCACEAE Willey and Hickson, 1909		
Subfamily DINOGYMNIOIDEAE (Sarjeant and Downie, 1974) Fensome et al., 1993		
Alisogymnium euclaense (Cookson and Eisenack, 1970a) Lentin and Vozzhennikova, 1990	BC	SH
Dinogymnium acuminatum Evitt et al., 1967	BC*	SH*
Dinogymnium albertii Clarke and Verdier, 1967	BC	
Dinogymnium denticulatum (Alberti, 1961) Evitt et al., 1967	SH	
Dinogymnium heterocostatum (Deflandre, 1936b) Evitt et al., 1967	BC	
Dinogymnium spp. Evitt et al., 1967	SH	
Subclass PERIDINIPHYCIDAE Fensome et al., 1993		
Order GONYAULACALES Taylor, 1980		
Suborder CLADOPYXIINEAE Fensome et al., 1993		
Family CLADOPYXIACEAE Stein, 1883		
Microdinium bensonii subsp. *pilatum* Slimani, 1994	BC	
Microdinium glabrum Cookson and Eisenack, 1974	BC	
Microdinium minutum Louwye, 1997	BC	
Microdinium reticulatum Vozzhennikova, 1967	BC	
Microdinium spp. Cookson and Eisenack, 1960a	SH	
Family UNCERTAIN		
Rhiptocorys veligera (Deflandre, 1937b) Lejeune-Carpentier and Sarjeant, 1983	BC	
Suborder GONIODOMINEAE Fensome et al., 1993		
Family GONIODOMACEAE Lindemann, 1928		
Subfamily PYRODINIOIDEAE Fensome et al., 1993		
Alisocysta circumtabulata (Drugg, 1967) Stover and Evitt, 1978	BC*	
Dinopterygium alatum (Cookson and Eisenack, 1962b) Fensome et al., 2009	BC	SH
Dinopterygium cf. *cladoides* Deflandre, 1935	BC	SH
Dinopterygium cladoides Deflandre, 1935	BC*	
Eisenackia? *knokkensis* Louwye, 1997 Fig. 7F, 12E	BC*‡	SH*
Hystrichosphaeridium bowerbankii Davey and Williams, 1966b	BC	SH
Hystrichosphaeridium recurvatum (White, 1842) Lejeune-Carpentier, 1940	BC	SH‡
Hystrichosphaeridium sp. 2 McIntyre, 1974	BC	
Hystrichosphaeridium spp. Deflandre, 1937b	BC	SH
Hystrichosphaeridium brevispinum (Davey and Williams, 1966b) Niechwedowicz, 2021	BC	SH
Hystrichosphaeridium tubiferum (Ehrenberg, 1837b) Deflandre, 1937b	BC	SH
Hystrichosphaeridium? *paracostatum* Cookson and Eisenack, 1974	SH	
Suborder GONYAULACINEAE (Autonym)		
Family GONYAULACACEAE Lindemann, 1928		
Subfamily LEPTODINIOIDEAE Fensome et al., 1993		
Eatonicysta? mutabilireta Pearce, 2010	SH*	
Kleithriasphaeridium loffrense Davey and Verdier, 1976		
Kleithriasphaeridium mantellii (Singh, 1971) Fensome et al., 2009	SH	
Litosphaeridium siphoniphorum subsp. *siphoniphorum* (Cookson and Eisenack, 1958) Davey and Williams, 1966b	BC	
Membranigonyaulax wilsonii Slimani, 1994	BC*	SH*
Oligosphaeridium complex (White, 1842) Davey and Williams, 1966b	BC	SH
Oligosphaeridium pulcherrimum Deflandre and Cookson, 1955	BC	SH

Genus *Rhynchodiniopsis* Deflandre, 1935
Type species. *Rhynchodiniopsis aptiana* Deflandre, 1935, pl. 5, fig. 10; pl. 8, figs 7–9.

Rhynchodiniopsis juneae sp. nov.
(Figs. 8B–C)

Etymology. Named in loving memory of June Webber, Grandmother of MAP who passed away on the 16th October 2022.
Holotype. Seaford Head, sample 149, England Finder (EF) location K23/4, Fig. 8B.
Other specimens. The operculum demonstrating the distinctive ornament (as a paratype) sample 144, EF location O37, Fig. 8C; see also EF: C22/4, G28/2, O22, O28/2, O29/2, O37, Q38/3, R45, S44/3, U16/3.
Type locality. Seaford Head, Sussex, England.
Type stratum. Newhaven Chalk Formation (lower Campanian, *Gonioteuthis quadrata* Zone).

Repository of the type material. Department of Earth Sciences, Natural History Museum, Cromwell Road, London SW7 5BD, UK. Holotype, NHMUK PM FD 1404 (1); paratype, NHMUK PM FD 1404 (2).

Diagnosis. A species of *Rhynchodiniopsis* possessing a foveolate periphragm and high parasutural crests.

Description. A large, elongate, acavate, murochorate dinoflagellate cyst, exhibiting minimal dorso-ventral compression and a prominent apical horn (average height 19 μm). The ambitus is sub-polygonal, complete length exceeds complete width (average w × l = 78 × 92 μm). Wall composed of a smooth endophragm and a closely appressed and thinner foveolate periphragm that forms parasutural crests (average maximum height 8 μm), accessory crests are absent. The foveolae are randomly distributed over the entire body, are circular to elongate, with the longest axis measuring 1–4 μm, and that impart a ragged appearance to the crests. Simple gonal spines slightly exceed the crests in height, thin spines or fine radial thickenings occur within the sutural crests. The paratabulation is indicated by the parasutural crests and conforms to the standard gonyaulacoid formula 4′, 6″, 6c, ?s, 6‴, 1p, 1⁗, indicating an L-Type ventral, and sexiform hypocystal plate arrangement. Dextral torsion exists such that the boundary between the 4‴ and 5‴ paraplates is mid-dorsal. The archaeopyle is precingular formed by the loss of the 3″ plate, the operculum is detached.

Dimensions. Holotype (including apical horn and sutural crests), width 98 μm, length 97 μm; maximum sutural crest height 10 μm, apical horn length 28 μm. Range (including apical horn and sutural crests), width 60(78)98 μm, 24 individuals measured; length 69(91.9)105 μm, 14 individuals measured; maximum sutural crests height 4(7.7)11 μm, 23 individuals measured; apical horn length 10(19.4) 28 μm, 18 individuals measured.

Comparison. *Rhynchodiniopsis saliorum* Louwye, 1997 most closely resembles *R. juneae* sp. nov. but differs in possessing a scabrate wall and lacks foveolae. *Rhynchodiniopsis fimbriata* Duxbury 1980 and *R. foveolata* Snape 1992 are similar in having fenestrate crests, but which are significantly lower than those of *R. juneae* sp. nov. In addition, *Rhynchodiniopsis fimbriata* has a finely reticulate wall, and the foveolae in *R. foveolata* are concentrated to the cingular and penitabular areas.

Rhynchodiniopsis saliorum Louwye, 1997	BC*‡	SH*
Figs. 8D, 12I		
Rhynchodiniopsis spp. Deflandre, 1935	SH	
Subfamily CRIBROPERIDINIOIDEAE Fensome et al., 1993		
Apteodinium deflandrei (Clarke and Verdier, 1967) Lucas-Clark, 1987	BC	SH
Apteodinium spp. Eisenack, 1958a	BC	SH
Cordosphaeridium catherineae Pearce, 2010	BC*	SH*
Figs. 7C, 12C		
Cribroperidinium spp. Neale and Sarjeant, 1962	BC	SH
Cribroperidinium wilsonii (Yun Hyesu, 1981) Poulsen, 1996	BC	
Florentinia buspina Davey and Verdier, 1976	BC	SH
Florentinia clavigera (Deflandre, 1937b) Davey and Verdier, 1973, p.192	SH	
Florentinia deanei (Davey and Williams, 1966b) Davey and Verdier, 1973	SH	
Florentinia ferox (Deflandre, 1937b) Duxbury, 1980	SH	
Florentinia hypomagna Yun Hyesu, 1981	BC	
Florentinia laciniata Davey and Verdier, 1973	BC	
Florentinia mayi Kirsch, 1991	SH*	
Florentinia radiculata (Davey and Williams, 1966b) Davey and Verdier, 1973	BC	
Florentinia spp. Davey and Verdier, 1973	BC	SH
Florentinia tenera (Davey and Verdier, 1976) Duxbury, 1980	BC	
Kallosphaeridium spp. de Coninck, 1969	SH	
Subfamily GONYAULACOIDEAE (Autonym)		
Achomosphaera granulata Mao Shaozhi, 1989	SH	
Achomosphaera ramulifera (Deflandre, 1937b) Evitt, 1963	BC	SH
Achomosphaera regiensis Corradini, 1973	BC	SH‡
Achomosphaera spp. Evitt, 1963	SH	
Cannosphaeropsis utinensis Wetzel, 1933b	BC*	
Fig. 12A		
Hystrichosphaeropsis ovum Deflandre, 1935	BC*	SH*
Hystrichosphaeropsis quasicribrata (Wetzel, 1961) Gocht, 1976	BC*	
Hystrichostrogylon (vermiculate)	BC	
Hystrichostrogylon membraniphorum membraniphorum Agelopoulos, 1964	SH	
Hystrichostrogylon membraniphorum subsp. *granulatum* Heilmann-Clausen in Heilmann-Clausen and Costa, 1989	BC	SH
Pterodinium cingulatum subsp. *cingulatum* (Wetzel, 1933b) Below, 1981a	BC	SH
Pterodinium cingulatum subsp. *granulatum* (Clarke and Verdier, 1967) Lentin and Williams, 1981	BC	
Pterodinium cingulatum subsp. *reticulatum* (Davey and Williams, 1966a) Lentin and Williams, 1981	BC	
Spiniferites foveolatus Schiøler, 1993	BC	
Spiniferites jarvisii Pearce, 2010	BC*	
Fig. 12K		
Spiniferites membranaceus (Rossignol, 1964) Sarjeant, 1970	BC	SH
Spiniferites multispinulus Pearce, 2010	SH*	
Spiniferites ramosus subsp. *aquilus* Pearce, 2010	BC	
Spiniferites ramosus subsp. *ginakrogiae*, Pearce, 2018	BC	
Spiniferites ramosus subsp. *gracilis* (Davey and Williams, 1966a) Lentin and Williams, 1973	BC	SH
Spiniferites ramosus subsp. *granomembranaceus* (Davey and Williams, 1966a) Lentin and Williams, 1973	BC	
Spiniferites ramosus subsp. *granosus* (Davey and Williams, 1966a) Lentin and Williams, 1973	BC	SH
Spiniferites ramosus subsp. *maeandriformis* (Corradini, 1973) Lentin and Williams, 1975	BC*	
Spiniferites ramosus subsp. *ramosus* (Ehrenberg, 1837b) Mantell, 1854	BC*‡	SH*‡
Spiniferites ramosus subsp. *reticulatus* (Davey and Williams, 1966a) Lentin and Williams, 1973	BC	SH
Spiniferites spp. Mantell, 1850	BC	SH
Spiniferites twistringiensis (Maier, 1959) Fensome et al., 1990	BC‡	SH‡
Turnhosphaera hypoflata (Yun Hyesu, 1981) Slimani, 1994	BC*	SH*
Subfamily UNCERTAIN		
Callaiosphaeridium asymmetricum (Deflandre and Courteville, 1939) Davey and Williams, 1966b	BC	
Cometodinium obscurum Deflandre and Courteville, 1939	BC	SH
Cometodinium whitei (Deflandre and Courteville, 1939) Stover and Evitt, 1978	BC	
Cometodinium? *comatum* Srivastava, 1984	BC	SH
Coronifera hebospina (Yun Hyesu, 1981) Peyrot, 2011	SH	
Coronifera oceanica Cookson and Eisenack, 1958	BC	SH
Coronifera striolata (Deflandre, 1937) Stover and Evitt, 1978 *sensu* Schiøler 1992	BC*	SH*
Hystrichodinium pulchrum Deflandre, 1935	BC	SH
Pervosphaeridium intervelum Kirsch, 1991	SH*	
Pervosphaeridium monasteriense Yun Hyesu, 1981	SH*	
Pervosphaeridium pseudhystrichodinium (Deflandre, 1937b) Yun Hyesu, 1981	BC*‡	SH*
Pervosphaeridium spp. Yun Hyesu, 1981	BC	
Sentusidinium euteichum (Davey, 1969a) Wood et al., 2016	BC	SH
Sentusidinium explanatum (Bujak in Bujak et al., 1980) Wood et al., 2016	SH	
Sentusidinium ringnesiorum (Manum and Cookson, 1964) Wood et al., 2016	BC	SH
Sentusidinium spp. Sarjeant and Stover, 1978	BC*‡	SH*
Surculosphaeridium belowii Yun Hyesu, 1981	BC	SH
Surculosphaeridium convocatum Fensome et al., 2016	BC	
Surculosphaeridium longifurcatum (Firtion, 1952) Davey et al., 1966	BC*‡	SH*‡
Figs. 8H, 12L		
Surculosphaeridium spinicongregatum Yun Hyesu, 1981	SH	
Surculosphaeridium spp. Davey et al., 1966	BC	
Surculosphaeridium? *basifurcatum* Yun Hyesu, 1981	SH	
Surculosphaeridium? *cassospinum* Yun Hyesu, 1981	BC	SH
Trichodinium castanea Deflandre, 1935 ex Clarke and Verdier, 1967	BC*	SH*
Family AREOLIGERACEAE Evitt, 1963b		
Areoligeraceae (undiff.)	SH	
Canningia glomerata Fensome et al., 2019b	BC*‡	SH*‡
Fig. 7A		
Canningia reticulata Cookson and Eisenack, 1960b	SH	
Canningia senonica Clarke and Verdier, 1967	SH*‡	
Fig. 7B		
Canningia spp. Cookson and Eisenack, 1960b	BC	
Circulodinium distinctum (Deflandre and Cookson, 1955) Jansonius, 1986	BC*‡	SH*
Circulodinium latoaculeum (Yun Hyesu, 1981) Prince et al., 1999	BC	
Senoniasphaera congrensa (Prince et al., 2008) Fensome et al., 2019b	BC*‡	SH*‡
Fig. 8E		
Senoniasphaera macroreticulata Prince et al., 2008	SH*‡	
Fig. 8F		
Senoniasphaera filoreticulata (Slimani, 1994) Fensome et al., 2019b	SH*	
Senoniasphaera protrusa Clarke and Verdier, 1967	BC*‡	SH*‡
Figs. 8G, 12J		
Senoniasphaera spp. Clarke and Verdier, 1967	BC	SH
Senoniasphaera turonica (Prössl, 1990 ex Prössl, 1992b) Pearce et al., 2011	SH*	
Tenua colliveri (Cookson and Eisenack, 1960b) Fensome et al., 2019b	BC*	SH*
Tenua hystrix Eisenack, 1958a	SH	
Trimuridinium whitenessense (Prince et al., 2008) Fensome et al., 2019b	SH*	
Fig. 8I		
Suborder CERATIINEAE Fensome et al., 1993		
Family CERATIACEAE Willey and Hickson, 1909		
Muderongia simplex Alberti, 1961	BC	
Odontochitina costata Alberti, 1961	BC*	SH*
Odontochitina diducta Pearce, 2010	BC*	SH*
Fig. 7J		
Odontochitina operculata (Wetzel, 1933a) Deflandre and Cookson, 1955	BC*‡	SH*
Odontochitina porifera Cookson, 1956	BC*‡	SH*
Figs. 7K, 12H		
Odontochitina spp. Deflandre, 1937b	BC	
Xenascus australensis Cookson and Eisenack, 1969	BC	SH
Xenascus blastema (Davey, 1970) Stover and Helby, 1987a	BC	
Xenascus ceratioides (Deflandre, 1937b) Lentin and Williams, 1973	BC*	SH*
Xenascus perforatus (Vozzhennikova, 1967) Yun Hyesu, 1981	SH*‡	
Fig. 8K		
Xenascus sarjeantii (Corradini, 1973) Stover and Evitt, 1978	SH	
Xenascus sp. SS (short spines)	SH	
Xenascus spp. Cookson and Eisenack, 1969	BC	SH
Xenascus yunii Prince et al., 2008	BC	SH

Suborder UNCERTAIN
Family UNCERTAIN

Batiacasphaera spp. Drugg, 1970b	BC	
Caligodinium aceras (Manum and Cookson, 1964) Lentin and Williams, 1973	SH	
Caligodinium amiculum Drugg, 1970b	BC	
Cassiculosphaeridia reticulata Davey, 1969a	BC*	SH*
Cassiculosphaeridia? intermedia Slimani, 1994	SH	
Chlamydophorella discreta Clarke and Verdier, 1967	BC	SH
Chlamydophorella nyei Cookson and Eisenack, 1958	SH	
Culversphaera velata (Clarke and Verdier, 1967) Prince et al., 2008 Fig. 7D	BC*	SH*‡
Dapsilidinium laminaspinosum (Davey and Williams, 1966b) Lentin and Williams, 1981	BC	SH
Dapsilidinium spp. Bujak et al., 1980	BC	SH
Dapsilidinium? pumilum (Davey and Williams, 1966b) Lentin and Williams, 1981	SH	
Dapsilidinium? simplex (White, 1842) Bujak et al., 1980	SH	
Desmocysta plekta Duxbury, 1983	SH	
Dimidium striatum (Clarke and Verdier, 1967) Pearce, 2010 Figs. 7E, 12D	BC*	SH*
Disphaeria macropyla Cookson and Eisenack, 1960	BC*	SH*
Downiesphaeridium armatum (Deflandre, 1937b) Islam, 1993	BC	SH
Downiesphaeridium flexuosum (Davey et al., 1966) Islam, 1993	SH	
Downiesphaeridium spp. Islam, 1993	BC	
Downiesphaeridium? aciculare (Davey, 1969a) Islam, 1993	BC	SH
Ellipsodinium membraniferum Prince et al., 2008 Figs. 7G, 12F	BC*	SH*
Ellipsodinium rugulosum Clarke and Verdier, 1967	BC*	SH*
Exochosphaeridium arnace Davey and Verdier, 1973	BC	SH
Exochosphaeridium majus (Lejeune-Carpentier, 1940) Peyrot, 2011	BC*	SH*
Exochosphaeridium majus (Lejeune-Carpentier, 1940) Peyrot, 2011 (robust type)	SH*	
Exochosphaeridium phragmites Davey et al., 1966	BC	SH
Heterosphaeridium bellii Radmacher et al., 2014	SH	
Heterosphaeridium conjunctum Cookson and Eisenack, 1968	SH	
Heterosphaeridium cordiforme Yun Hyesu, 1981	SH	
Heterosphaeridium difficile (Manum and Cookson, 1964) Ioannides, 1986 Fig. 12G	BC*	
Heterosphaeridium heteracanthum (Deflandre and Cookson, 1955) Eisenack and Kjellström, 1972 Fig. 7H	BC	SH‡
Heterosphaeridium heteracanthum sensu Pearce et al., 2003	BC*	SH
Heterosphaeridium sp. G (gracile)	SH*	
Heterosphaeridium spinaconjunctum Yun Hyesu, 1981	SH	
Heterosphaeridium spp. Cookson and Eisenack, 1968	SH	
Heterosphaeridium verdieri Yun Hyesu, 1981 Fig. 7I	SH‡	
Impletosphaeridium clavulum (Davey, 1969a) Islam, 1993	BC	SH
Impletosphaeridium spp. Morgenroth, 1966a	BC	
Membranilarnacia polycladiata Cookson and Eisenack in Eisenack, 1963a	BC	SH
Membranilarnacia pterococcoides (Wetzel, 1933b) Eisenack, 1963a	SH*	
Membranilarnacia wilsonii Pearce, 2010	BC	SH
Montanarocysta aemiliana Corradini, 1973	BC*	SH*
Neosphaerodictyon filosum Slimani, 2003	BC*	SH*
Raetiaedinium truncigerum (Deflandre, 1937b) Kirsch, 1991	BC*	SH*
Raphidodinium fucatum Deflandre, 1936b	BC*	SH*
Tanyosphaeridium xanthiopyxides (Wetzel, 1933b ex Deflandre, 1937b) Stover and Evitt, 1978	BC	SH
Trigonopyxidia ginella (Cookson and Eisenack, 1960a) Downie and Sarjeant, 1965	BC	
Wallodinium luna (Cookson and Eisenack, 1960a) Lentin and Williams, 1973	BC	

Order PERIDINIALES Haeckel, 1894b
Suborder PERIDINIINEAE (Autonym)
Family PERIDINIACEAE Ehrenberg, 1831
Subfamily PALAEOPERIDINIOIDEAE (Vozzhennikova, 1961) Bujak and Davies, 1983

Laciniadinium firmum (Harland, 1973) Morgan, 1977	BC*	
Laciniadinium spp. McIntyre, 1975	BC	
Palaeohystrichophora infusorioides Deflandre, 1935 Fig. 8A	BC*‡	SH*‡
Palaeoperidinium pyrophorum (Ehrenberg, 1837b ex Wetzel, 1933a) Sarjeant, 1967b	BC*	SH*
Subtilisphaera pontis-mariae (Deflandre, 1936b) Lentin and Williams, 1976	BC‡	SH‡
Subtilisphaera spp. Jain and Millepied, 1973	BC	SH

Subfamily DEFLANDREOIDEAE Bujak and Davies, 1983

Alterbidinium ioannidesii Pearce, 2010 Fig. 8L	BC*	
Alterbidinium spp. Lentin and Williams, 1985	BC	
Chatangiella islae Pearce et al., 2019 Fig. 12B	BC*	
Chatangiella ditissima (McIntyre, 1975) Lentin and Williams, 1976	BC*	
Chatangiella granulifera (Manum, 1963) Lentin and Williams, 1976	BC	
Chatangiella manumii (Vozzhennikova, 1967) Lentin and Williams, 1976	SH*	
Chatangiella spp. Vozzhennikova, 1967	BC	
Chatangiella victoriensis (Cookson and Manum, 1964) Lentin and Williams, 1976	BC	
Chatangiella williamsii Yun Hyesu, 1981	BC	
Isabelidinium cooksoniae (Alberti, 1959b) Lentin and Williams, 1977a	BC	SH
Isabelidinium glabrum (Cookson and Eisenack, 1969) Lentin and Williams, 1977a	BC	
Isabelidinium microarmum (McIntyre, 1975) Lentin and Williams, 1977a	BC*	
Spinidinium echinoideum (Cookson and Eisenack, 1960a) Lentin and Williams, 1976	BC*‡	SH*
Trithyrodinium evittii Drugg, 1967	BC*	
Trithyrodinium sabulum Mao Shaozhi and Norris, 1988	BC	
Trithyrodinium cf. *sabulum* Mao Shaozhi and Norris, 1988	BC	
Trithyrodinium vermiculatum (Cookson and Eisenack, 1961a) Lentin and Williams, 1976	BC	

Subfamily OVOIDINIOIDEAE (Norris, 1978) Bujak and Davies, 1983

Bosedinia spp. He Chengquan, 1984b	SH	
Leberidocysta chlamydata (Cookson and Eisenack, 1962b) Stover and Evitt, 1978	BC	SH
Leberidocysta defloccata (Davey and Verdier, 1973) Stover and Evitt, 1978	SH‡	

Subclass PERIDINIPHYCIDAE Fensome et al., 1993
Order UNCERTAIN
Family UNCERTAIN

Palaeotetradinium silicorum Deflandre, 1936b	BC	
Whitecliffia spinosa (Clarke and Verdier, 1967) Pearce, 2010 Fig. 8J	SH*‡	

Subclass DINOPHYSIPHYCIDAE Möhn 1984 ex Fensome et al., 1993
Order NANNOCERATOPSIALES Piel and Evitt 1980
Family NANNOCERATOPSIACEAE Gocht, 1970b

Nannoceratopsis gracilis Alberti, 1961	BC	

Subclass UNCERTAIN
Order UNCERTAIN
Family UNCERTAIN

Prolixosphaeridium? nanus (Wetzel, 1933b ex Lentin and Williams, 1985) Sarjeant, 1985b	SH	
dinocyst (cavate, chorate, murochorate, proximate, proximochorate, undiff.)	BC	

Additional marine palynomorphs:

acritarch (acanthomorph)	SH	
acritarch (undiff.)	BC	
algal cyst (cavate) (*incertae sedis*)	SH	
algal cyst (granulate/scabrate) (*incertae sedis*)	BC	SH
algal cyst (large) (*incertae sedis*)	BC	SH
algal cyst (reticulate) (*incertae sedis*)	BC	
algal cyst (small, thick wall) (*incertae sedis*)	SH	
algal cyst (smooth) (*incertae sedis*)	BC	SH
algal cyst? (diffuse edge) (*incertae sedis*)	SH	
Botryococcus spp. Kützing, 1849	BC	
Comasphaeridium cometes Valensi 1949 (acritarch)	SH	
Crassosphaera spp. Cookson and Manum, 1960 (Prasinophyceae)	BC	SH
Cymatiosphaera spp. Wetzel, 1933 (Prasinophyceae)	BC	SH
Cymatiosphaera spp. Wetzel, 1933 (small, thick) (Prasinophyceae)	SH	
Fromea fragilis (Cookson and Eisenack, 1962b) Stover and Evitt, 1978	BC	
Fromea laevigata (Drugg, 1967) Stover and Evitt, 1978 (acritarch)	BC	
Leiosphaeridia spp. Eisenack, 1958 (large) (Prasinophyceae)	SH	
Leiosphaeridia spp. Eisenack, 1958 (Prasinophyceae)	SH‡,	BC‡
Micrhystridium spp. Deflandre, 1937b	BC	
Microforaminiferal-test-linings (large, fragments)	SH	
Microforaminiferal-test-linings (planispiral)	SH	
Nummus similis (Cookson and Eisenack, 1960b) Burger, 1980b (acritarch)	SH	
Palaeostomocystis reticulata Deflandre, 1937b	BC*	
Palambages morulosa Wetzel, 1961	BC	
Paralecaniella indentata (Deflandre and Cookson, 1955) Cookson and Eisenack, 1970 (acritarch)	BC	SH
Paralecaniella indentata (striate) (acritarch)	BC	
Pediastrum spp. Meyen, 1829	BC	
Prasinophyceae (undiff.)	SH	
Pterospermella aureolata (Cookson and Eisenack, 1958) Eisenack, 1972 (large) (Prasinophyceae)	BC	
Pterospermella aureolata (Cookson and Eisenack, 1958) Eisenack, 1972 (Prasinophyceae)	BC	SH
Pterospermella australiensis (Deflandre and Cookson, 1955) Eisenack et al., 1973 (large) (Prasinophyceae)	SH	
Pterospermella australiensis (Deflandre and Cookson, 1955) Eisenack et al., 1973 (Prasinophyceae)	BC	SH
Pterospermella eurypteris (Cookson and Eisenack, 1958) Eisenack et al., 1973 (Prasinophyceae)	BC	SH
Pterospermella ginginensis (Deflandre and Cookson, 1955) Eisenack et al. 1973 (Prasinophyceae)	BC	SH
Tasmanites spp. Newton, 1875 (Prasinophyceae)	BC	SH
Veryhachium spp. Deunff, 1954b (acritarch)	BC	

Additional terrestrial palynomorphs:

Alnipollenites verus	BC	
Aquilapollenites spp.	BC*	
Araucariacites australis	BC	
Baculatisporites comaumensis	BC	
Biretisporites potoniaei	BC	
bisaccate pollen	BC	
Callialasporites dampieri	BC	SH
Callialasporites microvelatus	BC	
Cerebropollenites macroverrucosus	BC	
Chasmatosporites apertus	BC	
Chasmatosporites hians	BC	
Cicatricosisporites spp.	BC	
Classopollis torosus	SH	
Converrucosisporites spp.	BC	
Corollina meyeriana (tetrad)	BC	
Cyathidites minor	BC	SH
Deltoidospora spp.	BC	SH
Densoisporites velatus	BC	
Densosporites spp.	BC	
Dictyophyllidites crassexinus	BC	
Dictyophyllidites spp.	BC	
Echinatisporis spp.	BC	
Ericipites spp.	BC	
Exesipollenites tumulus	BC	
Foraminisporis spp.	BC	
Foveotriletes spp.	SH	
fungal hyphae	BC*	SH*
fungal spores (cluster)	BC	SH
Gleicheniidites senonicus	BC	SH
Gleicheniidites spp.	BC	
Inaperturopollenites hiatus	BC	
Inaperturopollenites spp.	BC	
Ischyosporites variegatus	BC	
Kurtzipites spp.	BC	
Laevigatosporites spp.	BC	
Matonisporites crassiangulatus	SH	
Monoporites spp.	BC	
Neoraistrickia spp.	BC	
Ornamentifera spp.	BC	
Osmundacidites spp.	BC	SH
Ovalipollis pseudoalatus	BC	
pollen (undiff.)	BC	
Retitricolpites spp.	BC	
Retitricolporites spp.	BC	
Retitriletes spp.	BC	
Rugulatisporites spp.	BC	
Spheripollenites psilatus	SH	
spore (indet.)	BC	
Todisporites minor	BC	
tricolpate pollen (undiff.)	SH	
Tricolpites spp.	BC	
triporate pollen (undiff.)	SH	
triporate spp.	BC	
Verrucosisporites spp.	BC	
zooclast (undiff.)	BC*	SH*

Appendix B. Supplementary data

Supplementary data to this article can be found online at https://doi.org/10.1016/j.cretres.2022.105415.